

# Sharp Spectral Thresholds for Multi-View Spiked Wigner Models

Xiaodong Yang <sup>\*1</sup>, Subhabrata Sen <sup>†1</sup>, and Yue M. Lu <sup>‡1,2</sup>

<sup>1</sup>Department of Statistics, Harvard University

<sup>2</sup>Applied Mathematics, Harvard University

May 20, 2026

## Abstract

Motivated by multimodal estimation, we study a multi-view spiked Wigner model in which several noisy matrix observations contain correlated latent spikes. We derive a spectral estimator for the latent spikes by linearizing approximate message passing (AMP). Our main result is an explicit sharp transition formula for its spectrum: for  $L \geq 2$  views, letting  $\lambda$  be the  $L$ -dimensional vector of spike strengths and  $B$  the  $L \times L$  limiting Gram matrix of the spikes, the critical parameter is

$$\text{SNR}(\lambda, B) = \lambda_{\max} \left[ \text{Diag}(\sqrt{\lambda})(B \odot B) \text{Diag}(\sqrt{\lambda}) \right].$$

When  $\text{SNR}(\lambda, B) < 1$ , the linearized AMP matrix has no outlier beyond the right edge of its bulk spectrum. When  $\text{SNR}(\lambda, B) > 1$ , an informative outlier is pinned at the distinguished point 1, and the associated eigenvector has explicit, nontrivial overlaps with the latent signals. Thus  $\text{SNR}(\lambda, B) = 1$  gives the exact spectral weak-recovery threshold for the linearized AMP method. To establish our results, we analyze the correlated Gaussian noise matrix through a matrix Dyson equation and combine this deterministic description with finite-rank perturbation arguments adapted to the multi-view spike structure. We also show that, for a broad class of spike priors, the spectral threshold  $\text{SNR}(\lambda, B) = 1$  coincides with the information-theoretic threshold for weak recovery, ruling out a statistical-computational gap for this class of priors.

## Contents

<b>1</b>	<b>Introduction</b>	<b>2</b>
<b>2</b>	<b>Main results</b>	<b>4</b>
2.1	The linearized AMP matrix . . . . .	5
2.2	The bulk law and spectral phase transition . . . . .	6
2.3	Information-theoretic thresholds . . . . .	9
2.4	Related work . . . . .	10
2.5	Numerical results . . . . .	13

---

\*xyang@g.harvard.edu

†subhabratasen@fas.harvard.edu

‡yuelu@seas.harvard.edu

<b>3</b>	<b>Proof outlines</b>	<b>15</b>
3.1	The bulk spectrum . . . . .	15
3.2	Outlier eigenvalues and eigenvectors . . . . .	16
3.3	The phase transition threshold . . . . .	18
<b>4</b>	<b>The matrix Dyson equation: existence and stability</b>	<b>20</b>
4.1	Existence, uniqueness, and the limiting measure . . . . .	20
4.2	Stability of the matrix Dyson equation . . . . .	21
<b>5</b>	<b>Proof of the bulk law</b>	<b>26</b>
5.1	Setup and main inputs . . . . .	26
5.2	The partial trace equation . . . . .	27
5.3	Stieltjes transforms and tested deterministic equivalents . . . . .	31
5.4	Proof of Theorem 2.6 . . . . .	33
<b>6</b>	<b>Outlier eigenvalues and eigenvector overlaps</b>	<b>33</b>
6.1	The outlier equation . . . . .	34
6.2	Spectral projection for a simple outlier . . . . .	36
6.3	Matrix overlaps and two-resolvent equivalents . . . . .	37
<b>7</b>	<b>Variational analysis of the matrix Dyson equation at <math>z = 1</math></b>	<b>41</b>
7.1	Variational formulation . . . . .	41
7.2	Local minimizers of the variational objective . . . . .	43
7.3	Proof of Proposition 7.1 . . . . .	46
<b>8</b>	<b>Emergence of outlier eigenvalues</b>	<b>46</b>
8.1	Counting outliers to the right . . . . .	47
8.2	Top outlier eigenvalue at 1 . . . . .	48
8.3	Simplifying the overlap formulas . . . . .	51
8.4	Proofs of the main spectral theorems . . . . .	53
<b>9</b>	<b>Derivation of the spectral algorithm</b>	<b>54</b>
<b>10</b>	<b>Discussion</b>	<b>55</b>
<b>A</b>	<b>Linearizing Bayes optimal AMP</b>	<b>60</b>
A.1	Expansion around the origin . . . . .	60
A.2	Gaussian prior . . . . .	61
<b>B</b>	<b>Standard facts for the self-consistent equation</b>	<b>64</b>
<b>C</b>	<b>Proofs for the information-theoretical thresholds</b>	<b>64</b>
<b>D</b>	<b>Gaussian concentration for the noise resolvent</b>	<b>66</b>

# 1 Introduction

Multi-view data arise when several related measurements are collected on the same underlying units. In many applications, each view is individually noisy, while the signals shared across views

are correlated. A natural statistical question is how to combine the views so that weak information in individual measurements can be aggregated into a reliable estimator. We study this question through a stylized multiview spiked matrix model, which is motivated by multimodal PCA and related multiview inference problems [Flu84, NM24, YLS25].

For a fixed number of views  $L \geq 1$ , we observe symmetric matrices

$$A^{(l)} = \sqrt{\frac{\lambda_l}{n}} X^{(l)} X^{(l)\top} + W^{(l)} \in \mathbb{R}^{n \times n}, \quad 1 \leq l \leq L. \quad (1.1)$$

Here  $X^{(l)} \in \mathbb{R}^n$  is the latent signal in view  $l$ ,  $W^{(l)}$  is an independent Gaussian Orthogonal Ensemble noise matrix, and  $\lambda_l$  is the signal-to-noise parameter of the corresponding view. The spike vectors are generally correlated across views; writing  $X = [X^{(1)}, \dots, X^{(L)}]$ , their empirical covariance converges to a fixed matrix  $B$ . We work in the asymptotic regime where  $n \rightarrow \infty$  while  $L$ ,  $\lambda = (\lambda_1, \dots, \lambda_L)$ , and  $B$  remain fixed. This is the critical regime in which the signal and noise terms in (1.1) have comparable spectral size.

When  $L = 1$ , the model reduces to the classical rank-one spiked Wigner model, or an idealized setting for principal component analysis [Joh01]. In that case, the top eigenvalue and eigenvector undergo the Baik–Ben Arous–Peche transition: above a critical signal-to-noise level, an outlier eigenvalue separates from the bulk and the associated eigenvector has nontrivial correlation with the signal [BBAP05, KY13, BGN11]. The corresponding information-theoretic thresholds for weak recovery are also well understood [DAM17, LM19, PWBM18]. Our goal is to identify the analogous sharp spectral transition in the multiview setting, where the views must be combined according to both their individual strengths  $\lambda_l$  and their correlation structure  $B$ .

The model (1.1) was studied in recent work by the first two authors, who identified recovery limits and introduced an approximate message passing (AMP) algorithm for signal recovery [Bol14, FVRS22, YLS25]. This line of work was motivated in part by community detection in multilayer network models [YLS25]; we return to this connection in Section 2.4. The AMP algorithm reaches the desired recovery threshold when suitably initialized, but it requires a warm start. This motivates the central question of the present paper: can one construct a principled spectral method which reaches the same threshold and provides such an initialization?

We answer this question by studying the matrix obtained from linearizing the multiview AMP iteration. Our main result gives an explicit phase transition parameter:

$$\text{SNR}(\lambda, B) = \lambda_{\max} \left( \text{Diag}(\sqrt{\lambda})(B \odot B) \text{Diag}(\sqrt{\lambda}) \right). \quad (1.2)$$

When  $\text{SNR}(\lambda, B) < 1$ , the linearized AMP matrix has no outliers beyond the right edge of the spectrum. When  $\text{SNR}(\lambda, B) > 1$ , an outlier eigenvalue appears at 1 and the associated eigenvector has nonzero asymptotic overlap with the latent signals. We characterize these overlaps explicitly. For several natural distributions on the spikes, this spectral threshold coincides with the information-theoretic threshold, so the model exhibits no statistical-computational gap in these cases.

The proof has two main ingredients. First, we analyze the bulk spectrum of the linearized AMP matrix through a matrix Dyson equation. The correlated Gaussian noise has a finite-dimensional Kronecker structure, and the matrix Dyson equation gives the deterministic description needed for both the bulk law and the spike-direction resolvent estimates. Second, we identify the special point  $z = 1$  in this deterministic equation and connect the resulting condition to the replica-symmetric free energy of the Gaussian-prior problem. This yields the explicit threshold  $\text{SNR}(\lambda, B) = 1$ .

The rest of the paper is organized as follows. Section 2 introduces the linearized AMP matrix and states the main results. Section 3 gives a proof roadmap. Section 4 studies the associated matrix Dyson equation. Sections 5 and 6 prove the bulk law and characterize the outlier eigenvalues and

eigenvectors. Sections 7 and 8 establish the explicit phase transition formula and prove the main informative-eigenvector result. Section 9 derives the spectral operator from the linearized AMP iteration. We close with a short discussion.

## 2 Main results

We state our main results in this section. We first fix notation and standing assumptions, then introduce the linearized AMP matrix which is the key object in our work.

**Notation.** For  $N \in \mathbb{N}$ , write  $[N] = \{1, \dots, N\}$ . We denote by  $\mathbb{C}^+ = \{z \in \mathbb{C} : \Im z > 0\}$  the upper half-plane, and write  $\text{tr}(A)$  for the unnormalized trace of a square matrix  $A$ . Normalized traces will always be written with their normalizing factor, for example  $n^{-1} \text{tr}(A)$  or  $(nL)^{-1} \text{tr}(A)$ . For  $\lambda = (\lambda_1, \dots, \lambda_L)$ , set  $\Lambda := \text{Diag}(\lambda)$ . For an  $N \times N$  self-adjoint matrix  $A$ , we write  $\sigma_1(A) \geq \dots \geq \sigma_N(A)$  for its eigenvalues, counted with multiplicity.

The maps  $\text{diag} : \mathbb{R}^{L \times L} \rightarrow \mathbb{R}^L$  and  $\text{Diag} : \mathbb{R}^L \rightarrow \mathbb{R}^{L \times L}$  extract the diagonal of a matrix and form the corresponding diagonal matrix. Thus  $\text{Diag}(\text{diag}(M))$  is the diagonal matrix obtained from  $M$  by keeping its diagonal entries and setting all off-diagonal entries to zero. We write  $A \odot B$  for the Hadamard product and  $A \otimes B$  for the Kronecker product. We shall use the identity

$$\text{diag}(A \text{Diag}(c) B^\top) = (A \odot B) c \in \mathbb{C}^m,$$

valid for all  $c \in \mathbb{C}^n$  and  $A, B \in \mathbb{C}^{m \times n}$ .

Let  $M_L(\mathbb{R})$  and  $M_L(\mathbb{C})$  be the spaces of  $L \times L$  real and complex matrices. For  $A \in M_L(\mathbb{C})$ , set  $A^\dagger := \bar{A}^\top$ . We write

$$\text{Sym}_L(\mathbb{R}) = \{A \in M_L(\mathbb{R}) : A^\top = A\}, \quad \text{Sym}_L^+(\mathbb{R}) = \{A \in \text{Sym}_L(\mathbb{R}) : A \geq 0\}.$$

The notation for symmetric matrices is extended complex-linearly:

$$\text{Sym}_L(\mathbb{C}) = \{A + iB : A, B \in \text{Sym}_L(\mathbb{R})\} = \{A \in M_L(\mathbb{C}) : A^\top = A\}.$$

This convention is distinct from Hermitian symmetry and is the natural one for the matrix Dyson equations below. For  $A = A_1 + iA_2 \in \text{Sym}_L(\mathbb{C})$  with  $A_1, A_2 \in \text{Sym}_L(\mathbb{R})$ , we write  $\Im A := A_2$ ; for a scalar  $z \in \mathbb{C}$ ,  $\Im z$  has its usual meaning. For self-adjoint matrices  $A$  and  $B$ , we use the Loewner order:  $A \leq B$  means that  $B - A$  is positive semidefinite, and  $A < B$  means that  $B - A$  is positive definite. We write  $X_n \xrightarrow{\mathbb{P}} X$  for convergence in probability.

**Assumptions.** We now state the standing assumptions used throughout the paper.

**Definition 2.1** (Reducible covariance matrices). *A covariance matrix  $\Sigma \in \mathbb{R}^{L \times L}$  is reducible if, after a simultaneous permutation of the views, it can be written as a block diagonal matrix  $\text{Diag}(\Sigma_1, \Sigma_2)$  with two nonempty blocks. Otherwise it is irreducible.*

**Assumption 2.2.** *The first assumption specifies the noise matrices in (1.1), while the remaining assumptions concern the spikes and their limiting Gram matrix.*

(A1) *For each  $l \in [L], i, j \in [n]$ , the matrix entries satisfy  $W_{ij}^{(l)} = W_{ji}^{(l)} \sim \mathcal{N}(0, 1 + \mathbf{1}\{i = j\})$ . These Gaussians are independent.*

(A2) There exists a fixed matrix  $B \in \text{Sym}_L^+(\mathbb{R})$  which describes the limiting Gram matrix of the spikes. More precisely, denoting  $X := [X^{(1)}, \dots, X^{(L)}] \in \mathbb{R}^{n \times L}$ , for any  $\epsilon > 0$  and  $D > 0$ , and for all sufficiently large  $n$ ,

$$\mathbb{P}\left(\|X^\top X/n - B\| \geq \frac{1}{n^{1/2-\epsilon}}\right) \leq n^{-D}.$$

(A3) Each view has positive signal strength:  $\lambda_l > 0$  for every  $l \in [L]$ .

(A4) We take  $B$  to be irreducible and positive definite, and use the normalization  $B_{ll} = 1$  for every  $l \in [L]$ .

**Remark 2.3.** Assumption A2 holds if the spike entries  $\{(X_i^{(l)} : 1 \leq l \leq L) : 1 \leq i \leq n\}$  are sampled i.i.d. from an underlying prior with the corresponding concentration bounds. The weaker empirical assumption stated above is sufficient for our spectral results.

The reductions in Assumption A3 and the normalization in Assumption A4 are made without loss of generality. If  $\lambda_l = 0$  for some  $l \in [L]$ , the corresponding view  $A^{(l)}$  in (1.1) does not contribute to signal recovery; we may therefore discard it and work with the remaining views. The condition  $B_{ll} \equiv 1$  is simply a choice of scale for the spikes, corresponding to  $\|X^{(l)}\|_2 \approx \sqrt{n}$ ; any non-unit diagonal entries of  $B$  can be absorbed into  $\lambda$  by rescaling the spike vectors.

The positive semidefiniteness of  $B$  in Assumption A2 is automatic for a Gram or second-moment matrix, while the positive-definiteness requirement in Assumption A4 is a nondegeneracy condition. Equivalently, every nonzero linear combination of the view signals has positive asymptotic second moment; in statistical terms, each view contains a nonzero innovation beyond what can be explained linearly by the other views. This excludes perfectly correlated signals and, more generally, cases in which one signal direction is an exact linear combination of the others. Such singular cases lie on the boundary of the present formulation; one should first reduce to the lower-dimensional span of the signals before applying the results below.

Finally, the reducible case will be explained after the linearized AMP matrix is introduced in the next subsection. The irreducibility assumption lets us state the outlier and eigenvector results without carrying a block decomposition of the views.

## 2.1 The linearized AMP matrix

We next introduce the linearized AMP matrix, which is of central interest in this work. The guiding idea is simple. To estimate the latent vectors from the observation matrices in (1.1), one would like to combine information across the  $L$  views, using the covariance matrix  $B$  to encode how the latent signals in different views are related. A natural iterative implementation of this idea is provided by approximate message passing. If this nonlinear iteration is expanded to first order near the non-informative estimate, the result is a linear spectral method. This linearization follows the AMP formulation in [YLS25]; the derivation is postponed to Section 9. For the main results below, the following self-adjoint matrix is the focal object.

**Definition 2.4** (Linearized AMP matrix). Let  $V = \sqrt{B} \in \mathbb{R}^{L \times L}$  denote the symmetric square root of  $B$ . We define the linearized AMP matrix as

$$H = (V \otimes I_n) \text{Diag} \left( \sqrt{\frac{\lambda_1}{n}} A^{(1)} - \lambda_1 I_n, \dots, \sqrt{\frac{\lambda_L}{n}} A^{(L)} - \lambda_L I_n \right) (V \otimes I_n) \in \mathbb{R}^{Ln \times Ln}. \quad (2.1)$$

Our spectral estimator is based on a top eigenvector of  $H$ , so the first step is to translate such an eigenvector back into the signal space. The matrix  $H$  acts on vectors in  $\mathbb{R}^{nL}$ , while the latent

signal is the matrix  $X \in \mathbb{R}^{n \times L}$  in (1.1). Thus an eigenvector should be viewed as  $L$  length- $n$  blocks, one for each view. For  $v = (v^{(1)}, \dots, v^{(L)}) \in \mathbb{R}^{nL}$ , with  $v^{(l)} \in \mathbb{R}^n$ , define its matricization by

$$\text{mat}(v) := \begin{bmatrix} v^{(1)} & \dots & v^{(L)} \end{bmatrix} \in \mathbb{R}^{n \times L}.$$

This operation only reshapes the vector and does not change its norm. Thus, if  $\nu_n$  is a unit eigenvector, then  $\text{mat}(\nu_n)$  has Frobenius norm one, whereas the latent signal matrix  $X$  has columns of norm of order  $\sqrt{n}$ . To put the estimator on the same scale as the signal, we use the rescaled matrix-valued estimator

$$\hat{X}(\nu_n) := \sqrt{n} \text{mat}(\nu_n). \quad (2.2)$$

As usual for an eigenvector, this estimator is defined only up to a global sign. The central question is whether this estimator is correlated with the latent signal  $X$  in the asymptotic limit. We show that the answer exhibits a sharp phase transition, governed by an explicit signal-to-noise ratio.

**Remark 2.5** (Reducible covariance matrices). *We can now explain why the irreducibility condition in Assumption A4, in the sense of Definition 2.1, loses no generality. If  $B$  is reducible, then after permuting the views there is a partition  $S_1 \cup \dots \cup S_k = [L]$  such that*

$$B = \text{Diag}(B_1, \dots, B_k), \quad \lambda = (\tilde{\lambda}_1, \dots, \tilde{\lambda}_k), \quad \dim(B_j) = \dim(\tilde{\lambda}_j) = |S_j|,$$

where each  $B_j$  is irreducible. The same permutation makes  $V = \sqrt{B}$  block diagonal with blocks  $V_j = \sqrt{B_j}$ . Consequently, the matrix  $H$  decomposes as a direct sum of the corresponding component matrices

$$H^{[j]} = (V_j \otimes I_n) \text{Diag} \left\{ \sqrt{\lambda_l/n} A^{(l)} - \lambda_l I_n : l \in S_j \right\} (V_j \otimes I_n), \quad 1 \leq j \leq k.$$

Thus the irreducibility assumption is made without loss of generality for the analysis. It lets us state the outlier and eigenvector results without carrying this component decomposition throughout the paper.

For our subsequent analysis, it is convenient to decompose  $H$  into a low-rank “signal component” and a “noise component.” Recalling the observation model in (1.1), we write

$$H = H_0 + H_1, \quad (2.3)$$

where

$$H_0 := (V \otimes I_n) \text{Diag} \left[ \frac{\lambda_1}{n} X^{(1)} \left( X^{(1)} \right)^\top, \dots, \frac{\lambda_L}{n} X^{(L)} \left( X^{(L)} \right)^\top \right] (V \otimes I_n), \quad (2.4)$$

$$H_1 := (V \otimes I_n) \text{Diag} \left( \sqrt{\frac{\lambda_1}{n}} W^{(1)}, \dots, \sqrt{\frac{\lambda_L}{n}} W^{(L)} \right) (V \otimes I_n) - [V \text{Diag}(\lambda) V] \otimes I_n. \quad (2.5)$$

## 2.2 The bulk law and spectral phase transition

We now state the limiting spectral law for the linearized AMP matrix  $H$ .

**Theorem 2.6.** *Suppose that Assumptions A1–A4 hold. There exists a compactly supported probability measure  $\mu$  on  $\mathbb{R}$  such that, if*

$$\hat{\mu}_H := \frac{1}{nL} \sum_{j=1}^{nL} \delta_{\sigma_j(H)}$$

is the empirical spectral measure of  $H$ , then  $\hat{\mu}_H$  converges weakly to  $\mu$  in probability. Let

$$\sigma_+ := \max \text{supp}(\mu) \quad (2.6)$$

denote the upper edge of this limiting bulk spectrum. Then, for every fixed  $\epsilon > 0$ ,

$$\mathbb{P}(\#\{j \in [nL] : \sigma_j(H) > \sigma_+ + \epsilon\} \leq L) \rightarrow 1.$$

Theorem 2.6 is proved in Section 5. The limiting measure  $\mu$  can be specified explicitly through a matrix Dyson equation, a standard deterministic self-consistent equation for correlated random matrix ensembles [AEK19, AEKN19]. Because our model has an  $L$ -view block structure, this equation naturally produces a matrix-valued object before one obtains the scalar spectral law. More precisely, Section 4 constructs a compactly supported  $\text{Sym}_L^+(\mathbb{R})$ -valued measure  $\xi$  on  $\mathbb{R}$  with total mass  $\xi(\mathbb{R}) = B$ , characterized by this matrix Dyson equation. The limiting measure  $\mu$  in Theorem 2.6 is

$$\mu = \frac{1}{L} \text{tr} (B^{-1}\xi). \quad (2.7)$$

In this sense, the scalar bulk law is the normalized trace projection of the matrix-valued measure  $\nu$ . We write its matrix-valued Stieltjes transform as

$$M(z) := - \int_{\mathbb{R}} \frac{\xi(d\tau)}{\tau - z}, \quad z \in \mathbb{C}^+, \quad (2.8)$$

so that  $-(1/L) \text{tr} [B^{-1}M(z)]$  is the Stieltjes transform of  $\mu$ . Section 4 identifies  $M(z)$  as the valid solution of the corresponding matrix Dyson equation.

Note that the low-rank perturbation  $H_0$  can create at most  $L$  outlying eigenvalues in the spectrum of  $H$ . We next study the outlying eigenvalues and the recovery performance of the corresponding eigenvectors. The relevant parameter is the signal-to-noise ratio  $\text{SNR}(\lambda, B)$  defined in (1.2). It gives a sharp spectral phase transition in the spectrum of  $H$ : when  $\text{SNR}(\lambda, B) < 1$ , there is no outlier eigenvalue above the right edge  $\sigma_+$  of the bulk spectrum; in contrast, if  $\text{SNR}(\lambda, B) > 1$ , there is an outlier eigenvalue of  $H$  near 1 with high probability.

**Theorem 2.7.** *Suppose that Assumptions A1–A4 hold, and recall that  $\sigma_+$  is the upper edge of the limiting bulk spectrum defined in (2.6). Then  $\sigma_+ < 1$  whenever  $\text{SNR}(\lambda, B) \neq 1$ , and the top eigenvalue of  $H$  undergoes the following phase transition.*

(i) *If  $\text{SNR}(\lambda, B) < 1$ , then no eigenvalue separates from the right edge of the bulk:*

$$\sigma_1(H) \xrightarrow{\mathbb{P}} \sigma_+.$$

(ii) *If  $\text{SNR}(\lambda, B) > 1$ , then an outlier emerges at the point 1:*

$$\sigma_1(H) \xrightarrow{\mathbb{P}} 1.$$

*Moreover, with high probability as  $n \rightarrow \infty$ , this top eigenvalue is simple and separated from the rest of the spectrum: there exists  $\rho \in [\sigma_+, 1)$  such that  $\sigma_2(H) \xrightarrow{\mathbb{P}} \rho$ .*

The proof is given in Subsection 8.4, after the deterministic phase-transition analysis in Section 7.

In the informative phase  $\text{SNR}(\lambda, B) > 1$ , the last theorem still leaves open the possibility of additional outliers to the right of the bulk spectrum. Our next result allows us to characterize the number of outlying eigenvalues.

**Proposition 2.8.** Let  $M_+$  denote the real boundary value of the matrix-valued Stieltjes transform (2.8) at the right bulk edge  $\sigma_+$ ; the existence of this boundary value is shown in Subsection 8.1. Define  $L_0$  to be the number of eigenvalues of

$$\sqrt{\Lambda} [B \odot M_+] \sqrt{\Lambda}$$

that are strictly larger than 1. Then there exists  $\epsilon_0 > 0$  such that, for every fixed  $\epsilon \in (0, \epsilon_0)$  and  $D > 0$ ,

$$\mathbb{P}(\#\{j \in [nL] : \sigma_j(H) > \sigma_+ + \epsilon\} = L_0) \geq 1 - n^{-D}$$

for all sufficiently large  $n$ . In particular, if  $\text{SNR}(\lambda, B) > 1$ , then  $L_0 \geq 1$  and the first eigenvalue after the outlier group returns to the bulk edge:

$$\sigma_{L_0+1}(H) \xrightarrow{\mathbb{P}} \sigma_+.$$

Proposition 2.8 is proved in Subsection 8.1. Unlike the leading outlier, whose emergence is governed by the simple formula  $\text{SNR}(\lambda, B) > 1$ , the later outliers do not appear to admit an equally simple closed-form threshold. Proposition 2.8 nevertheless gives a finite-dimensional characterization of how many such outliers occur, and this criterion can be evaluated numerically; see the illustration in Figure 2.

We now turn from eigenvalues to recovery. In the informative regime  $\text{SNR}(\lambda, B) > 1$ , let  $\nu_n$  be a top eigenvector of  $H$  and use the matrix-valued estimator  $\hat{X}(\nu_n) = \sqrt{n} \text{mat}(\nu_n)$  introduced in (2.2). The next theorem identifies its asymptotic overlap with the latent signal matrix  $X$ .

**Theorem 2.9.** Suppose that Assumptions A1–A4 hold and that  $\text{SNR}(\lambda, B) > 1$ . The matrix-valued Stieltjes transform (2.8) admits a real value  $M(1) \in \text{Sym}_L^+(\mathbb{R})$  at  $z = 1$ , and this value satisfies  $M(1) < B$ .

Let  $\nu_n \in \mathbb{R}^{nL}$  be a unit eigenvector associated with the largest eigenvalue of  $H$ , and set  $\hat{X} = \sqrt{n} \text{mat}(\nu_n)$ . Then, after choosing the global sign of  $\nu_n$  appropriately,

$$\begin{aligned} \frac{1}{n} \hat{X}^\top X &\xrightarrow{\mathbb{P}} \Sigma_1 := \frac{1}{\sqrt{c^*}} V^{-1} [B - M(1)], \\ \frac{1}{n} \hat{X}^\top \hat{X} &\xrightarrow{\mathbb{P}} \Sigma_2 := \frac{1}{c^*} [I - V^{-1} M(1) V^{-1}]. \end{aligned} \tag{2.9}$$

where

$$c^* := \sum_{l=1}^L \lambda_l M_{ll}(1) [1 - M_{ll}(1)] > 0.$$

In particular,  $\Sigma_1 \neq 0$ , so the estimator  $\hat{X}$  has nontrivial asymptotic correlation with the latent signal.

The proof is given in Subsection 8.4; the overlap formulas are obtained from the general outlier analysis in Section 6.

Together, Theorems 2.7 and 2.9 give a sharp spectral transition for the model (1.1). Below the threshold, the top eigenvalue does not separate from the right edge of the bulk. Above the threshold, a distinguished outlier appears at 1, and Theorem 2.9 shows that its eigenvector yields a matrix-valued estimator with nonvanishing overlap with the latent signal.

### 2.3 Information-theoretic thresholds

The spectral results above identify  $\text{SNR}(\lambda, B) = 1$  as the threshold for the linearized AMP estimator. It is then natural to ask whether this threshold is only algorithmic, or whether it also reflects an intrinsic statistical barrier. Building on the free-energy analysis in [YLS25], we show that, for several natural classes of spikes, the same threshold is information-theoretic: below it, no estimator can have nonvanishing overlap with the planted signal, while above it Theorem 2.9 gives weak recovery by the spectral estimator. Thus, for these problems, the spectral method is optimal at the level of the weak-recovery threshold. We formulate the lower bound under the following distributional assumption on the spikes.

**Assumption 2.10.** *Every  $(X_i^{(1)}, \dots, X_i^{(L)})$  is drawn i.i.d. from a distribution  $p(x)$  with mean zero and second moment  $B$ , such that Assumption A2 holds.*

The following proposition gives two sufficient conditions under which the information-theoretic threshold coincides with the spectral threshold  $\text{SNR}(\lambda, B) \leq 1$ . We expect that  $\text{SNR}(\lambda, B) = 1$  is the fundamental weak-recovery threshold more generally, but a full characterization of the class of priors which satisfy this equivalence is an intriguing open question. Additionally, based on similar results in other high-dimensional models [KMM<sup>+</sup>13, PWBM18, LM19], we conjecture  $\text{SNR}(\lambda, B) = 1$  to be the algorithmic threshold for weak recovery in the multi-view spiked matrix problem (1.1).

**Proposition 2.11.** *Under Assumption 2.10, suppose further that  $p(\cdot)$  satisfies at least one of the two conditions below:*

(#) **Concave state evolution mapping.** *Define the state evolution mapping  $T : [0, +\infty)^L \rightarrow [0, +\infty)^L$  as*

$$T_l(\gamma) = \mathbb{E} \left[ \mathcal{X}_l \frac{\int_{\mathbb{R}^L} x_l \exp \left\{ -\frac{1}{2} \sum_{i=1}^L (\sqrt{\gamma_l} \mathcal{X}_i + \mathcal{W}_i - \sqrt{\gamma_l} x_l)^2 \right\} dp(x)}{\int_{\mathbb{R}^L} \exp \left\{ -\frac{1}{2} \sum_{i=1}^L (\sqrt{\gamma_l} \mathcal{X}_i + \mathcal{W}_i - \sqrt{\gamma_l} x_l)^2 \right\} dp(x)} \right],$$

where the expectation is evaluated with respect to independent random vectors  $\mathcal{X} \sim p(x)$  and  $\mathcal{W} \sim \mathcal{N}(0, I_L)$ . We require that for any fixed  $\gamma \in [0, +\infty)^L$  with  $\gamma \neq 0$ , the mapping  $t \in [0, +\infty) \mapsto T_l(t\gamma)$  is strictly concave for any  $l \in [L]$ .

(b) **Strictly sub-Gaussian overlaps.** *For any  $a \in (0, +\infty)^L$  and  $\mu \in \mathbb{R}^L$ ,*

$$\log \left[ \mathbb{E} \exp \left( \sum_{l=1}^L \mu_l a_l \mathcal{X}^{(l)} \overline{\mathcal{X}}^{(l)} \right) \right] \leq \frac{1}{2} \|\mu\|^2 \sigma_{\max} [\text{Diag}(a) B^{\odot 2} \text{Diag}(a)],$$

where  $\mathcal{X}, \overline{\mathcal{X}}$  are drawn independently from  $p(x)$ . This definition originates from Definition A.10 of [YLS25].

Then, whenever  $\text{SNR}(\lambda, B) < 1$ , every estimator  $\hat{X}(A) \in \mathbb{R}^{n \times L}$  computed from the observation model (1.1) has vanishing overlap with the planted signal:

$$\frac{1}{n} \hat{X}(A)^\top X \xrightarrow{\mathbb{P}} 0_{L \times L}.$$

The conditions (#) and (b) can be difficult to interpret at first glance. The following corollary presents concrete priors that are covered by the sufficient conditions introduced above.

**Corollary 2.12.** *We provide two canonical examples that satisfy the previous conditions:*

- (a) *When  $p(\cdot) = \mathcal{N}(0, B)$ , condition (#) holds.*
- (b) *When  $x$  is supported on  $\{\pm 1\}^L$  and  $\mathbb{E}x = 0$ , many priors  $p(x)$  with covariance matrices  $B$  satisfy condition (b). Interesting instances arise from community detection on multiple networks, and include: (i)  $B = (1 - \rho^2)I_L + \rho^2 \mathbf{1}_L \mathbf{1}_L^\top$  which corresponds to the hierarchical structure in [CLM22]; (ii)  $B_{l_1 l_2} = \rho^{|l_1 - l_2|}$  which corresponds to the dynamical structure in [MM17].*

Combining Corollary 2.12 with Theorem 2.9, these canonical priors exhibit no gap between the spectral weak-recovery threshold and the information-theoretic threshold for the problem (1.1). The proofs of Proposition 2.11 and Corollary 2.12 are given in Appendix C.

## 2.4 Related work

In this section, we situate our results in the wider context of high-dimensional estimation and highlight some connections with recent progress in this area.

**Spiked matrices and PCA.** Principal Component Analysis (PCA) is a classical technique for recovering low-dimensional hidden signals from high-dimensional data. Spiked random matrices [Joh01] have emerged as a natural testbed for studying the fundamental limits of signal recovery in this context. The celebrated Baik-Ben Arous-Peche transition [BBAP05] characterizes the behavior of the top eigenvalue and the associated eigenvector: above a critical threshold, the spectrum has an outlier eigenvalue and the top eigenvector is correlated with the latent signal, while below the threshold the top eigenvector is uncorrelated with the signal. Our results generalize this phenomenon to the multi-view spiked matrix setting (1.1).

**Multi-view spiked models.** Multi-view spiked models of the form (1.1) have been investigated recently by several authors (see e.g. [NM24, YLS25, Ree20, KZ25] and references therein). In [NM24], these models are motivated by applications in single-cell data analysis. They also arise naturally in past work by the first two authors on multi-layer network models [YLS25]. Prior works have developed recovery algorithms based on Approximate Message Passing (AMP) [NM24, YLS25, RR23]. A practical challenge is that AMP algorithms require a warm start, which is not immediately available. Prior work has investigated optimal recovery in spiked matrices by AMP algorithms initialized with an appropriate spectral estimator [MV21]. It would be interesting to explore the performance of AMP algorithms initialized with the spectral estimator introduced here. This is significantly beyond the scope of the current manuscript; we leave it for future work.

Recent work [Li25] develops algorithms for signal estimation in two-view spiked random matrix models based on subgraph counts of specific cycles. Subgraph-counting algorithms are typically quasi-polynomial time and are therefore less efficient than the spectral methods developed here. Finally, [MZ25] analyzes the performance of the Partial Least Squares (PLS) algorithm in this setup. This algorithm is suboptimal compared to the spectral method introduced here and requires a higher SNR to guarantee signal recovery.

**Connections with community detection.** The multi-view spiked Wigner model (1.1) is closely connected with the community detection problem on multi-layer networks. In this problem, one observes  $L \geq 2$  graphs on the same set of  $[n]$  vertices. Let  $\{E_l : l \in [L]\}$  denote the edges in layer  $l$ . The graphs are constructed as follows: each vertex  $i \in [n]$  has a “local” community assignment

in each layer  $l \in [L]$ , denoted  $X_i^{(l)} \in \{\pm 1\}$ . Given the local community assignments, the edges are sampled as

$$\mathbb{P}(\{i, j\} \in E_l) = \begin{cases} \frac{a_l}{n} & \text{if } X_i^{(l)} = X_j^{(l)}, \\ \frac{b_l}{n} & \text{otherwise.} \end{cases}$$

The edges are all independent, and  $a_l$  and  $b_l$  are  $n$ -dependent sequences that govern the connection probabilities in layer  $l$ . The main task in this context is to recover the local communities  $\{X_i^{(l)} : i \in [n], l \in [L]\}$  from the observed graphs. To connect this setting with (1.1), we encode the data through the layer-wise adjacency matrices  $A^{(l)}(i, j) = \mathbf{1}(\{i, j\} \in E_l)$ . Setting

$$d_l = \frac{a_l + b_l}{2}, \quad \lambda^{(l)} = \frac{(a_l - b_l)^2}{2(a_l + b_l)},$$

one obtains the usual centered and rescaled adjacency matrix

$$\bar{A}^{(l)}(i, j) = \frac{A^{(l)}(i, j) - d_l/n}{\sqrt{(d_l/n)(1 - d_l/n)}}.$$

Assuming  $1 \ll d_l \ll n$  and  $\lambda_l = O(1)$ , the leading signal term of  $\bar{A}^{(l)}(i, j)$  is of size  $\sqrt{\lambda_l/n} X_i^{(l)} X_j^{(l)}$ , while the variance is of order one. In this sense, the Gaussian model (1.1) is the dense random-matrix analogue of the multi-layer community-detection model. This connection is well known for spiked random matrices [DAM17], and was exploited in past work by the first two authors [YLS25]. Given the ubiquity of universality phenomena in random matrix theory, we expect that the spectral algorithm introduced here can be adapted directly to community detection on multi-layer networks, provided the observed networks are sufficiently dense. We leave a rigorous proof of this universality to future work.

This conceptual connection has also been leveraged in other recent works. Building on the ideas of [Li25], the follow-up work [GHL26] extends the walk-based approach to establish the information-theoretic threshold in the sparse graph version of the multi-layer network model investigated in [YLS25]. This resolves several questions left open in [YLS25].

**Spectral methods from linearized message passing.** Our spectral algorithm is obtained by linearizing an appropriate AMP algorithm near the “uninformative” fixed point. This general strategy has been successful for several high-dimensional inference problems. For spiked matrices, this recipe reduces to the naive spectral method, which computes the top eigenvector of the observed matrix. In other problems, this approach suggests spectral operators that attain the information-theoretic threshold for signal recovery. Notable examples include the non-backtracking operator for community detection [KMM<sup>+</sup>13], spectral methods for single-index models [LL20, MM18, LAL19], contextual stochastic block models [BCSvH24], and spiked models with heterogeneity [MKK24].

The linearized operators are analyzed using different techniques depending on the application. For dense linearized operators, prior work uses techniques from AMP [ZMV22], develops new tools from free probability [BCSvH24], or uses well-established results from random matrices [MKK24]. In our setting, the correlated multi-view noise leads naturally to a matrix Dyson equation and to a finite-dimensional outlier equation. The main task is to combine these deterministic random-matrix tools with the spike structure carefully enough to obtain explicit eigenvalue and eigenvector formulas.

It is particularly fruitful to compare our results to the recent work [MKK24], which studies the recovery of  $X \in \mathbb{R}^N$  from  $Y = \sqrt{\frac{1}{N}}XX^\top + H \odot (\Delta^{\odot 1/2})$ , where  $H$  has i.i.d. entries and  $\Delta$

admits a block structure. The entries of the spike  $X$  are assumed to be i.i.d. The authors study the spectral operator obtained by linearizing AMP. While the strategies adopted in the two works are similar, there are crucial differences in the random-matrix objects that appear. In contrast to the setting in [MKK24], we study the effect of correlations among the entries of the spike vector. The resulting noise matrix (2.5) has a structured correlated form, and its deterministic description is expressed through the matrix Dyson equation used throughout this paper. The spiked matrix with heterogeneous noise has also been analyzed using the Lehner formula [Leh99] in [BCSvH24]. It would be interesting to understand whether that free-probabilistic perspective can also be connected to the present multi-view model.

Prior analyses of spectral methods using Approximate Message Passing (AMP) [ZM24, ZJVM24] have also influenced our analysis. In these works, one tracks the top eigenvector using an appropriate AMP algorithm, and the performance of the spectral estimator is characterized through AMP state evolution. In our setting, it is challenging to rigorously establish this correspondence between the spectral estimator and an appropriate AMP algorithm, since we lack detailed information on spectral gaps in the bulk spectrum. However, state evolution suggests simplified expressions for the asymptotic overlaps in Theorem 2.9. Inspired by this prediction, we provide an independent proof of the correctness of these expressions. We defer additional details to Appendix A.2.

**Concurrent work.** While completing this manuscript, we became aware of concurrent work by Du, Hu, and Lepsveridze [DHL26]. Their paper develops spectral algorithms for several correlated two-view models, including high-dimensional canonical correlation analysis and the two-view correlated spiked Wigner and Wishart models. In particular, their correlated spiked Wigner model overlaps with the special case  $L = 2$  of our setting.

There are several important differences between the two works. First, in the two-view setting, [DHL26] constructs spectral procedures that are agnostic to the unknown model parameters: after replacing the correlation parameter by its critical value, they search over candidate signal strengths and detect separation from a common bulk edge. This parameter-free feature is statistically attractive, since the covariance structure of the latent signals may not be known a priori. By contrast, the matrix studied in the present paper uses the limiting Gram matrix  $B$  explicitly. On the other hand, our analysis applies to an arbitrary fixed number of views  $L \geq 2$  and to a general positive definite limiting Gram matrix  $B$ . Extending parameter-agnostic spectral methods beyond the special two-view structure remains an interesting open problem.

Second, one of the main contributions of the present paper is the explicit phase-transition formula  $\text{SNR}(\lambda, B) = 1$ , with  $\text{SNR}(\lambda, B)$  defined in (1.2), for an arbitrary fixed number of views. This formula is written directly in terms of the signal-strength vector  $\lambda$  and the full limiting Gram matrix  $B$ . In the overlapping two-view Wigner case, the threshold in [DHL26] is expressed in the native parameters of their model; after translating notation, it agrees with the  $L = 2$  specialization of our formula. For general  $L$ , however, the problem is genuinely multidimensional. Our proof identifies the threshold by connecting the outlier equation for the linearized AMP matrix with the variational structure of the replica-symmetric free energy with a Gaussian prior [YLS25]. This step requires a separate deterministic analysis of the matrix Dyson equation at  $z = 1$ .

**Matrix Dyson equation.** To characterize the emergence of outliers in our setting, we analyze the noise matrix  $H_1$  in (2.5) through a matrix Dyson equation. This connects our work to a broad random matrix literature on correlated ensembles and Kronecker random matrices [AEK19, AEKN19, AEKS20, AEK20]. In particular, the Hermitian Kronecker framework of [AEKN19] contains the noise component  $H_1$  and provides important input on the location of its spectrum.

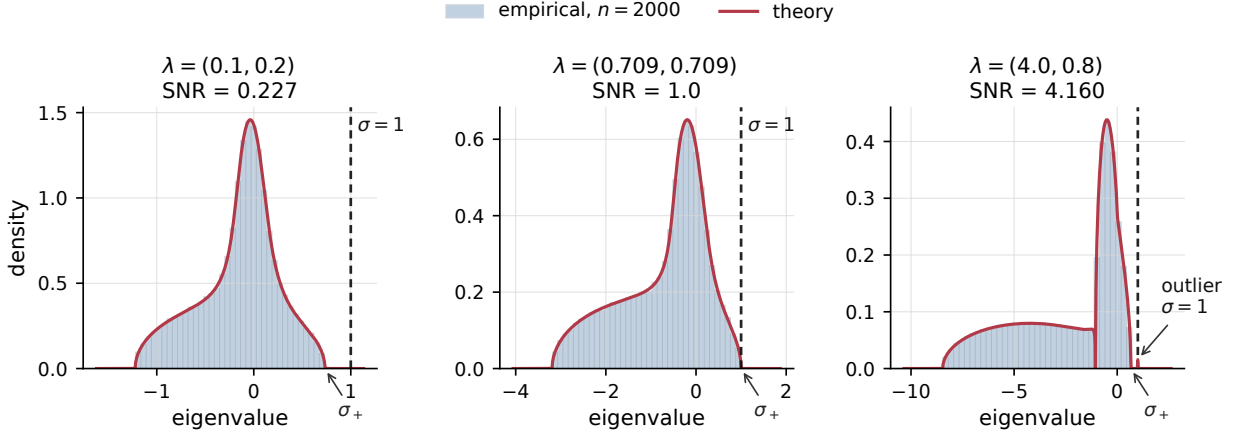


Figure 1: Comparing empirical spectral distribution with theoretical predictions. Throughout, we take  $L = 2$  and  $B = 0.64\mathbf{1}_2\mathbf{1}_2^\top + 0.36I_2$ . Going from left to right, we take  $\lambda = (0.1, 0.2)$ ,  $\lambda = (0.709, 0.709)$  and  $\lambda = (4.0, 0.8)$  respectively. To simulate the histograms, we set  $n = 2000$  and sample Bernoulli spikes  $X \in \{\pm 1\}^{n \times L}$  with the given covariance  $B$ . Then the spectrum is computed for  $H$  defined in (2.1). The arrows mark the right edge  $\sigma_+$  of the bulk spectrum; in the right panel, the small bump at  $\sigma = 1$  highlights the outlier.

What remains specific to the present paper is the way this noise analysis is coupled to the finite-rank signal component: we need deterministic equivalents adapted to the spike directions, matrix-valued overlap formulas, and a separate finite-dimensional analysis of the outlier equation. These are the ingredients that lead to the explicit phase-transition formula  $\text{SNR}(\lambda, B) = 1$ .

## 2.5 Numerical results

We close this section with numerical illustrations of the preceding results. The experiments are designed to show the three main spectral phenomena in a finite-dimensional sample: the deterministic bulk law, the emergence of the distinguished outlier at the phase transition, and the agreement between the predicted and empirical eigenvector overlaps. The theoretical curves are computed from the finite-dimensional deterministic equations associated with the matrix Dyson equation developed later in the paper, while the empirical points come from direct diagonalization of the linearized AMP matrix  $H$  in (2.1).

Figure 1 compares the empirical spectral distribution with the limiting bulk density in three regimes. In the left panel, the signal-to-noise ratio is below the transition, and the spectrum is well described by the bulk law with no visible separated eigenvalue. The middle panel is close to the transition and illustrates the movement of the right bulk edge toward the critical location. In the right panel, the model is in the informative regime: the bulk is still accurately captured by the limiting measure, while an additional eigenvalue separates and appears near the distinguished point 1. The agreement in all three panels supports both the bulk law in Theorem 2.6 and the spectral transition described in Theorem 2.7.

Figure 2 gives a more detailed view of the outlier behavior and the associated recovery formulas along a one-parameter ray  $\lambda = t(0.5, 0.8, 1.3)$  for  $t > 0$ . Panel (a) tracks the leading eigenvalues as  $t$  increases. The first dashed line is the threshold  $\text{SNR}(\lambda, B) = 1$ : after this point the leading outlier is pinned at 1, as predicted by Theorem 2.7. The later dashed lines mark the emergence of additional outliers. These subsequent thresholds are not governed by the simple scalar criterion  $\text{SNR}(\lambda, B) = 1$ ,

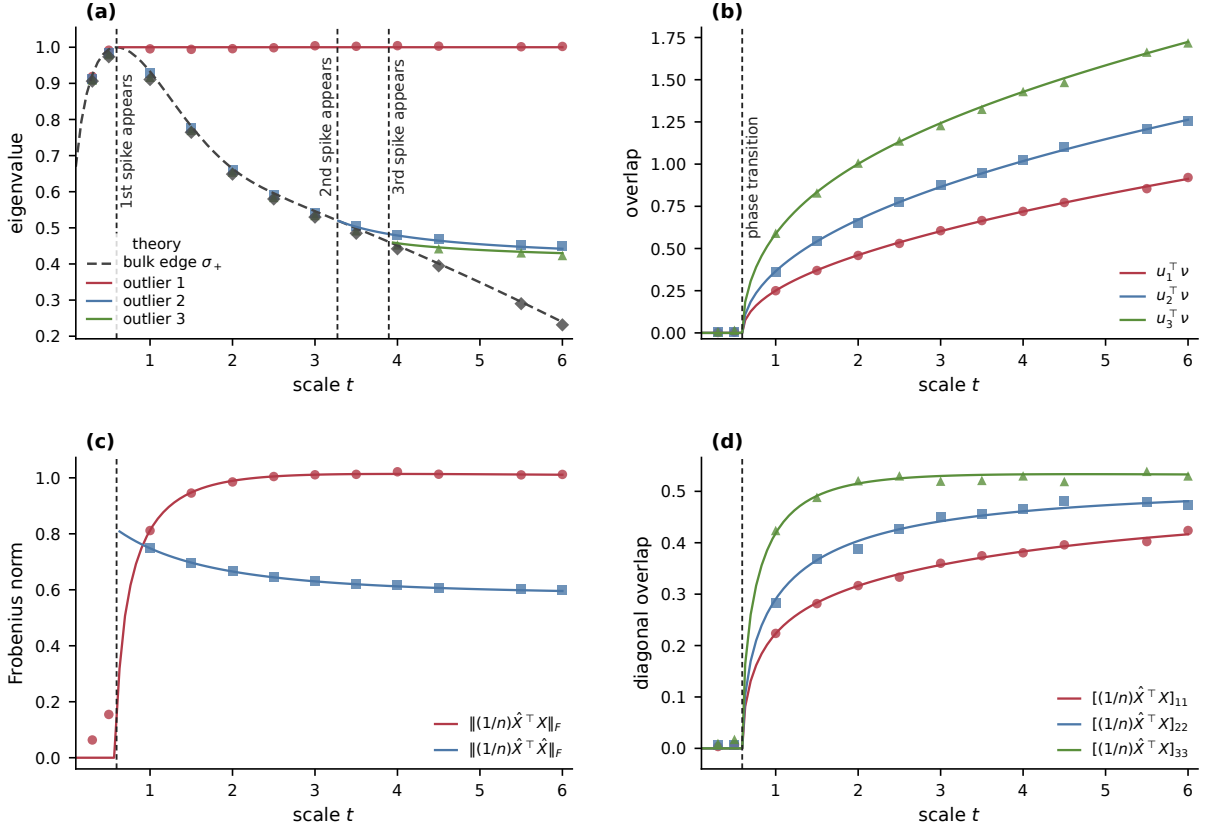


Figure 2: Comparing empirical top eigenvalues and overlaps with theoretical predictions. Throughout, we take  $L = 3$  and  $B = 0.64\mathbf{1}_3\mathbf{1}_3^\top + 0.36I_3$ . In all panels, we use  $\lambda = t(0.5, 0.8, 1.3)$  with  $0.1 \leq t \leq 6$ . For  $t \in \{0.3, 0.5, 1.0, 1.5, 2.0, 2.5, 3.0, 3.5, 4.0, 4.5, 5.5, 6.0\}$ , each scattered point averages 10 independent numerical simulations with  $n = 3000$ ; the curves are theoretical predictions. Panel (a) shows the top 4 eigenvalues, with the 4-th tracking the bulk edge  $\sigma_+$ . The vertical dashed lines mark where the first, second, and third spike eigenvalues appear. Panel (b) compares  $u_l^\top \nu_n$  for each  $l \in [L]$ , where  $\nu_n$  is the eigenvector whose eigenvalue is closest to 1 and  $u_l$  is the  $l$ th signal direction in the rank- $L$  factorization of the spike component. Panel (c) compares  $\|(1/n)\hat{X}^\top X\|_F$  with  $\|\Sigma_1\|_F$  and  $\|(1/n)\hat{X}^\top \hat{X}\|_F$  with  $\|\Sigma_2\|_F$ , where  $\hat{X} = \sqrt{n} \text{mat}(\nu_n)$  is the signal-scale matrix estimator and  $\Sigma_1, \Sigma_2$  are defined in (2.9). Panel (d) compares the diagonal entries of  $(1/n)\hat{X}^\top X$  with those of  $\Sigma_1$ .

but they are captured by the finite-dimensional outlier equations underlying Proposition 2.8. Panel (b) compares the scalar overlaps between the eigenvector and the signal directions in the rank- $L$  spike component. Panels (c) and (d) then display the matrix-valued overlaps of the signal-scale estimator  $\hat{X} = \sqrt{n} \text{mat}(\nu_n)$ : panel (c) shows the Frobenius norms of the two overlap matrices, while panel (d) shows the diagonal entries of  $(1/n)\hat{X}^\top X$ . These are the quantities predicted by Theorem 2.9.

### 3 Proof outlines

This section gives the proof roadmap for the main spectral claims of Section 2.2. Our argument has three main components. First, we identify the limiting bulk spectrum of the linearized AMP operator  $H$  in (2.1) by using the decomposition  $H = H_0 + H_1$  in (2.3) and analyzing the resolvent of the noise component  $H_1$  through the matrix Dyson equation developed in Section 4. Second, we use the finite-rank structure of  $H_0$  to reduce the outlier eigenvalues, together with the associated eigenvector overlaps, to a deterministic  $L$ -dimensional equation. Third, we analyze this deterministic equation at the special point  $z = 1$  and show that its behavior changes exactly when the signal-to-noise ratio  $\text{SNR}(\lambda, B)$  defined in (1.2) crosses one. The goal of this section is to make the proof readable before the technical estimates begin, and to serve as an atlas for where those estimates are established.

**Stochastic domination.** We will use stochastic domination throughout the proofs as a convenient way to quantify the typical size of random quantities. We use the standard notion from [EKY13, EY17, EKYY13]. Let

$$X = \left( X^{(n)}(u) : n \in \mathbb{N}, u \in U_n \right), \quad Y = \left( Y^{(n)}(u) : n \in \mathbb{N}, u \in U_n \right),$$

where  $U_n$  may depend on  $n$ . We say that  $X$  is stochastically dominated by  $Y$ , uniformly in  $u \in U_n$ , if for every  $\epsilon > 0$  and  $D > 0$ ,

$$\sup_{u \in U_n} \mathbb{P} [ |X(u)| > n^\epsilon |Y(u)| ] \leq n^{-D}$$

for all sufficiently large  $n \geq n_0(\epsilon, D)$ . In this case we write  $X = \mathcal{O}_<(Y)$ .

#### 3.1 The bulk spectrum

We first explain the mechanism behind the bulk law in Theorem 2.6; the formal proof is given in Section 5. Recall from (2.1) and (2.3) that the linearized AMP operator can be decomposed as  $H = H_0 + H_1$ . Here  $H_0$  is the signal component and has rank at most  $L$ , while  $H_1$  is the noise component. This distinction is useful because the two pieces affect different parts of the spectrum. The finite-rank matrix  $H_0$  can create a bounded number of outlying eigenvalues, but it cannot change the limiting empirical spectral distribution. Consequently, the bulk spectrum of  $H$  is governed by the noise matrix  $H_1$ .

The main task is therefore to identify the limiting spectral distribution of  $H_1$ . This is done through its resolvent, for  $z \in \mathbb{C}^+$ ,

$$G(z) = (H_1 - zI_{nL})^{-1}. \tag{3.1}$$

The deterministic approximation to  $G(z)$  is expressed in terms of the matrix-valued Stieltjes transform  $M(z)$  introduced in (2.8). In the notation of Section 4, this is the case  $\Gamma = 0$  of the perturbed matrix Dyson equation introduced there. Recall from (2.7) that  $\mu$  is obtained from the positive semidefinite matrix-valued measure  $\nu$  by taking the normalized trace against  $B^{-1}$ . The technical input we use here is the resolvent comparison below.

**Proposition 3.1** (Resolvent deterministic equivalent). *Fix  $\epsilon > 0$ , and let  $\mathcal{U}(\epsilon)$  be the spectral domain in (4.3). Uniformly for  $z \in \mathcal{U}(\epsilon)$ , define*

$$\mathcal{G}(z) := [-V^{-1}M(z)V^{-1}] \otimes I_n.$$

Then for every deterministic matrix  $A \in \mathbb{C}^{nL \times nL}$ ,

$$\mathrm{tr} [A(G(z) - \mathcal{G}(z))] = \mathcal{O}_{<} \left( \frac{\|A\|_F}{\sqrt{n}(\Im z)^4} \right).$$

Proposition 5.3 in Section 5 is a more general version of Proposition 3.1. It says that the random resolvent  $G(z)$  is asymptotically indistinguishable, when tested against deterministic matrices, from the block-constant deterministic matrix  $\mathcal{G}(z)$ . Choosing  $A = I_{nL}/(nL)$  gives the convergence of normalized traces in the form

$$\frac{1}{nL} \mathrm{tr} G(z) + \frac{1}{L} \mathrm{tr} [B^{-1}M(z)] = \mathcal{O}_{<} \left( \frac{1}{n(\Im z)^4} \right).$$

By the Stieltjes representation from Proposition 4.2, the deterministic term is the Stieltjes transform of the self-consistent density of states  $\mu$  introduced in (2.7). This identifies the limiting empirical spectral distribution of  $H_1$ . Section 5 also proves the companion no-outside-spectrum estimate, Lemma 5.5, which rules out eigenvalues of  $H_1$  away from  $\mathrm{supp}(\mu)$  with high probability.

**Remark 3.2.** *The noise matrix  $H_1$  is a correlated Gaussian matrix with a Kronecker structure, so the matrix Dyson equation literature [AEK19, Erd19, AEKN19, AEKS20, AEK20] provides the natural starting point for the analysis. In this paper we keep the resulting deterministic equation in an explicit finite-dimensional form, which is useful both for the stability estimates in Section 4 and for the spike-direction deterministic equivalents in Section 5.*

### 3.2 Outlier eigenvalues and eigenvectors

We next explain how the finite-rank signal component creates the outliers stated in Theorems 2.7 and 2.9. Recall from (2.3) that  $H = H_0 + H_1$ , where  $H_1$  is the noise matrix whose bulk law was discussed above. The signal component  $H_0$  has rank at most  $L$  and can be factored as  $H_0 = UU^\top$ , with  $U \in \mathbb{R}^{nL \times L}$  given by

$$U = [u_1, \dots, u_L] \in \mathbb{R}^{nL \times L}, \text{ with } u_l = \sqrt{\frac{\lambda_l}{n}} \begin{bmatrix} V_{1l} \\ V_{2l} \\ \dots \\ V_{Ll} \end{bmatrix} \otimes X^{(l)} \in \mathbb{R}^{nL \times 1}, \quad \forall l \in [L].$$

Consequently, the question of eigenvalues outside the bulk reduces to a fixed-dimensional one. Recall from (3.1) that  $G(z)$  denotes the resolvent of the noise component, initially for  $z \in \mathbb{C}^+$ . The same formula extends to real  $z$  outside  $\mathrm{spec}(H_1)$ . Whenever the inverses below exist, the Woodbury formula gives

$$\begin{aligned} (H - zI_{nL})^{-1} &= G(z) - G(z)U\mathcal{Q}_n(z)^{-1}U^\top G(z), \\ \mathcal{Q}_n(z) &:= I_L + U^\top G(z)U \in \mathbb{C}^{L \times L}. \end{aligned} \tag{3.2}$$

Thus, away from the spectrum of  $H_1$ , a point  $z$  is an eigenvalue of  $H$  precisely when  $\mathcal{Q}_n(z)$  is singular. This is the same determinant reduction that appears in finite-rank deformations of Wigner matrices [BGN11], but here the limiting resolvent is matrix-valued because the views are correlated.

The deterministic equivalent from Proposition 3.1, together with the spike concentration assumption in Assumption A2, gives the deterministic limit of the finite-dimensional matrix  $\mathcal{Q}_n(z)$ :

$$\mathcal{Q}(z) := I_L - \sqrt{\Lambda} [B \odot M(z)] \sqrt{\Lambda} \in \mathbb{C}^{L \times L}.$$

Here  $M(z)$  is the matrix-valued Stieltjes transform introduced in (2.8); equivalently, it is the  $\Gamma = 0$  valid solution of the matrix Dyson equation in Section 4. The measure  $\mu$  whose support defines the bulk was introduced in (2.7) and Definition 4.3. The candidate outlier locations are therefore the real solutions outside the bulk support:

$$\det \mathcal{Q}(\sigma) = 0, \quad \sigma \in \mathbb{R} \setminus \text{supp}(\mu).$$

This determinant reduction is rigorously established in Subsection 6.1 and formalized as follows.

**Proposition 3.3** (Outlier eigenvalue equation). *Let*

$$\Psi_0 = \{\sigma \in \mathbb{R} \setminus \text{supp}(\mu) : \det [\mathcal{Q}(\sigma)] = 0\},$$

with roots counted according to the order of the zero of  $\det \mathcal{Q}$ . For any fixed  $\epsilon > 0$  small enough, and for all sufficiently large  $n$ , the elements of  $\Psi_0$  are in one-to-one correspondence with the eigenvalues of  $H$  outside  $\text{supp}(\mu) + (-\epsilon, \epsilon)$ , up to multiplicity. If  $\sigma \in \Psi_0$  has multiplicity  $\text{deg}(\sigma) \geq 1$ , and  $\sigma_n$  is a corresponding eigenvalue of  $H$ , then

$$|\sigma - \sigma_n| = \mathcal{O}_<\left(n^{-\frac{1}{2\text{deg}(\sigma)+8}}\right).$$

We also characterize the eigenvectors associated with simple outliers. The next proposition identifies the limiting rank-one projection onto the outlier eigenspace, tested against arbitrary deterministic directions.

**Proposition 3.4** (Outlier eigenvector alignment). *Suppose that  $\sigma \in \Psi_0$  is simple, and let  $\sigma_n$  be the corresponding eigenvalue of  $H$  from Proposition 3.3. Let  $\nu_n \in \mathbb{R}^{nL}$  be a unit eigenvector associated with  $\sigma_n$ . Let  $w \in \mathbb{R}^L$  be the normalized null vector of  $\mathcal{Q}(\sigma)$ , so that  $\mathcal{Q}(\sigma)w = 0$  and  $\|w\| = 1$ . Then, uniformly for deterministic unit vectors  $\xi_1, \xi_2 \in \mathbb{C}^{nL}$ ,*

$$\left| (\xi_1^\top \nu_n)(\nu_n^\top \xi_2) - \frac{(\xi_1^\top \mathcal{G}(\sigma)Uw)(w^\top U^\top \mathcal{G}(\sigma)\xi_2)}{w^\top \mathcal{Q}'(\sigma)w} \right| = \mathcal{O}_<(n^{-1/10}).$$

The proof of Proposition 3.4, given in Subsection 6.2, is a contour version of the preceding determinant reduction. For the sketch, suppose that  $\sigma \in \Psi_0$  is simple and that  $\sigma_n$  is the corresponding eigenvalue of  $H$ . Choose a small circle  $\partial B(\sigma, r)$  enclosing  $\sigma_n$  and no other eigenvalue of  $H$ . The spectral projection onto the associated one-dimensional eigenspace is then recovered from the resolvent by Cauchy's formula:

$$\begin{aligned} & \frac{1}{2\pi i} \oint_{\partial B(\sigma, r)} \xi_1^\top (H - zI_{nL})^{-1} \xi_2 dz \\ &= \frac{1}{2\pi i} \oint_{\partial B(\sigma, r)} \left[ \frac{\xi_1^\top \nu_n \nu_n^\top \xi_2}{\sigma_n - z} + \sum_{(\tilde{\sigma}, \tilde{\nu})} \frac{\xi_1^\top \tilde{\nu} \tilde{\nu}^\top \xi_2}{\tilde{\sigma} - z} \right] dz = -\xi_1^\top \nu_n \nu_n^\top \xi_2, \end{aligned}$$

where the summation in the intermediate expression is over all other eigenpairs  $(\tilde{\sigma}, \tilde{\nu})$  of  $H$ . All other eigenvalues lie outside the contour, so their contributions integrate to zero. On the other hand, using (3.2) and replacing the random objects by their deterministic equivalents yields

$$\begin{aligned} \frac{1}{2\pi i} \oint_{\partial B(\sigma, r)} \xi_1^\top (H - zI_{nL})^{-1} \xi_2 dz &= \frac{1}{2\pi i} \oint_{\partial B(\sigma, r)} \xi_1^\top [\mathcal{G}(z) - \mathcal{G}(z)U\mathcal{Q}(z)^{-1}U^\top \mathcal{G}(z)] \xi_2 dz + \mathcal{O}_<(n^{-1/10}) \\ &= -\frac{1}{2\pi i} \oint_{\partial B(\sigma, r)} [\xi_1^\top \mathcal{G}(z)U] \mathcal{Q}(z)^{-1} [U^\top \mathcal{G}(z)\xi_2] dz + \mathcal{O}_<(n^{-1/10}). \end{aligned}$$

Since  $\sigma$  is a simple zero of  $\det \mathcal{Q}(z)$ , the matrix  $\mathcal{Q}(z)^{-1}$  has a simple pole at  $\sigma$ . If  $w$  spans the null space of  $\mathcal{Q}(\sigma)$ , the residue calculation gives

$$\frac{1}{2\pi i} \oint_{\partial B(\sigma, r)} [\xi_1^\top \mathcal{G}(z) U] \mathcal{Q}(z)^{-1} [U^\top \mathcal{G}(z) \xi_2] dz = \frac{[\xi_1^\top \mathcal{G}(\sigma) U w] [w^\top U^\top \mathcal{G}(\sigma) \xi_2]}{w^\top \mathcal{Q}'(\sigma) w}.$$

This explains why the null vector  $w$  of the  $L$ -dimensional matrix  $\mathcal{Q}(\sigma)$  controls the direction of the high-dimensional eigenvector  $\nu_n$ .

For signal recovery, the scalar overlap in Proposition 3.4 is not the most natural final object. As explained in Section 2.1, the signal-scale estimator is the rescaled matrixed eigenvector  $\hat{X} = \sqrt{n} \text{mat}(\nu_n)$  from (2.2), because the target signal is the matrix  $X \in \mathbb{R}^{n \times L}$  in (1.1). Equivalently, at the unit-eigenvector scale used in the spectral proof, the overlap  $\text{mat}(\nu_n)^\top X / \sqrt{n} = (1/n) \hat{X}^\top X$  gives all view-by-signal correlations at once: its  $(a, b)$  entry measures the alignment between the  $a$ th block of the eigenvector and the  $b$ th latent signal. The next proposition records these matrix-valued overlaps; this is the form needed for the recovery formulas and is one of the places where the multi-view structure of the model appears explicitly.

**Proposition 3.5** (Matrix overlaps). *Under the assumptions of Proposition 3.4, after choosing the global sign of  $\nu_n$  consistently,*

$$\left\| \frac{1}{\sqrt{n}} \text{mat}(\nu_n)^\top X - \frac{1}{\sqrt{w^\top \mathcal{Q}'(\sigma) w}} V^{-1} M(\sigma) \text{Diag}(w \odot \sqrt{\lambda}) B \right\| = \mathcal{O}_<(n^{-1/10}).$$

Moreover, the block self-overlap matrix  $\text{mat}(\nu_n)^\top \text{mat}(\nu_n) = (1/n) \hat{X}^\top \hat{X}$  equals an explicit  $L \times L$  matrix determined by  $M(\sigma)$ ,  $B$ ,  $\lambda$ , and  $w$ , up to an error  $\mathcal{O}_<(n^{-1/20})$ ; the formula is given in Proposition 6.3 in Subsection 6.3.

The proof of Proposition 3.5 is completed in Subsection 6.3. The overlap with  $X$  follows by testing the eigenvector formula against the spike directions. The block self-overlap  $\text{mat}(\nu_n)^\top \text{mat}(\nu_n)$  is more subtle. Its entries compare different view blocks of the same eigenvector, and after the spectral projection is written as a contour integral, these entries lead to expressions with two resolvents and a deterministic block matrix inserted between them. The deterministic equivalent for a single resolvent is not enough to evaluate such quantities. This is exactly why we introduced the perturbation  $\Gamma$  in the matrix Dyson equation (mat). By differentiating the deterministic equivalent with respect to  $\Gamma$ , we extract the needed two-resolvent correlations and obtain the self-overlap formula.

### 3.3 The phase transition threshold

The preceding subsection gives a general asymptotic description of outliers: outside the bulk support, their possible locations are the real roots of

$$\det \mathcal{Q}(\sigma) = 0, \quad \mathcal{Q}(\sigma) = I_L - \sqrt{\Lambda} [B \odot M(\sigma)] \sqrt{\Lambda}.$$

It also explains how the corresponding eigenvector overlaps are recovered from the null space of  $\mathcal{Q}(\sigma)$ . To prove Theorems 2.7 and 2.9, we must therefore identify when this deterministic equation creates the particular outlier responsible for weak recovery.

The special feature of the present model is that this root-creation problem has an explicit phase-transition threshold: it occurs exactly when the signal-to-noise ratio  $\text{SNR}(\lambda, B)$  defined in (1.2)

crosses one. The deterministic reason is encoded in the solution of the matrix Dyson equation at the special point  $z = 1$ . Below the threshold, the determinant equation has no root at 1; above the threshold, 1 becomes the distinguished outlier location and the associated eigenvector has nontrivial overlap with the signal. This subsection explains the deterministic mechanism behind this transition and points to the later sections where the calculations are carried out.

The main input is Proposition 7.1, proved in Section 7. It states, in particular, that when  $\text{SNR}(\lambda, B) < 1$ , the valid continuation of the matrix-valued Stieltjes transform satisfies

$$M(1) = B,$$

whereas when  $\text{SNR}(\lambda, B) > 1$ , the valid solution satisfies

$$0 < M(1) < B.$$

Thus the phase transition is already visible at the level of the deterministic matrix Dyson equation. The point  $M = B$  is the trivial solution at  $z = 1$ ; it is stable below the threshold and is replaced, above the threshold, by a smaller positive definite solution.

We next translate this deterministic transition into the spectral transition for  $H$ . If  $\text{SNR}(\lambda, B) < 1$ , then  $M(1) = B$  gives

$$\mathcal{Q}(1) = I_L - \sqrt{\Lambda} [B \odot B] \sqrt{\Lambda} > 0,$$

so the determinant equation has no root at 1. In the informative regime, Proposition 7.1 gives  $M(1) < B$ , and Section 8 uses the self-consistent equation at  $z = 1$  to construct an explicit nonzero vector in the kernel of  $\mathcal{Q}(1)$ . Hence  $\det \mathcal{Q}(1) = 0$ , and Proposition 3.3 turns this deterministic root into an outlier eigenvalue of  $H$  near 1.

We regard the explicit phase-transition formula (1.2), with threshold  $\text{SNR}(\lambda, B) = 1$ , as one of the main contributions of the paper. It is not a direct consequence of general matrix Dyson equation theory. That theory provides the deterministic description of the correlated Gaussian noise, but the phase transition also requires locating the real roots of the finite-dimensional determinant equation  $\det \mathcal{Q}(\sigma) = 0$  and explaining why the relevant threshold reduces to the explicit formula  $\text{SNR}(\lambda, B) = 1$ . Our model lies between two familiar regimes: it is more structured than a general correlated Gaussian ensemble, because the covariance structure comes from the multi-view AMP linearization, but it is still substantially richer than the one-dimensional BBP setting, where the relevant self-consistent equation can be solved in closed form.

The key additional idea is to connect the matrix Dyson equation at the special point  $z = 1$  with the TAP variational structure of the underlying inference problem. Section 7 makes this connection through the functional (7.2), a finite-dimensional counterpart of the replica-symmetric free energy for the Gaussian version of the observation model (1.1); see, for example, the general discussion in [MS24]. After a change of variables, solving the MDE at  $z = 1$  becomes a problem about local minimizers of this explicit objective. The trivial point corresponds to  $M = B$ , and the Hessian at this point changes sign exactly when  $\text{SNR}(\lambda, B)$  crosses one.

This variational viewpoint explains why the same stability criterion that governs the uninformative TAP solution also governs the creation of the spectral outlier at 1. More broadly, it suggests a potentially deeper connection between matrix Dyson equations, linearized AMP operators, and free-energy landscapes in other high-dimensional inference problems. Related uses of linearized AMP and spectral methods appear in [ZM24, ZJVM24, MKK24]; our analysis indicates that the associated deterministic MDEs may sometimes be understood more explicitly by uncovering the variational structure inherited from the underlying inference model.

The subsequent technical sections separate the deterministic and spectral parts of this argument. Section 7 proves the deterministic input, namely Proposition 7.1, by analyzing the variational

functional (7.2) and showing how the MDE solution at  $z = 1$  changes when  $\text{SNR}(\lambda, B)$  crosses one. Section 8 then converts this deterministic information into the spectral statements of Theorems 2.7 and 2.9: it counts the outliers to the right of the bulk edge, identifies the outlier at 1 when  $\text{SNR}(\lambda, B) > 1$ , and simplifies the eigenvector-overlap formulas from Proposition 6.3.

## 4 The matrix Dyson equation: existence and stability

The purpose of this section is to introduce and analyze the deterministic self-consistent equation that controls the noise component  $H_1$  in the decomposition (2.3). This equation constructs the matrix-valued measure  $\xi$  and the limiting bulk measure  $\mu$  used in Theorem 2.6, and it formalizes the Stieltjes-transform description in (2.8). It is also the deterministic object that appears in the resolvent estimates of Section 5.

**Definition 4.1** (Matrix Dyson equation and valid solution). *For a spectral parameter  $z \in \mathbb{C}$  and a deterministic perturbation  $\Gamma \in \text{Sym}_L(\mathbb{R})$ , we consider the matrix Dyson equation*

$$M^{-1} = zB^{-1} - V^{-1}\Gamma V^{-1} + \text{Diag}(\lambda) - \text{Diag}\{\lambda \odot \text{diag}(M)\}, \quad M \in \text{Sym}_L(\mathbb{C}). \quad (\text{mat})$$

When  $z \in \mathbb{C}^+$ , we call  $M(z; \Gamma)$  a valid solution if it satisfies (mat) and  $\Im M(z; \Gamma) < 0$ .

When  $\Gamma = 0$ , the valid solution will be the matrix-valued Stieltjes transform  $M(z)$  introduced in (2.8). The perturbation  $\Gamma$  is not needed for the bulk law, but it will be useful later when studying overlaps between spike eigenvectors and the target signals, where one differentiates resolvents with respect to finite-dimensional perturbations.

In this section, we establish two types of facts. First, existence, uniqueness, and the Stieltjes representation of the solution to (mat) are standard consequences of the matrix Dyson equation framework [AEK19, Erd19, AEKN19, AEKS20, AEK20]. Second, we record the quantitative stability estimate needed later in the resolvent analysis. The proof uses the explicit finite-dimensional form of the variance operator in our model; see Remark 4.6.

### 4.1 Existence, uniqueness, and the limiting measure

The self-consistent equation (mat) belongs to the general class of matrix Dyson equations studied in prior work [AEK19, Erd19, AEKN19, AEKS20, AEK20], after the change of variables given in Appendix B. We use the general existence and representation theory for these equations to obtain the valid solution in the upper half-plane and the corresponding matrix-valued Stieltjes representation.

**Proposition 4.2.** (i) *For any fixed  $\Gamma \in \text{Sym}_L(\mathbb{R})$  and any  $z \in \mathbb{C}^+$ , (mat) admits a unique valid solution  $M(z; \Gamma) \in \text{Sym}_L(\mathbb{C})$ .*

(ii) *For any fixed  $\Gamma \in \text{Sym}_L(\mathbb{R})$ , there exists a compactly-supported  $\text{Sym}_L^+(\mathbb{R})$ -valued measure  $\xi_\Gamma$  such that  $\xi_\Gamma(\mathbb{R}) = B$ , and for any  $z \in \mathbb{C}^+$ ,*

$$M(z; \Gamma) = - \int_{\mathbb{R}} \frac{\xi_\Gamma(d\tau)}{\tau - z} \in \text{Sym}_L(\mathbb{C}). \quad (4.1)$$

Proposition 4.2 is a direct consequence of existing results on matrix Dyson equations, after reducing (mat) to the standard form. We provide the proof in Appendix B for completeness.

**Definition 4.3.** Let  $\xi_\Gamma$  be the measure introduced in Proposition 4.2. We call  $\xi_\Gamma$  the generating measure with perturbation  $\Gamma$ , and define

$$\mu_\Gamma = \frac{1}{L} \operatorname{tr} (B^{-1} \xi_\Gamma). \quad (4.2)$$

In the terminology of [AEKN19, AEK19],  $\mu_\Gamma$  is the self-consistent density of states.

**Remark 4.4.** When  $\Gamma = 0$ , we suppress the perturbation from the notation:

$$M(z) := M(z; 0), \quad \xi := \xi_0, \quad \mu := \mu_0.$$

The same convention applies to any  $\Gamma$ -dependent object introduced below; for example,  $\mathcal{U}(\epsilon)$  means  $\mathcal{U}_0(\epsilon)$ . With this convention,  $\xi$  and  $\mu$  agree with the limiting measures introduced informally in (2.7).

The measure  $\mu_\Gamma$  is a compactly-supported probability measure on  $\mathbb{R}$ , since

$$\mu_\Gamma(\mathbb{R}) = \frac{1}{L} \operatorname{tr} [B^{-1} \xi_\Gamma(\mathbb{R})] = 1.$$

Since  $B^{-1} > 0$  and  $\xi_\Gamma$  is positive semidefinite valued, the scalar measure  $\mu_\Gamma$  and the matrix-valued measure  $\xi_\Gamma$  have the same support. The Stieltjes representation (4.1) implies that  $M(z; \Gamma)$  extends analytically from  $\mathbb{C}^+$  to  $\mathbb{C} \setminus \operatorname{supp}(\mu_\Gamma)$ . The following proposition gives the corresponding criterion for locating  $\operatorname{supp}(\mu_\Gamma)$ .

**Proposition 4.5.** Fix  $\Gamma \in \operatorname{Sym}_L(\mathbb{R})$ . An interval  $(a, b) \subseteq \mathbb{R}$  is outside  $\operatorname{supp}(\mu_\Gamma)$  if and only if  $M(z; \Gamma)$  admits a continuous extension onto  $(a, b)$  with  $M(\sigma; \Gamma) \in \operatorname{Sym}_L(\mathbb{R})$  for any  $\sigma \in (a, b)$ .

*Proof.* If  $(a, b) \cap \operatorname{supp}(\mu_\Gamma) = \emptyset$ , the continuous extension follows trivially from (4.1). Conversely, suppose that  $M(z; \Gamma)$  admits the prescribed extension. Using the inverse formula of Stieltjes transforms [Erd19, Lemma 2.1.4], for any  $(a_1, b_1) \subset (a, b)$ , it holds that

$$\frac{1}{2} [\xi_\Gamma(\{a_1\}) + \xi_\Gamma(\{b_1\})] + \xi_\Gamma((a_1, b_1)) = - \lim_{\eta \rightarrow 0^+} \frac{1}{\pi} \int_{a_1}^{b_1} \Im M(E + i\eta; \Gamma) dE = 0.$$

Since  $\xi_\Gamma$  is a positive semidefinite matrix-valued measure, all terms on the left-hand side are positive semidefinite matrices. Hence it further implies that each term vanishes individually, i.e.,

$$\xi_\Gamma(\{a_1\}) = 0, \quad \xi_\Gamma(\{b_1\}) = 0, \quad \xi_\Gamma((a_1, b_1)) = 0.$$

Therefore,  $\xi_\Gamma$  vanishes on every subinterval of  $(a, b)$ . Since  $\operatorname{supp}(\xi_\Gamma) = \operatorname{supp}(\mu_\Gamma)$ , this shows that  $(a, b) \cap \operatorname{supp}(\mu_\Gamma) = \emptyset$ .  $\square$

## 4.2 Stability of the matrix Dyson equation

We next prove the quantitative stability estimate that will be used in the resolvent analysis of Section 5. Roughly speaking, the estimate says that if a matrix nearly satisfies the quadratic form of the matrix Dyson equation (mat), then it must be close to the valid solution  $M(z; \Gamma)$ , uniformly for spectral parameters away from  $\operatorname{supp}(\mu_\Gamma)$ . The next remark records the particular structure of the variance operator that will be used in the proof.

**Remark 4.6** (Structure of the variance operator). *General matrix Dyson equations are often written in the form*

$$-M^{-1} = zI_N - A + \mathcal{S}[M],$$

where  $A$  is deterministic and  $\mathcal{S}$  encodes the covariance structure of the random matrix. For the equation (mat), the corresponding finite-dimensional variance operator has the simple form

$$\mathcal{S}[R] = \text{Diag} \{ \lambda \odot \text{diag}(R) \}.$$

It acts only on the diagonal of  $R$  and returns a diagonal matrix. The proof below uses this explicit form directly. This is convenient for our purposes because the later outlier and eigenvector calculations also take place in the same fixed-dimensional space.

**The stability domain.** For any  $\epsilon > 0$ , we define the  $\epsilon$ -stability domain by

$$\mathcal{U}_\Gamma(\epsilon) := \{ z \in \mathbb{C}^+ : \text{dist}(z, \text{supp } \mu_\Gamma) \geq \epsilon, |z| \leq \epsilon^{-1} \}, \quad \mathcal{U}(\epsilon) := \mathcal{U}_0(\epsilon). \quad (4.3)$$

This is the region where the limiting spectral parameter stays a fixed distance away from the bulk spectrum and where all stability estimates below are uniform.

**Proposition 4.7** (Stability of (mat) in its quadratic form). *There exist constants  $c, C > 0$ , depending only on  $(B, \lambda, \Gamma)$  and  $\epsilon$ , such that the following stability result holds uniformly over  $z \in \mathcal{U}_\Gamma(\epsilon)$ . If  $(\widetilde{M}, \Delta)$  satisfies*

$$I_L = \left( zB^{-1} - V^{-1}\Gamma V^{-1} + \Lambda - \text{Diag} \left\{ \lambda \odot \text{diag}(\widetilde{M}) \right\} \right) \widetilde{M} + \Delta, \quad \Im \widetilde{M} < 0, \quad \|\Delta\| \leq c, \quad (4.4)$$

then  $\|\widetilde{M} - M(z; \Gamma)\| \leq C \|\Delta\|$ , where  $M(z; \Gamma)$  is the valid solution from Proposition 4.2.

Note that our proof of Proposition 4.7 is adapted from the arguments in [AEKN19]. Since the general ensembles in [AEKN19] allow inhomogeneous variance profiles in each component, their self-consistent equation is expressed through a vector Dyson equation with matrix-valued variables. Our object is conciser, so we append a self-contained proof here to illustrate the key ideas in establishing the stability result.

The key point in Proposition 4.7 is the invertibility of the linearization of the matrix Dyson equation. Throughout the rest of this subsection,  $\Gamma$  is fixed and we write  $M = M(z; \Gamma)$ .

**Definition 4.8** (Stability operator). *Let  $\mathcal{S}, \mathcal{C}_R : M_L(\mathbb{C}) \rightarrow M_L(\mathbb{C})$  be given by*

$$\mathcal{S}[A] = \text{Diag} \{ \lambda \odot \text{diag}(A) \}, \quad \mathcal{C}_R[A] = RAR.$$

For the valid solution  $M = M(z; \Gamma)$ , define the stability operator

$$\mathcal{L}_z[A] := A - M \text{Diag} \{ \lambda \odot \text{diag}(A) \} M = (\text{Id} - \mathcal{C}_M \mathcal{S})[A].$$

The operator  $\mathcal{L}_z$  appears by differentiating the quadratic form of the self-consistent equation. Indeed, if  $\widetilde{M}(\Delta)$  is a local solution of (4.4) with  $\widetilde{M}(0) = M$ , then for a direction  $R \in M_L(\mathbb{C})$ ,

$$\mathcal{L}_z \left[ \nabla_R \widetilde{M}(0) \right] = -MR.$$

Thus the desired stability follows once  $\mathcal{L}_z^{-1}$  is bounded uniformly on the domain (4.3). The next lemma provides this input.

**Lemma 4.9** (Invertibility of the stability operator). *Uniformly over  $z \in \mathbb{C}^+$ , the following bounds hold:*

(i) *The solution and its inverse satisfy*

$$\|M(z; \Gamma)\| \leq \frac{C(B, \Gamma)}{\text{dist}(z, \text{supp } \mu_\Gamma)}, \quad (4.5)$$

$$\|M(z; \Gamma)^{-1}\| \leq C(B, \lambda, \Gamma) (1 + |z| + \|M(z; \Gamma)\|). \quad (4.6)$$

(ii) *The inverse of the stability operator satisfies*

$$\|\mathcal{L}_z^{-1}\| \leq C(B, \lambda, \Gamma) \frac{\|M(z; \Gamma)\| \|M(z; \Gamma)^{-1}\|^9}{\text{dist}(z, \text{supp } \mu_\Gamma)^8}. \quad (4.7)$$

In particular, the right-hand side of (4.7) is uniformly bounded on  $\mathcal{U}_\Gamma(\epsilon)$ .

*Proof.* The bound (4.5) follows from the Stieltjes-transform representation of the valid solution, while (4.6) follows directly from (mat). Indeed,

$$\begin{aligned} \|M^{-1}\| &\leq \|zB^{-1} - V^{-1}\Gamma V^{-1}\| + \|\text{Diag}(\lambda)\| + \|\text{Diag}\{\lambda \odot \text{diag}(M)\}\| \\ &\leq C(B, \lambda, \Gamma) (1 + |z| + \|M\|). \end{aligned}$$

The nontrivial part is the bound on  $\mathcal{L}_z^{-1}$ . The argument follows the saturated-operator method of [AEK19, AEKN19], specialized to the finite-dimensional operator  $\mathcal{S}[R] = \text{Diag}\{\lambda \odot \text{diag}(R)\}$ .

*Step 1. Auxiliary operators.* Define

$$\mathcal{K}_R : M_L(\mathbb{C}) \rightarrow M_L(\mathbb{C}), \quad \mathcal{K}_R[A] = R^\dagger A R, \quad \forall R \in M_L(\mathbb{C}).$$

If  $R$  is Hermitian, in particular if  $R \in \text{Sym}_L(\mathbb{R})$ , then  $\mathcal{C}_R = \mathcal{K}_R$ . We use the identity

$$\Im(M^{-1}) = -(M^\dagger)^{-1} [\Im M] M^{-1}.$$

Taking the imaginary part of (mat) gives

$$-\Im M = \Im z \cdot \mathcal{K}_M[B^{-1}] - \mathcal{K}_M \mathcal{S}[\Im M]. \quad (4.8)$$

Introduce

$$T := \mathcal{C}_{\sqrt{-\Im M}}^{-1} [\Re M] + iI, \quad W := (T^\dagger T)^{1/4}, \quad U := T(T^\dagger T)^{-1/2}. \quad (4.9)$$

Since  $T$  is normal and  $T^\dagger T = T T^\dagger$ ,

$$M = \left(W \sqrt{-\Im M}\right)^\dagger U^\dagger \left(W \sqrt{-\Im M}\right).$$

Consequently,

$$\mathcal{K}_M = \mathcal{C}_{\sqrt{-\Im M}} \mathcal{C}_W \mathcal{K}_{U^\dagger} \mathcal{C}_W \mathcal{C}_{\sqrt{-\Im M}}.$$

Define the saturated operator  $\mathcal{F} : M_L(\mathbb{C}) \rightarrow M_L(\mathbb{C})$  by

$$\mathcal{F} := \mathcal{C}_W \mathcal{C}_{\sqrt{-\Im M}} \mathcal{S} \mathcal{C}_{\sqrt{-\Im M}} \mathcal{C}_W. \quad (4.10)$$

The operator  $\mathcal{F}$  preserves the cone of positive semidefinite matrices. Hence a Perron-Frobenius theorem for cone-preserving operators gives a normalized matrix  $F$  with  $\|F\| = 1$ ,  $F \geq 0$ , and  $\mathcal{F}[F] = \|\mathcal{F}\| F$ .

*Step 2. The saturated equation.* Applying the inverse of  $\mathcal{C}_{\sqrt{-\Im M}} \mathcal{C}_W \mathcal{K}_{U^\dagger}$  to both sides of (4.8), we obtain

$$W^{-2} = \Im z \cdot \mathcal{C}_W \mathcal{C}_{\sqrt{-\Im M}} [B^{-1}] + \mathcal{F} [W^{-2}].$$

For the left-hand side we used the commutation of  $W$  and  $U$ , which implies

$$\mathcal{K}_{U^\dagger}^{-1} \mathcal{C}_W^{-1} \mathcal{C}_{\sqrt{-\Im M}}^{-1} [-\Im M] = U^\dagger W^{-2} U = W^{-2}.$$

Taking the matrix inner product with  $F$  yields

$$1 - \|\mathcal{F}\| = \frac{\Im z \langle F, \mathcal{C}_W \mathcal{C}_{\sqrt{-\Im M}} [B^{-1}] \rangle}{\langle F, W^{-2} \rangle}. \quad (4.11)$$

*Step 3. Bounding the saturation gap.* The Stieltjes representation and the fact that  $\text{supp}(\mu_\Gamma) \subset \mathbb{R}$  imply

$$-\Im M \leq \frac{C(B, \Gamma) \Im z}{\text{dist}(z, \text{supp } \mu_\Gamma)^2} I_L. \quad (4.12)$$

Since  $\mathcal{K}_M \mathcal{S}$  is positivity preserving and  $\Im M < 0$ , equation (4.8) also gives

$$-\Im M \geq \Im z \mathcal{K}_M [B^{-1}] \geq \sigma_{\max}(B)^{-1} \Im z \cdot M^\dagger M \geq \sigma_{\max}(B)^{-1} \Im z \|M^{-1}\|^{-2} I_L. \quad (4.13)$$

From the definition of  $W$  in (4.9),

$$\begin{aligned} W^4 &= \mathcal{C}_{\sqrt{-\Im M}}^{-1} (\mathcal{C}_{\Re M} + \mathcal{C}_{-\Im M}) [(-\Im M)^{-1}] \\ &\geq c(B, \Gamma) (\Im z)^{-1} \text{dist}(z, \text{supp } \mu_\Gamma)^2 \mathcal{C}_{\sqrt{-\Im M}}^{-1} [MM^\dagger + M^\dagger M] \\ &\geq c(B, \Gamma) \|M^{-1}\|^{-2} (\Im z)^{-2} \text{dist}(z, \text{supp } \mu_\Gamma)^4 I_L, \end{aligned} \quad (4.14)$$

where we used  $MM^\dagger + M^\dagger M \geq 2 \|M^{-1}\|^{-2} I_L$  and (4.12). Similarly,

$$\begin{aligned} W^4 &= \mathcal{C}_{\sqrt{-\Im M}}^{-1} (\mathcal{C}_{\Re M} + \mathcal{C}_{-\Im M}) [(-\Im M)^{-1}] \\ &\leq C(B) (\Im z)^{-1} \|M^{-1}\|^2 \mathcal{C}_{\sqrt{-\Im M}}^{-1} [MM^\dagger + M^\dagger M] \\ &\leq C(B) \|M\|^2 (\Im z)^{-2} \|M^{-1}\|^4 I_L. \end{aligned} \quad (4.15)$$

We now bound the numerator and denominator in (4.11). For the numerator,

$$\begin{aligned} \langle F, \mathcal{C}_W \mathcal{C}_{\sqrt{-\Im M}} [B^{-1}] \rangle &\geq c(B) \langle F, \mathcal{C}_W [-\Im M] \rangle \\ &\geq c(B) \Im z \|M^{-1}\|^{-2} \langle F, W^2 \rangle \\ &= c(B) \Im z \|M^{-1}\|^{-2} \text{tr} [\sqrt{F} W^2 \sqrt{F}] \\ &\geq c(B, \Gamma) \|M^{-1}\|^{-3} \text{dist}(z, \text{supp } \mu_\Gamma)^2 \text{tr}(F). \end{aligned}$$

For the denominator,

$$\langle F, W^{-2} \rangle \leq C(B, \Gamma) \|M^{-1}\| (\Im z) \text{dist}(z, \text{supp } \mu_\Gamma)^{-2} \text{tr}(F).$$

Combining these estimates with (4.11), we obtain

$$1 - \|\mathcal{F}\| \geq c(B, \Gamma) \frac{\text{dist}(z, \text{supp } \mu_\Gamma)^4}{\|M^{-1}\|^4}. \quad (4.16)$$

*Step 4. Inverting the stability operator.* By the definitions (4.9) and (4.10),

$$\mathcal{L}_z = \mathcal{C}_{\sqrt{-\Im M}} \mathcal{C}_W \mathcal{C}_{U^\dagger} (\mathcal{C}_U - \mathcal{F}) \mathcal{C}_W^{-1} \mathcal{C}_{\sqrt{-\Im M}}^{-1}.$$

Since  $U$  is unitary,  $\|\mathcal{C}_{U^\dagger}\| = 1$ , and (4.16) implies

$$\|(\mathcal{C}_U - \mathcal{F})^{-1}\| \leq (1 - \|\mathcal{F}\|)^{-1} \leq C(B, \Gamma) \frac{\|M^{-1}\|^4}{\text{dist}(z, \text{supp } \mu_\Gamma)^4}.$$

Finally, using (4.12), (4.13), (4.14), and (4.15),

$$\begin{aligned} \|\mathcal{C}_{\sqrt{-\Im M}}\| &\leq C(B, \Gamma) (\Im z) \text{dist}(z, \text{supp } \mu_\Gamma)^{-2}, \\ \|\mathcal{C}_{\sqrt{-\Im M}}^{-1}\| &\leq C(B) (\Im z)^{-1} \|M^{-1}\|^2, \\ \|\mathcal{C}_W\| &\leq C(B) \|M\| (\Im z)^{-1} \|M^{-1}\|^2, \\ \|\mathcal{C}_W^{-1}\| &\leq C(B, \Gamma) \|M^{-1}\| (\Im z) \text{dist}(z, \text{supp } \mu_\Gamma)^{-2}. \end{aligned}$$

Multiplying the displayed bounds gives (4.7).  $\square$

**Lemma 4.10** (Quantitative implicit function theorem, Lemma 4.10 of [AEK19]). *Let  $T : \mathbb{C}^A \times \mathbb{C}^D \rightarrow \mathbb{C}^A$  be continuously differentiable with  $T(0, 0) = 0$  and invertible partial derivative  $\nabla^{(1)}T(0, 0) \in M_A(\mathbb{C})$ . Assume  $\mathbb{C}^A$  and  $\mathbb{C}^D$  are equipped with norms  $\|\cdot\|$  and let the induced operator norms be denoted by the same symbol. Suppose there exist constants  $\delta > 0$  and  $C_1, C_2 < \infty$  such that:*

1.  $\|(\nabla^{(1)}T(0, 0))^{-1}\| \leq C_1$ ;
2.  $\|\text{Id}_{\mathbb{C}^A} - (\nabla^{(1)}T(0, 0))^{-1} \nabla^{(1)}T(a, d)\| \leq \frac{1}{2}$  for every  $(a, d) \in B_\delta^A \times B_\delta^D$ ;
3.  $\|\nabla^{(2)}T(a, d)\| \leq C_2$  for every  $(a, d) \in B_\delta^A \times B_\delta^D$ .

Then there exists  $\epsilon > 0$ , depending only on  $(\delta, C_1, C_2)$ , and a unique continuously differentiable function  $f : B_\epsilon^D \rightarrow B_\delta^A$  such that

$$\begin{aligned} T(f(d), d) &= 0 \quad \text{for all } d \in B_\epsilon^D, \\ Df(d) &= -(\nabla^{(1)}T(f(d), d))^{-1} \nabla^{(2)}T(f(d), d). \end{aligned}$$

Therefore,  $Df(d)$  is uniformly bounded by a constant depending only on  $(C_1, C_2)$  for  $d \in B_\epsilon$ . Moreover, if  $T$  is analytic, then  $f$  is analytic.

*Proof of Proposition 4.7.* We apply Lemma 4.10 to the map  $\mathcal{J} : M_L(\mathbb{C}) \times M_L(\mathbb{C}) \rightarrow M_L(\mathbb{C})$  defined by

$$\mathcal{J} \left[ \widetilde{M}, \Delta \right] = -I_L + \left( zB^{-1} - V^{-1}\Gamma V^{-1} + \Lambda - \text{Diag} \left\{ \lambda \odot \text{diag}(\widetilde{M}) \right\} \right) \widetilde{M} + \Delta.$$

The perturbed equation (4.4) is equivalent to  $\mathcal{J}[\widetilde{M}, \Delta] = 0$ , and the equation with  $\Delta = 0$  is  $\mathcal{J}[M(z; \Gamma), 0] = 0$ . For a direction  $R \in M_L(\mathbb{C})$ ,

$$\begin{aligned} \nabla_R^{(\widetilde{M})} \mathcal{J}[\widetilde{M}, \Delta] &= \left( zB^{-1} - V^{-1}\Gamma V^{-1} + \Lambda - \text{Diag} \left\{ \lambda \odot \text{diag}(\widetilde{M}) \right\} \right) R \\ &\quad - \text{Diag} \left\{ \lambda \odot \text{diag}(R) \right\} \widetilde{M}. \end{aligned}$$

Evaluating at  $(M(z; \Gamma), 0)$  and using (mat),

$$\nabla_R^{(\widetilde{M})} \mathcal{J}[M(z; \Gamma), 0] = M(z; \Gamma)^{-1} \mathcal{L}_z[R].$$

Lemma 4.9, together with the definition of  $\mathcal{U}_\Gamma(\epsilon)$  in (4.3), gives a uniform bound on the inverse of this derivative for  $z \in \mathcal{U}_\Gamma(\epsilon)$ . The derivative of  $\mathcal{J}$  is continuous in  $\widetilde{M}$ , so the second hypothesis of Lemma 4.10 holds on a sufficiently small uniform neighborhood. Finally,  $\nabla_R^{(\Delta)} \mathcal{J}[\widetilde{M}, \Delta] = R$ , so the third hypothesis is immediate.

Lemma 4.10 yields a local solution map  $\Delta \mapsto \widetilde{M}(\Delta)$  with uniformly bounded derivative. Therefore  $\|\widetilde{M} - M(z; \Gamma)\| \leq C \|\Delta\|$  whenever  $\|\Delta\| \leq c$ .  $\square$

## 5 Proof of the bulk law

The goal of this section is to prove the bulk law in Theorem 2.6. Recall from (2.3) that the linearized AMP matrix decomposes as  $H = H_0 + H_1$ , where  $H_0$  is the signal component and has rank at most  $L$ , while  $H_1$  is the correlated Gaussian noise component. Since adding a matrix of rank at most  $L$  does not change the limiting empirical spectral distribution, the bulk law is determined by the spectrum of  $H_1$ . We therefore prove deterministic equivalents for the resolvent of  $H_1$  and identify their limit with the solution of the matrix Dyson equation introduced in Section 4. For later use in the eigenvector-overlap analysis, we carry out the argument for the slightly perturbed matrix  $H_1 + \Gamma \otimes I_n$ , where  $\Gamma \in \text{Sym}_L(\mathbb{R})$  is deterministic. The bulk law itself corresponds to the special case  $\Gamma = 0$ ; throughout the paper, notation without  $\Gamma$  refers to this unperturbed case.

### 5.1 Setup and main inputs

For  $z \in \mathbb{C}^+$  and  $\Gamma \in \text{Sym}_L(\mathbb{R})$ , we define a generalized resolvent for the noise matrix  $H_1$  given in (2.5),

$$G(z; \Gamma) = (H_1 + \Gamma \otimes I_n - zI_{nL})^{-1} \in \mathbb{C}^{nL \times nL}. \quad (5.1)$$

The rest of this section rigorously establishes the connection between  $G(z; \Gamma)$  and  $M(z; \Gamma)$ , the unique solution to (mat) defined in Section 4. We also introduce the partial trace operator  $\text{Tr} : M_{nL}(\mathbb{C}) \rightarrow M_L(\mathbb{C})$ , defined by

$$A = \left\{ A_{ij}^{lk} : i, j \in [n], l, k \in [L] \right\} \mapsto \text{Tr}(A) = \left\{ \sum_{i=1}^n A_{ii}^{lk} : l, k \in [L] \right\}. \quad (5.2)$$

Here  $A$  is viewed as an  $L \times L$  block matrix whose blocks are  $n \times n$ . We shall repeatedly use

$$\begin{aligned} \text{Tr}(A_0 \otimes I_n) &= nA_0, & A_0 &\in M_L(\mathbb{C}), \\ \text{Tr}[(A_1 \otimes I_n)A_2(A_3 \otimes I_n)] &= A_1 \text{Tr}[A_2] A_3, & A_1, A_3 &\in M_L(\mathbb{C}), A_2 \in M_{nL}(\mathbb{C}). \end{aligned}$$

We will need a concentration estimate for the normalized partial trace of the resolvent. The standard proof is given in Appendix D; it yields that for every deviation level  $\delta > 0$ ,

$$\mathbb{P} \left( \left\| \frac{1}{n} \text{Tr} [G(z; \Gamma)] - \mathbb{E} \left\{ \frac{1}{n} \text{Tr} [G(z; \Gamma)] \right\} \right\|_F \geq \delta \right) \leq 2 \exp \left( -C (\Im z)^4 n^2 \delta^2 \right). \quad (5.3)$$

Since  $L$  stays fixed throughout the paper, the Frobenius norm  $\|\cdot\|_F$  in (5.3) can be replaced by any matrix norm on  $\text{Sym}_L(\mathbb{C})$ , up to changing constants.

**Definition 5.1** (Deterministic equivalent resolvent). *Fix  $\Gamma \in \text{Sym}_L(\mathbb{R})$  and let  $M(z; \Gamma)$  be the valid solution of the matrix Dyson equation (mat). For  $z \in \mathbb{C}^+$ , define*

$$\mathcal{G}(z; \Gamma) := [-V^{-1}M(z; \Gamma)V^{-1}] \otimes I_n \in \mathbb{C}^{nL \times nL}.$$

When  $\Gamma = 0$ , we write  $\mathcal{G}(z) := \mathcal{G}(z; 0)$ .

The following two propositions connect the random resolvent  $G(z; \Gamma)$  to the deterministic matrix  $\mathcal{G}(z; \Gamma)$ . The first identifies the normalized partial trace, and the second gives convergence in the sense of deterministic equivalents [HLN07].

**Proposition 5.2** (Partial-trace deterministic equivalent). *Recall the domain  $\mathcal{U}_\Gamma(\epsilon)$  in (4.3). Uniformly over  $z \in \mathcal{U}_\Gamma(\epsilon)$ , we have*

$$\frac{1}{n} \text{Tr} [G(z; \Gamma)] = -V^{-1}M(z; \Gamma)V^{-1} + \mathcal{O}_< \left( \frac{1}{n(\Im z)^3} \right),$$

where  $M(z; \Gamma)$  is the unique valid solution from Proposition 4.2.

**Proposition 5.3.** *For any fixed  $\epsilon > 0$ , uniformly over  $z \in \mathcal{U}_\Gamma(\epsilon)$  and deterministic matrices  $A \in \mathbb{C}^{nL \times nL}$ , the following holds*

$$\text{tr} [AG(z; \Gamma)] = \text{tr} [A\mathcal{G}(z; \Gamma)] + \mathcal{O}_< \left( \frac{1}{\sqrt{n}(\Im z)^4} \|A\|_F \right).$$

We prove these two propositions in the next two subsections. We then derive a no-outside-spectrum estimate for the noise matrix and use it, together with the rank bound on  $H_0$ , to complete the proof of Theorem 2.6.

## 5.2 The partial trace equation

We now prove Proposition 5.2. The averaged object that naturally appears in the computation is

$$\mathcal{T}_{G,n} := \frac{1}{n} \text{Tr} [(V \otimes I_n)G(z; \Gamma)(V \otimes I_n)].$$

The main step is to derive a finite-dimensional relation for  $\mathcal{T}_{G,n}$  by applying Stein's lemma and then taking the partial trace. After concentration, this relation becomes an approximate version of the matrix Dyson equation in the variable  $\mathcal{T} = -M(z; \Gamma)$ . The stability estimate from Proposition 4.7 then identifies  $\mathbb{E}\mathcal{T}_{G,n}$  with  $-M(z; \Gamma)$ ; a final use of concentration gives the random partial-trace estimate in Proposition 5.2.

*Proof of Proposition 5.2.* In the proof, for notational convenience, write  $G = G(z; \Gamma)$  and  $\tilde{V}_n = V \otimes I_n$ . For convenience, write  $\tilde{H}_1$  for the mean-zero random part of  $H_1$ ,

$$\tilde{H}_1 = H_1 - \mathbb{E}H_1 = \tilde{V}_n \text{Diag} \left( \sqrt{\frac{\lambda_1}{n}} W^{(1)}, \dots, \sqrt{\frac{\lambda_L}{n}} W^{(L)} \right) \tilde{V}_n.$$

In what follows, we will consistently use  $e_i^l$  to denote the one-hot length- $nL$  vector with only the  $i$ -th entry in the  $l$ -th block being 1. Then decompose  $\tilde{H}_1$  into a sum of independent components:

$$\begin{aligned} \tilde{H}_1 &= \sum_{i=1}^n \sum_{l=1}^L \sqrt{\frac{\lambda_l}{n}} W_{ii}^{(l)} \tilde{V}_n \left[ e_i^l (e_i^l)^\top \right] \tilde{V}_n \\ &\quad + \sum_{1 \leq i < j \leq n} \sum_{l=1}^L \sqrt{\frac{\lambda_l}{n}} W_{ij}^{(l)} \tilde{V}_n \left[ e_i^l (e_j^l)^\top + e_j^l (e_i^l)^\top \right] \tilde{V}_n, \end{aligned} \quad (5.4)$$

Using the decomposition in (5.4), we can deduce that

$$\begin{aligned} \mathbb{E} \left[ G\tilde{H}_1 \right] &= \mathbb{E} \left\{ \sum_{i=1}^n \sum_{l=1}^L \sqrt{\frac{\lambda_l}{n}} \mathbb{E}_{ii,l} \left[ W_{ii}^{(l)} G \right] \tilde{V}_n \left[ e_i^l (e_i^l)^\top \right] \tilde{V}_n \right. \\ &\quad \left. + \sum_{1 \leq i < j \leq n} \sum_{l=1}^L \sqrt{\frac{\lambda_l}{n}} \mathbb{E}_{ij,l} \left[ W_{ij}^{(l)} G \right] \tilde{V}_n \left[ e_i^l (e_j^l)^\top + e_j^l (e_i^l)^\top \right] \tilde{V}_n \right\}, \end{aligned} \quad (5.5)$$

where  $\mathbb{E}_{ij,l}(\cdot)$  denote the *partial* expectation with respect to the scalar Gaussian  $W_{ij}^{(l)}$ , while keeping all the other random variables fixed. By Stein's lemma and standard resolvent identities,

$$\begin{aligned} \mathbb{E}_{ii,l} \left[ W_{ii}^{(l)} G \right] &= -\sqrt{\frac{\lambda_l}{n}} \mathbb{E}_{ii,l} \left[ G \tilde{V}_n \left[ 2e_i^l (e_i^l)^\top \right] \tilde{V}_n G \right], \\ \mathbb{E}_{ij,l} \left[ W_{ij}^{(l)} G \right] &= -\sqrt{\frac{\lambda_l}{n}} \mathbb{E}_{ij,l} \left[ G \tilde{V}_n \left[ e_i^l (e_j^l)^\top + e_j^l (e_i^l)^\top \right] \tilde{V}_n G \right]. \end{aligned}$$

Substituting these expressions into (5.5) yields

$$\begin{aligned} &\mathbb{E} \left[ G\tilde{H}_1 \right] \\ &= -\mathbb{E} \left\{ \sum_{i=1}^n \sum_{l=1}^L \frac{2\lambda_l}{n} \mathbb{E}_{ii,l} \left[ G \tilde{V}_n \left[ e_i^l (e_i^l)^\top \right] \tilde{V}_n G \right] \tilde{V}_n \left[ e_i^l (e_i^l)^\top \right] \tilde{V}_n \right. \\ &\quad \left. + \sum_{i < j} \sum_{l=1}^L \frac{\lambda_l}{n} \mathbb{E}_{ij,l} \left[ G \tilde{V}_n \left[ e_i^l (e_j^l)^\top + e_j^l (e_i^l)^\top \right] \tilde{V}_n G \right] \tilde{V}_n \left[ e_i^l (e_j^l)^\top + e_j^l (e_i^l)^\top \right] \tilde{V}_n \right\} \\ &= -\sum_{l=1}^L \frac{\lambda_l}{n} \mathbb{E} \left\{ G \tilde{V}_n \left[ 2 \sum_{i=1}^n e_i^l (e_i^l)^\top \tilde{V}_n G \tilde{V}_n e_i^l (e_i^l)^\top \right. \right. \\ &\quad \left. \left. + \sum_{i < j} \left( e_i^l (e_j^l)^\top + e_j^l (e_i^l)^\top \right) \tilde{V}_n G \tilde{V}_n \left( e_i^l (e_j^l)^\top + e_j^l (e_i^l)^\top \right) \right] \tilde{V}_n \right\}. \end{aligned}$$

By applying the following identity

$$\begin{aligned} & 2 \sum_{i=1}^n e_i^l (e_i^l)^\top \tilde{V}_n G \tilde{V}_n e_i^l (e_i^l)^\top + \sum_{i < j} \left( e_i^l (e_j^l)^\top + e_j^l (e_i^l)^\top \right) \tilde{V}_n G \tilde{V}_n \left( e_i^l (e_j^l)^\top + e_j^l (e_i^l)^\top \right) \\ &= \sum_{i,j=1}^n e_i^l (\tilde{V}_n G \tilde{V}_n)_{ji}^{ll} (e_j^l)^\top + \sum_{i,j=1}^n e_i^l (\tilde{V}_n G \tilde{V}_n)_{jj}^{ll} (e_i^l)^\top, \end{aligned}$$

we can further rephrase  $\mathbb{E} [G \tilde{H}_1]$  by

$$\mathbb{E} [G \tilde{H}_1] = -\mathbb{E} [G \tilde{V}_n \text{Diag} \{ \lambda_1 E_1, \dots, \lambda_L E_L \} \tilde{V}_n], \quad (5.6)$$

where each  $E_l$  is an  $n \times n$  matrix whose entries are given by

$$\begin{aligned} (E_l)_{ij} &= \frac{\sum_{k=1}^n (\tilde{V}_n G \tilde{V}_n)_{kk}^{ll}}{n} \mathbb{1}_{i=j} + \frac{(\tilde{V}_n G \tilde{V}_n)_{ji}^{ll}}{n} \\ &= \frac{1}{n} \text{Tr} [\tilde{V}_n G \tilde{V}_n]^{ll} \mathbb{1}_{i=j} + \frac{(\tilde{V}_n G \tilde{V}_n)_{ji}^{ll}}{n}. \end{aligned}$$

Introduce a vector  $\hat{\chi} = \text{diag} \left\{ \frac{1}{n} \text{Tr} [\tilde{V}_n G \tilde{V}_n] \right\} \in \mathbb{C}^L$  whose coordinates are given by

$$\hat{\chi}_l = \frac{1}{n} \sum_{i=1}^n (\tilde{V}_n G \tilde{V}_n)_{ii}^{ll}.$$

It is straightforward to show that

$$E_l = \hat{\chi}_l I_n + \frac{1}{n} \Delta_l, \quad l \in [L],$$

where  $\Delta_1, \Delta_2, \dots, \Delta_L$  are  $n \times n$  residual matrices such that  $\Delta_{l,ij} = (\tilde{V}_n G \tilde{V}_n)_{ji}^{ll}$ . Therefore, we are able to rewrite  $\tilde{V}_n \text{Diag} \{ \lambda_1 E_1, \dots, \lambda_L E_L \} \tilde{V}_n$  into the following form,

$$\begin{aligned} & \text{Diag} \{ \lambda_1 E_1, \dots, \lambda_L E_L \} \\ &= \text{Diag} \left\{ \lambda_l \left( \hat{\chi}_l I_n + \frac{1}{n} \Delta_l \right); l \in [L] \right\} \\ &= \text{Diag} (\lambda \odot \hat{\chi}) \otimes I_n + \frac{1}{n} \text{Diag} \{ \lambda_1 \Delta_1, \dots, \lambda_L \Delta_L \}. \end{aligned}$$

From definition (5.1), we find that

$$\tilde{V}_n G \tilde{V}_n = [\tilde{V}_n^{-1} \tilde{H}_1 \tilde{V}_n^{-1} - \Lambda \otimes I_n + (V^{-1} \Gamma V^{-1}) \otimes I_n - z (B^{-1} \otimes I_n)]^{-1}.$$

It further induces that

$$I_{nL} = \tilde{V}_n G \tilde{H}_1 \tilde{V}_n^{-1} - \tilde{V}_n G \tilde{V}_n [\Lambda \otimes I_n] + \tilde{V}_n G \tilde{V}_n [V^{-1} \Gamma V^{-1} \otimes I_n] - z \tilde{V}_n G \tilde{V}_n (B^{-1} \otimes I_n).$$

Taking expectation and plugging in (5.6), it follows that

$$I_{nL} = \mathbb{E} \left\{ \tilde{V}_n G \tilde{V}_n \cdot \left[ -\text{Diag} (\lambda \odot \hat{\chi}) \otimes I_n - (\Lambda - V^{-1} \Gamma V^{-1}) \otimes I_n - z B^{-1} \otimes I_n \right] \right\} - \tilde{\Delta},$$

where  $\tilde{\Delta}$  satisfies the following

$$\tilde{\Delta} = \frac{1}{n} \mathbb{E} \left[ \tilde{V}_n G \tilde{V}_n \cdot \text{Diag} \{ \lambda_1 \Delta_1, \dots, \lambda_L \Delta_L \} \right].$$

Subsequently, let  $\mathcal{T}_{G,n} := \frac{1}{n} \text{Tr} \left[ \tilde{V}_n G \tilde{V}_n \right] \in \text{Sym}_L(\mathbb{C})$ . Applying the partial trace (5.2) and noting that  $\text{Tr}(A(A_1 \otimes I_n)) = \text{Tr}(A)A_1$ , we conclude that

$$I_L = \mathbb{E} \left\{ \mathcal{T}_{G,n} \cdot \left[ -\text{Diag}(\lambda \odot \text{diag}(\mathcal{T}_{G,n})) - (\Lambda - V^{-1} \Gamma V^{-1}) - zB^{-1} \right] \right\} - \frac{1}{n} \text{Tr} \left[ \tilde{\Delta} \right].$$

For simplicity, let

$$F(\mathcal{T}) = I_L - \mathcal{T} \cdot \left[ -\text{Diag}(\lambda \odot \text{diag}(\mathcal{T})) - (\Lambda - V^{-1} \Gamma V^{-1}) - zB^{-1} \right]$$

be a functional in  $\mathcal{T} \in \text{Sym}_L(\mathbb{C})$ . Then the previous equation yields that

$$\|\mathbb{E}F(\mathcal{T}_{G,n})\| = \frac{1}{n} \left\| \text{Tr} \left[ \tilde{\Delta} \right] \right\| \leq \frac{C}{n(\Im z)^2}. \quad (5.7)$$

Since  $\|\mathcal{T}_{G,n}\| \leq C(B, \lambda)/\Im z$  is almost surely bounded,

$$\|\nabla F(c\mathcal{T}_{G,n} + (1-c)\mathbb{E}\mathcal{T}_{G,n})\| \leq C(B, \lambda)/\Im z, \quad \forall c \in [0, 1].$$

Since  $\mathcal{T}_{G,n} = V \left( \frac{1}{n} \text{Tr} [G] \right) V$  and  $V$  is fixed, the concentration estimate (5.3) gives

$$\begin{aligned} \|\mathbb{E}F(\mathcal{T}_{G,n}) - F(\mathbb{E}\mathcal{T}_{G,n})\| &\leq C/\Im z \cdot \mathbb{E} \|\mathcal{T}_{G,n} - \mathbb{E}\mathcal{T}_{G,n}\| \\ &\leq C/\Im z \int_0^\infty \mathbb{P}(\|\mathcal{T}_{G,n} - \mathbb{E}\mathcal{T}_{G,n}\| \geq \delta) \, d\delta \\ &\leq \frac{C}{\Im z} \int_0^\infty \exp\left(-C(\Im z)^4 n^2 \delta^2\right) \, d\delta = \frac{C}{n(\Im z)^3}. \end{aligned}$$

In combination with (5.7), we end up with

$$\|F(\mathbb{E}\mathcal{T}_{G,n})\| \leq \frac{C}{n(\Im z)^3}.$$

Proposition 4.7 is stated for the left-handed quadratic form in (4.4). Since  $\mathbb{E}\mathcal{T}_{G,n}$  and the bracket in  $F(\mathbb{E}\mathcal{T}_{G,n})$  are complex symmetric, transposing the preceding display gives the same bound for the left-handed form. Applying Proposition 4.7 with  $\tilde{M} = -\mathbb{E}\mathcal{T}_{G,n}$  therefore implies that

$$\|\mathbb{E}\mathcal{T}_{G,n} + M(z; \Gamma)\| \leq \frac{C}{n(\Im z)^3}.$$

Since  $\mathcal{T}_{G,n} = V \left( \frac{1}{n} \text{Tr} [G] \right) V$ , this is equivalent to the same estimate for  $\mathbb{E} \left\{ \frac{1}{n} \text{Tr} [G] \right\} + V^{-1} M(z; \Gamma) V^{-1}$ . Lastly, the concentration inequality (5.3) gives the asserted stochastic domination estimate.  $\square$

### 5.3 Stieltjes transforms and tested deterministic equivalents

We now record two consequences of the partial-trace estimate. First, taking the trace gives convergence of the empirical spectral distribution of the noise matrix. Second, a slightly more detailed version of the same Stein expansion gives the deterministic equivalent in Proposition 5.3. We begin with the Stieltjes transforms

$$S_{\mathcal{L}_n}(z) := \frac{1}{nL} \operatorname{tr} \left[ (H_1 + \Gamma \otimes I_n - zI_{nL})^{-1} \right],$$

$$S_{\mu_\Gamma}(z) := \int_{\mathbb{R}} \frac{\mu_\Gamma(d\sigma)}{\sigma - z}.$$

Here  $\mu_\Gamma$  is the limiting distribution from Definition 4.3.

**Lemma 5.4.** *The empirical distribution  $\mathcal{L}_n := \frac{1}{nL} \sum_{j=1}^{nL} \delta_{\sigma_j(H_1 + \Gamma \otimes I_n)}$  converges weakly in probability to  $\mu_\Gamma$  in Definition 4.3.*

*Proof.* By Proposition 5.2, for every fixed  $z \in \mathbb{C}^+$ ,

$$S_{\mathcal{L}_n}(z) = \frac{1}{L} \operatorname{tr} \left[ \frac{1}{n} \operatorname{Tr} [G(z; \Gamma)] \right] = -\frac{1}{L} \operatorname{tr} [B^{-1}M(z; \Gamma)] + r_n(z), \quad r_n(z) \rightarrow 0 \quad \text{in probability.}$$

By the Stieltjes representation (4.1) and the definition of  $\mu_\Gamma$  in (4.2), the deterministic term equals  $S_{\mu_\Gamma}(z)$ . Hence  $S_{\mathcal{L}_n}(z)$  converges in probability to  $S_{\mu_\Gamma}(z)$  for every fixed  $z \in \mathbb{C}^+$ . The Stieltjes continuity theorem [AGZ10, Theorem 2.4.4] implies that  $\mathcal{L}_n$  converges weakly in probability to  $\mu_\Gamma$ .  $\square$

While the previous quantitative deterministic equivalent results can imply a global law on the spectrum of  $H_1 + \Gamma \otimes I_n$  via Lemma 5.4, it actually requires a slightly faster rate to guarantee the behavior of individual eigenvalues. For convenience, we use the main results of [AEKN19] to directly deduce the next lemma.

**Lemma 5.5** (No eigenvalues outside the limiting support). *For a compact set  $S \subset \mathbb{R}$ , write*

$$S^{(\delta)} := \{x \in \mathbb{R} : \operatorname{dist}(x, S) \leq \delta\}$$

*for its closed  $\delta$ -neighborhood. For any  $\delta, D > 0$ , we have*

$$\mathbb{P} \left[ \operatorname{spec}(H_1 + \Gamma \otimes I_n) \subseteq \operatorname{supp}(\mu_\Gamma)^{(\delta)} \right] \geq 1 - n^{-D}$$

*for all sufficiently large  $n$ .*

*Proof.* It can be verified that our model is also included in the general class of random matrices studied by Section 4 of [AEKN19], namely the definition in their equation (4.2). Directly through their Theorem 4.7, there exists a  $\delta_0 > 0$  such that for each  $D > 0$ , there exists a constant  $C_D > 0$  such that

$$\mathbb{P} \left[ \operatorname{spec}(H_1 + \Gamma \otimes I_n) \subseteq \left\{ \tau \in \mathbb{R} : \operatorname{dist}(\tau, \operatorname{supp}(\mu_\Gamma)) \leq N^{-\delta_0} \right\} \right] \geq 1 - \frac{C_D}{N^D}.$$

This result can yield the conclusion of this lemma.  $\square$

*Proof of Proposition 5.3.* Write  $G = G(z; \Gamma)$ ,  $\tilde{V}_n = V \otimes I_n$ , and

$$\mathcal{T}_{G,n} := \frac{1}{n} \text{Tr} \left[ \tilde{V}_n G \tilde{V}_n \right].$$

In the proof of Proposition 5.2, Stein's identity gave the full matrix relation

$$I_{nL} = \mathbb{E} \left\{ \tilde{V}_n G \tilde{V}_n \cdot \left[ -\text{Diag}(\lambda \odot \hat{\chi}) \otimes I_n - (\Lambda - V^{-1} \Gamma V^{-1}) \otimes I_n - z B^{-1} \otimes I_n \right] \right\} - \tilde{\Delta},$$

where

$$\begin{aligned} \tilde{\Delta} &= \frac{1}{n} \mathbb{E} \left[ \tilde{V}_n G \tilde{V}_n \cdot \text{Diag} \{ \lambda_1 \Delta_1, \dots, \lambda_L \Delta_L \} \right], \\ (\Delta_l)_{ij} &= (\tilde{V}_n G \tilde{V}_n)_{ji}^{ll}, \quad l \in [L], \\ \hat{\chi}_l &= \frac{1}{n} \sum_{i=1}^n (\tilde{V}_n G \tilde{V}_n)_{ii}^{ll}, \quad \forall l \in [L]. \end{aligned}$$

Since  $\|\tilde{V}_n G \tilde{V}_n\| \leq C(B)/\Im z$  and  $L$  is fixed,

$$\|\tilde{\Delta}\|_F \leq \frac{C(B, \lambda)}{\sqrt{n} (\Im z)^2}.$$

Proposition 5.2 implies  $\hat{\chi} + \text{diag} [M(z; \Gamma)] = \mathcal{O}_<(1/(n(\Im z)^3))$ ; integrating this stochastic domination, using the deterministic bound  $\|\mathcal{T}_{G,n}\| \leq C(B)/\Im z$ , gives the corresponding expectation estimate. Therefore,

$$\begin{aligned} &\left\| I_{nL} - \mathbb{E} \left( \tilde{V}_n G \tilde{V}_n \right) \cdot \left[ \text{Diag}(\lambda \odot \text{diag}(M(z; \Gamma))) \otimes I_n - (\Lambda - V^{-1} \Gamma V^{-1}) \otimes I_n - z B^{-1} \otimes I_n \right] \right\|_F \\ &\leq \frac{C(B, \lambda)}{\Im z} \mathbb{E} \|(\hat{\chi} + \text{diag} [M(z; \Gamma)]) \otimes I_n\|_F + \|\tilde{\Delta}\|_F \leq \frac{C(B, \lambda)}{\sqrt{n} (\Im z)^4}. \end{aligned}$$

Then we right multiply the matrix inside the norm bracket with a deterministic matrix

$$\left[ \text{Diag}(\lambda \odot \text{diag}(M(z; \Gamma))) - (\Lambda - V^{-1} \Gamma V^{-1}) - z B^{-1} \right]^{-1} \otimes I_n$$

which is equal to  $-M(z; \Gamma) \otimes I_n$  by **(mat)**. We obtain

$$\|\mathbb{E}G(z; \Gamma) - \mathcal{G}(z; \Gamma)\|_F \leq \frac{C(B, \lambda)}{\sqrt{n} (\Im z)^4}.$$

Thus

$$\text{tr} [A (\mathbb{E}G(z; \Gamma) - \mathcal{G}(z; \Gamma))] = \mathcal{O} \left( \frac{\|A\|_F}{\sqrt{n} (\Im z)^4} \right).$$

Finally, the same Gaussian concentration argument used in Appendix D, now with the Lipschitz constant measured in the Frobenius norm of  $A$ , gives

$$\text{tr} [A (G(z; \Gamma) - \mathbb{E}G(z; \Gamma))] = \mathcal{O}_< \left( \frac{\|A\|_F}{\sqrt{n} (\Im z)^2} \right).$$

Combining the last two displays proves the claim, after enlarging the constant in the weaker denominator  $(\Im z)^4$ .  $\square$

## 5.4 Proof of Theorem 2.6

Recall from (2.3) that  $H = H_0 + H_1$ , and that  $\text{rank}(H_0) \leq L$ . A standard rank inequality for Hermitian matrices gives

$$\sup_{x \in \mathbb{R}} |F_H(x) - F_{H_1}(x)| \leq \frac{\text{rank}(H - H_1)}{nL} \leq \frac{1}{n},$$

where  $F_A(x)$  denotes the empirical distribution function of the eigenvalues of  $A$ . By Lemma 5.4 with  $\Gamma = 0$ , the empirical spectral distribution of  $H_1$  converges weakly in probability to  $\mu$ . The preceding display transfers this convergence from  $H_1$  to  $H$ , proving the bulk convergence claimed in Theorem 2.6.

It remains to justify the statement that at most  $L$  eigenvalues can lie to the right of the limiting bulk. More precisely, fix  $\delta, D > 0$  and let  $\sigma_+ = \text{supp}(\mu)$ . By Lemma 5.5 with  $\Gamma = 0$ , with probability at least  $1 - n^{-D}$  for all sufficiently large  $n$ , the noise matrix  $H_1$  has no eigenvalues in  $(\sigma_+ + \delta, \infty)$ . On this event, the rank inequality for eigenvalue counting functions gives

$$\#\{j : \sigma_j(H) > \sigma_+ + \delta\} \leq \#\{j : \sigma_j(H_1) > \sigma_+ + \delta\} + \text{rank}(H - H_1) \leq L.$$

Hence, outside any fixed neighborhood of the right edge of the limiting support,  $H$  has at most  $L$  eigenvalues on the right. This proves the finite-rank nature of the possible right outliers claimed in Theorem 2.6.

## 6 Outlier eigenvalues and eigenvector overlaps

This section proves Propositions 3.3, 3.4, and 3.5 from the proof outline. We first reduce the outlier eigenvalues to the zeros of an  $L \times L$  deterministic matrix, then identify the corresponding one-dimensional spectral projections, and finally convert these projection formulas into the matrix overlaps needed for signal recovery.

We use the notation introduced in Section 3:  $H = H_0 + H_1$  with  $H_0 = UU^\top$ , the noise resolvent  $G(z)$  from (3.1), the finite-dimensional matrices  $\mathcal{Q}_n(z)$  and  $\mathcal{Q}(z)$  from (3.2), and the deterministic outlier set  $\Psi_0$  from Proposition 3.3. Throughout this section,  $M(z)$  denotes the  $\Gamma = 0$  solution of the matrix Dyson equation (mat).

Following the convention introduced in Lemma 5.5, for a closed set  $S \subset \mathbb{R}$  and  $\delta > 0$  we write

$$S^{(\delta)} := \{x \in \mathbb{R} : \text{dist}(x, S) \leq \delta\}$$

for its closed  $\delta$ -neighborhood. Fix  $\epsilon > 0$  small enough that every point of  $\Psi_0$  lies outside  $\text{supp}(\mu)^{(2\epsilon)}$ ; if  $\Psi_0 = \emptyset$ , choose any sufficiently small  $\epsilon$ . We will also use the real-line extension of the stability domain,

$$\bar{\mathcal{U}}(\epsilon) = \{z \in \mathbb{C} : \text{dist}(z, \text{supp}(\mu)) \geq \epsilon, |z| \leq \epsilon^{-1}\},$$

whose intersection with  $\mathbb{C}^+$  is the domain  $\mathcal{U}(\epsilon)$  from (4.3). The proofs below are carried out on the event

$$\mathcal{E} = \left\{ \text{spec}(H_1) \subseteq \text{supp}(\mu)^{(\epsilon/2)} \right\}.$$

Here  $\text{supp}(\mu)^{(\epsilon/2)}$  denotes the closed  $\epsilon/2$ -neighborhood of  $\text{supp}(\mu)$ , in the notation introduced in Lemma 5.5. By Lemma 5.5, for every  $D > 0$  we have  $\mathbb{P}(\mathcal{E}) > 1 - n^{-D}$  for all sufficiently large  $n$ . Thus estimates proved with stochastic domination on  $\mathcal{E}$  imply the unconditional estimates stated in Section 3.

## 6.1 The outlier equation

This subsection proves Proposition 3.3. The main point is to compare the finite-dimensional random matrix  $\mathcal{Q}_n(z)$  with its deterministic limit  $\mathcal{Q}(z)$ , and then to count the zeros of their determinants outside the bulk.

**Lemma 6.1.** *Uniformly over  $z \in \bar{U}(\epsilon) \cap \mathbb{R}^c$ , we have  $\|\mathcal{Q}_n(z) - \mathcal{Q}(z)\| = \mathcal{O}_< \left(1 / \left(\sqrt{n} |\Im z|^4\right)\right)$ .*

*Proof.* Conditional on the spikes, the entries of  $U^\top G(z)U$  are tested resolvent entries of the form  $\text{tr}[AG(z)]$ , with  $\|A\|_F = \mathcal{O}_<(1)$  by Assumption A2. Using Proposition 5.3 and symmetry across the real line, we conclude that uniformly over  $z \in \bar{U}(\epsilon) \cap \mathbb{R}^c$ ,

$$\|\mathcal{Q}_n(z) - (I_L + U^\top \mathcal{G}(z)U)\| = \mathcal{O}_< \left( \frac{1}{\sqrt{n} |\Im z|^4} \right).$$

Exploiting the tensor-product structures in both  $\mathcal{G}(z)$  and  $U$ ,

$$\begin{aligned} & U^\top \mathcal{G}(z)U \\ &= -\frac{1}{n} \text{diag} \left\{ \sqrt{\lambda_1} X^{(1)\top}, \dots, \sqrt{\lambda_L} X^{(L)\top} \right\} \{ [M(z)] \otimes I_n \} \text{diag} \left\{ \sqrt{\lambda_1} X^{(1)}, \dots, \sqrt{\lambda_L} X^{(L)} \right\} \\ &= -\left\{ \frac{1}{n} \left[ \sqrt{\lambda_1} X^{(1)}, \dots, \sqrt{\lambda_L} X^{(L)} \right]^\top \left[ \sqrt{\lambda_1} X^{(1)}, \dots, \sqrt{\lambda_L} X^{(L)} \right] \right\} \odot [M(z)]. \end{aligned}$$

Since  $M(z)$  is uniformly bounded on  $\bar{U}(\epsilon)$ , Assumption A2 gives

$$\left\| U^\top \mathcal{G}(z)U + \sqrt{\Lambda} [B \odot M(z)] \sqrt{\Lambda} \right\| = \mathcal{O}_< (1/\sqrt{n}).$$

Therefore, we can conclude our lemma.  $\square$

**Lemma 6.2.** *On the event  $\mathcal{E}$ , every eigenvalue  $\sigma_n \in \mathbb{R} \setminus \text{supp}(\mu)^{(\epsilon)}$  of  $H$  satisfies  $\det \mathcal{Q}_n(\sigma_n) = 0$ . Moreover, for all sufficiently large  $n$ , these eigenvalues are in one-to-one correspondence with the elements of  $\Psi_0$ , counted with multiplicity.*

*Proof.* On  $\mathcal{E}$ , every  $\sigma \in \mathbb{R} \setminus \text{supp}(\mu)^{(\epsilon)}$  is separated from  $\text{spec}(H_1)$ , so  $(H_1 - \sigma I_{nL})^{-1}$  is well defined. Using  $H_0 = UU^\top$  and Sylvester's identity,

$$\begin{aligned} 0 &= \det(H_0 + H_1 - \sigma I_{nL}) \\ &= \det(H_1 - \sigma I_{nL}) \cdot \det\left(I_{nL} + (H_1 - \sigma I_{nL})^{-1} H_0\right) \\ &= \det(H_1 - \sigma I_{nL}) \cdot \det\left(I_L + U^\top (H_1 - \sigma I_{nL})^{-1} U\right) = \det(H_1 - \sigma I_{nL}) \cdot \det \mathcal{Q}_n(\sigma). \end{aligned}$$

Since  $\det(H_1 - \sigma I_{nL}) \neq 0$ , we conclude that under event  $\mathcal{E}$ , every outlier eigenvalue  $\sigma_n \in \mathbb{R} \setminus \text{supp}(\mu)^{(\epsilon)}$  of  $H$  must satisfy  $\det \mathcal{Q}_n(\sigma_n) = 0$ .

Recall that under  $\mathcal{E}$ , both  $\mathcal{Q}_n(z)$  and  $\mathcal{Q}(z)$  are holomorphic on  $\bar{U}(\epsilon)$ . We now count their zeros by the argument principle. Consider any fixed interval  $[c, d] \subset \bar{U}(\epsilon) \cap \mathbb{R}$ , with both endpoints  $c, d$  not zeros of  $\det \mathcal{Q}(z)$ . To simplify the notation, first suppose that every zero of  $\det \mathcal{Q}(z)$  in the interval is simple; multiple zeros are handled by the same argument with multiplicities. Let  $\gamma \subset \bar{U}(\epsilon)$  be the boundary of a rectangle with vertical sides through  $c$  and  $d$  and with fixed height. For some  $\iota > 0$  to be chosen later, we split the contour  $\gamma = \gamma_1 \cup \gamma_2$  by

$$\gamma_1 := \{z \in \gamma : |\Im z| \leq n^{-\iota}\}, \quad \gamma_2 := \gamma \setminus \gamma_1.$$

We further choose the rectangle so that

$$|\gamma_1| \leq 10n^{-\iota}, \quad |\gamma_2| \leq 10|c-d|.$$

The number of zeros inside  $[c, d]$  is represented by

$$\begin{aligned} \text{Card}_{[c,d],n} &= \frac{1}{2\pi i} \oint_{\gamma} \frac{\partial_z \det \mathcal{Q}_n(z)}{\det \mathcal{Q}_n(z)} dz = \frac{1}{2\pi i} \oint_{\gamma} \text{tr} [\mathcal{Q}'_n(z) \mathcal{Q}_n(z)^{-1}] dz, \\ \text{Card}_{[c,d]} &= \frac{1}{2\pi i} \oint_{\gamma} \frac{\partial_z \det \mathcal{Q}(z)}{\det \mathcal{Q}(z)} dz = \frac{1}{2\pi i} \oint_{\gamma} \text{tr} [\mathcal{Q}'(z) \mathcal{Q}(z)^{-1}] dz. \end{aligned}$$

On  $z \in \gamma_1$ , since  $[c, d] \subset \bar{U}(\epsilon)$  is bounded away from  $\text{supp}(\mu)$ , the function  $\text{tr} [\mathcal{Q}'(z) \mathcal{Q}(z)^{-1}]$  is uniformly bounded. Under  $\mathcal{E}$ , the random quantity  $\text{tr} [\mathcal{Q}'_n(z) \mathcal{Q}_n(z)^{-1}]$  is also uniformly bounded. Since  $|\gamma_1|$  is small, the integral over this part is negligible.

On  $z \in \gamma_2$ , Lemma 6.1 gives  $\|\mathcal{Q}_n(z) - \mathcal{Q}(z)\| = \mathcal{O}_{<}(n^{4\iota-1/2})$  since  $|\Im z| \geq n^{-\iota}$ . This estimate is uniform in a small neighborhood of  $\gamma_2$ , so  $\|\mathcal{Q}'_n(z) - \mathcal{Q}'(z)\| = \mathcal{O}_{<}(n^{4\iota-1/2})$  as well. Since  $\gamma$  is fixed with endpoints  $c, d$  away from the zeros of  $\mathcal{Q}(z)$ , we have  $\min_{z \in \gamma_2} \sigma_{\min}(\mathcal{Q}(z)) \geq \kappa > 0$ . This guarantees that  $\|\mathcal{Q}_n(z)^{-1} - \mathcal{Q}(z)^{-1}\| = \mathcal{O}_{<}(n^{4\iota-1/2})$ , and hence uniformly over  $z \in \gamma_2$ ,

$$|\text{tr} [\mathcal{Q}'_n(z) \mathcal{Q}_n(z)^{-1}] - \text{tr} [\mathcal{Q}'(z) \mathcal{Q}(z)^{-1}]| = \mathcal{O}_{<}(n^{4\iota-1/2}).$$

Since  $|\gamma|$  stays bounded in  $n$ , choosing  $\iota = 1/10$  gives

$$|\text{Card}_{[c,d],n} - \text{Card}_{[c,d]}| = \mathcal{O}_{<}(n^{-\iota} + n^{4\iota-1/2}) = \mathcal{O}_{<}(n^{-1/10}).$$

Since the two quantities are integers, they must be equal for all sufficiently large  $n$ . The same contour argument applied around each connected component containing zeros of  $\det \mathcal{Q}$  gives the correspondence with multiplicities.  $\square$

We now prove the quantitative part of Proposition 3.3. The one-to-one correspondence follows from Lemma 6.2.

*Proof of Proposition 3.3.* For any  $\sigma \in \Psi_0$  with multiplicity  $m := \deg(\sigma) \geq 1$ , the function  $\det \mathcal{Q}(z)$  is holomorphic and has a zero of order  $m$  at  $\sigma$ . Hence

$$|\det \mathcal{Q}(z)| \geq c|z - \sigma|^m$$

locally around  $z \approx \sigma$ . We pick a rectangular contour

$$\gamma_{\sigma,\eta} : \quad \Re z \in [\sigma - 2\eta, \sigma + 2\eta], \quad \Im z \in [-\eta, \eta].$$

If  $\eta = n^{-\frac{1}{2(m+4)} + \delta}$  for any fixed  $\delta > 0$ , then

$$\frac{\sup_{z \in \mathbb{R}^c \cap \gamma_{\sigma,\eta}} |\det \mathcal{Q}_n(z) - \det \mathcal{Q}(z)|}{\inf_{z \in \mathbb{R}^c \cap \gamma_{\sigma,\eta}} |\det \mathcal{Q}(z)|} = \mathcal{O}_{<} \left( \frac{1}{\sqrt{n}\eta^4} \cdot \frac{1}{\eta^m} \right)$$

is vanishing. By continuity this also controls the real endpoints of the rectangle. Once the ratio is smaller than one, Rouché's theorem implies that  $\det \mathcal{Q}_n$  has exactly  $m$  zeros inside  $\gamma_{\sigma,\eta}$ , counted with multiplicity. By Lemma 6.2, these zeros are precisely the corresponding outlier eigenvalues of  $H$ , and hence  $|\sigma_n - \sigma| = \mathcal{O}_{<} \left( n^{-\frac{1}{2m+8}} \right)$ .  $\square$

## 6.2 Spectral projection for a simple outlier

We now prove Proposition 3.4. Assume throughout this subsection that  $\sigma \in \Psi_0$  is a simple outlier, and let  $\sigma_n$  be the corresponding eigenvalue of  $H$ . Choose a positively oriented rectangular contour  $\gamma \subset \bar{U}(\epsilon)$  enclosing  $\sigma$  and no other point of  $\Psi_0$ . By Proposition 3.3, for all sufficiently large  $n$  the contour encloses  $\sigma_n$  and no other eigenvalue of  $H$  outside the bulk.

The spectral projection onto the eigenspace of  $\sigma_n$  is recovered by Cauchy's formula:

$$\xi_1^\top \nu_n \nu_n^\top \xi_2 = -\frac{1}{2\pi i} \oint_{\gamma} \xi_1^\top (H - zI_{nL})^{-1} \xi_2 dz.$$

Using the Woodbury formula and the definition of  $\mathcal{Q}_n(z)$ ,

$$\begin{aligned} \xi_1^\top (H - zI_{nL})^{-1} \xi_2 &= \xi_1^\top G(z) \xi_2 - \xi_1^\top G(z) U [I_L + U^\top G(z) U]^{-1} U^\top G(z) \xi_2 \\ &= \xi_1^\top G(z) \xi_2 - \xi_1^\top G(z) U \mathcal{Q}_n(z)^{-1} U^\top G(z) \xi_2. \end{aligned}$$

On  $\mathcal{E}$ , the spectrum of  $H_1$  lies inside  $\text{supp}(\mu)^{(\epsilon/2)}$ , while  $\gamma$  is separated from  $\text{supp}(\mu)$ . Thus  $\xi_1^\top G(z) \xi_2$  has no pole inside  $\gamma$ , and its contour integral vanishes. Hence

$$\xi_1^\top \nu_n \nu_n^\top \xi_2 = \frac{1}{2\pi i} \oint_{\gamma} \xi_1^\top G(z) U \mathcal{Q}_n(z)^{-1} U^\top G(z) \xi_2 dz.$$

We will compare this integral with the deterministic one

$$A(\xi_1, \xi_2, U) := \frac{1}{2\pi i} \oint_{\gamma} \xi_1^\top \mathcal{G}(z) U \mathcal{Q}(z)^{-1} U^\top \mathcal{G}(z) \xi_2 dz. \quad (6.1)$$

For  $j = 1, 2$ , set

$$\begin{aligned} a_{n,j}(z) &:= U^\top G(z) \xi_j \in \mathbb{C}^L, \\ a_j(z) &:= U^\top \mathcal{G}(z) \xi_j \in \mathbb{C}^L. \end{aligned}$$

Let the rectangle  $\gamma$  have vertical sides  $\Re z = \sigma \pm E$  and horizontal sides  $\Im z = \pm \eta$ , where  $E, \eta > 0$  are fixed small constants chosen so that the enclosed real interval contains no point of  $\Psi_0$  other than  $\sigma$  and remains separated from  $\text{supp}(\mu)$ . Split

$$\begin{aligned} \gamma_1 &= \{z \in \gamma : |\Re z - \sigma| = E, |\Im z| \leq n^{-\iota}\}, \\ \gamma_2 &= \{z \in \gamma : |\Re z - \sigma| = E, n^{-\iota} \leq |\Im z| \leq \eta\}, \\ \gamma_3 &= \{z \in \gamma : |\Re z - \sigma| \leq E, |\Im z| = \eta\}. \end{aligned}$$

On  $\gamma_1$ , the deterministic factors  $a_1(z), a_2(z), \mathcal{Q}(z)^{-1}$  are uniformly bounded. On  $\mathcal{E}$ , the corresponding random factors  $a_{n,1}(z), a_{n,2}(z), \mathcal{Q}_n(z)^{-1}$  are also uniformly bounded for all sufficiently large  $n$ , because the vertical sides are separated from both the bulk spectrum and the outlier location. Since  $|\gamma_1| = \mathcal{O}(n^{-\iota})$ , this part of the contour contributes  $\mathcal{O}_{<}(n^{-\iota})$ .

On  $\gamma_2 \cup \gamma_3$ , the imaginary part is at least  $n^{-\iota}$ . Conditional on the spikes, each entry of  $a_{n,j}(z)$  is a tested resolvent entry, so Proposition 5.3 gives

$$\|a_{n,j}(z) - a_j(z)\| = \mathcal{O}_{<}(n^{4\iota-1/2}), \quad j = 1, 2,$$

uniformly on  $\gamma_2 \cup \gamma_3$ . This part of the contour is separated from the zero  $\sigma$  of  $\det \mathcal{Q}$ , and hence  $\sigma_{\min}(\mathcal{Q}(z)) \geq \kappa > 0$  there. Together with Lemma 6.1, this implies

$$\|\mathcal{Q}_n(z)^{-1} - \mathcal{Q}(z)^{-1}\| = \mathcal{O}_{<}(n^{4\iota-1/2})$$

uniformly on  $\gamma_2 \cup \gamma_3$ . A telescoping estimate then yields

$$\begin{aligned} & |a_{n,1}(z)^\top \mathcal{Q}_n(z)^{-1} a_{n,2}(z) - a_1(z)^\top \mathcal{Q}(z)^{-1} a_2(z)| \\ & \leq 2 \max\{\|a_1\|, \|a_{n,1}\|, \|a_2\|, \|a_{n,2}\|\} \cdot \max\{\|\mathcal{Q}_n(z)^{-1}\|, \|\mathcal{Q}(z)^{-1}\|\} \cdot \max_{j=1,2} |a_{n,j}(z) - a_j(z)| \\ & \quad + \max\{\|a_1\|, \|a_{n,1}\|, \|a_2\|, \|a_{n,2}\|\}^2 \cdot \|\mathcal{Q}_n(z)^{-1} - \mathcal{Q}(z)^{-1}\| \\ & = \mathcal{O}_{<}(n^{4\iota-1/2}). \end{aligned}$$

Combining the three pieces of the contour and taking  $\iota = 1/10$  gives

$$|\xi_1^\top \nu_n \nu_n^\top \xi_2 - A(\xi_1, \xi_2, U)| = \mathcal{O}_{<}(n^{-1/10}).$$

It remains to evaluate the deterministic contour integral. Since  $\sigma$  is a simple zero of  $\det \mathcal{Q}(z)$  and  $w$  spans the null space of  $\mathcal{Q}(\sigma)$ ,

$$\mathcal{Q}(z)^{-1} = \frac{1}{z - \sigma} \cdot \frac{w w^\top}{w^\top \mathcal{Q}'(\sigma) w} + \text{holomorphic terms}$$

in a neighborhood of  $\sigma$ . Taking the residue in (6.1) yields

$$A(\xi_1, \xi_2, U) = \frac{(\xi_1^\top \mathcal{G}(\sigma) U w)(w^\top U^\top \mathcal{G}(\sigma) \xi_2)}{w^\top \mathcal{Q}'(\sigma) w}.$$

This is the estimate claimed in Proposition 3.4. Since  $\mathbb{P}(\mathcal{E}) > 1 - n^{-D}$  for every  $D > 0$ , the same bound holds in the stated unconditional stochastic-domination form.

### 6.3 Matrix overlaps and two-resolvent equivalents

We now convert the spectral projection estimate into the overlaps used for signal recovery. As in Section 3, split  $\nu_n \in \mathbb{R}^{nL}$  into its  $L$  view blocks by

$$\nu_n^{(l)} := (e_l^\top \otimes I_n) \nu_n \in \mathbb{R}^n, \quad \text{mat}(\nu_n) := \begin{bmatrix} \nu_n^{(1)} & \dots & \nu_n^{(L)} \end{bmatrix} \in \mathbb{R}^{n \times L}.$$

The next proposition gives the detailed matrix-overlap formulas. In particular, part (b) is the first assertion of Proposition 3.5, while part (c) supplies the explicit self-overlap formula referred to there.

**Proposition 6.3** (Detailed matrix-overlap formulas). *In the setup of Proposition 3.4, let*

$$s(\nu_n) = \text{sign}(w^\top U^\top \nu_n) \in \{\pm 1\} \tag{6.2}$$

fix the global sign of  $\nu_n$ . Then:

(a)

$$\left\| U^\top \nu_n - s(\nu_n) \frac{w}{\sqrt{w^\top \mathcal{Q}'(\sigma) w}} \right\| = \mathcal{O}_{<}(n^{-1/10});$$

(b)

$$\left\| \frac{1}{\sqrt{n}} \text{mat}(\nu_n)^\top X - \frac{s(\nu_n)}{\sqrt{w^\top \mathcal{Q}'(\sigma)w}} \left\{ V^{-1} M(\sigma) \text{Diag} \left( w \odot \sqrt{\lambda} \right) B \right\} \right\| = \mathcal{O}_{<}(n^{-1/10});$$

(c) Let  $\mathcal{P}_\sigma$  be the linear operator on  $\text{Sym}_L(\mathbb{R})$  defined by

$$\mathcal{P}_\sigma[A] := M(\sigma) \left\{ A + \text{Diag} \left( \lambda \odot \left[ [I_L - M(\sigma)^{\odot 2} \Lambda]^{-1} \text{diag} (M(\sigma) A M(\sigma)) \right] \right) \right\} M(\sigma). \quad (6.3)$$

Then for any  $l_1, l_2 \in [L]$ ,

$$\left| \langle \nu_n^{(l_1)}, \nu_n^{(l_2)} \rangle - \frac{1}{2w^\top \mathcal{Q}'(\sigma)w} w^\top \left\{ \left( \sqrt{\Lambda} B \sqrt{\Lambda} \right) \odot \left( \mathcal{P}_\sigma \left[ V^{-1} (e_{l_1} e_{l_2}^\top + e_{l_2} e_{l_1}^\top) V^{-1} \right] \right) \right\} w \right| = \mathcal{O}_{<}(n^{-1/20}).$$

*Proof of Proposition 6.3(a).* Repeating the contour argument in the proof of Proposition 3.4, now with the spike directions  $U$  inserted on both sides, gives the same deterministic integral with  $U^\top \mathcal{G}(z) U$  in place of the deterministic test-vector factors. From Lemma 6.1,

$$\|U^\top \mathcal{G}(z) U + I_L - \mathcal{Q}(z)\| = \mathcal{O}_{<}(1/\sqrt{n}).$$

Evaluating at  $z = \sigma$  and using  $\mathcal{Q}(\sigma)w = 0$ , we obtain

$$\left\| U^\top \nu_n \nu_n^\top U - \frac{w w^\top}{w^\top \mathcal{Q}'(\sigma)w} \right\| = \mathcal{O}_{<}(n^{-1/10}).$$

The right-hand side is a rank-one projection scaled by  $(w^\top \mathcal{Q}'(\sigma)w)^{-1}$ . With the sign convention (6.2), this matrix estimate implies the claimed vector estimate for  $U^\top \nu_n$ .  $\square$

*Proof of Proposition 6.3(b).* We again use the contour argument from the proof of Proposition 3.4, this time testing against the spike direction  $e_{l_1} \otimes (X^{(l_2)}/\sqrt{n})$ . The following deterministic vector then appears:

$$\begin{aligned} & U^\top \mathcal{G}(\sigma) \left[ e_{l_1} \otimes X^{(l_2)}/\sqrt{n} \right] \\ &= -\frac{1}{n} \text{diag} \left\{ \sqrt{\lambda_1} X^{(1)\top}, \dots, \sqrt{\lambda_L} X^{(L)\top} \right\} \left\{ [M(\sigma) V^{-1}] \otimes I_n \right\} \left[ e_{l_1} \otimes X^{(l_2)} \right] \\ &= -\sum_{s=1}^L \sqrt{\lambda_s} (e_s e_s^\top M(\sigma) V^{-1} e_{l_1}) \left[ \frac{1}{n} X^{(s)\top} X^{(l_2)} \right]. \end{aligned}$$

Since  $M(z)$  is uniformly bounded on  $\bar{U}(\epsilon)$ , Assumption A2 gives

$$\left\| U^\top \mathcal{G}(\sigma) \left[ e_{l_1} \otimes X^{(l_2)}/\sqrt{n} \right] + \sqrt{\lambda} \odot [M(\sigma) V^{-1} e_{l_1}] \odot [B e_{l_2}] \right\| = \mathcal{O}_{<}(1/\sqrt{n}).$$

Let  $\xi_{l_1, l_2} := e_{l_1} \otimes X^{(l_2)}/\sqrt{n}$ . The eigenvalue equation gives

$$\nu_n = -(H_1 - \sigma_n I_{nL})^{-1} U U^\top \nu_n.$$

Using Proposition 6.3(a), the deterministic equivalent for  $U^\top G(\sigma_n) \xi_{l_1, l_2}$ , and the preceding display together with  $|\sigma_n - \sigma| = \mathcal{O}_{<}(n^{-1/10})$ , we obtain

$$\nu_n^\top \xi_{l_1, l_2} = -\frac{s(\nu_n)}{\sqrt{w^\top \mathcal{Q}'(\sigma)w}} w^\top U^\top \mathcal{G}(\sigma) \xi_{l_1, l_2} + \mathcal{O}_{<}(n^{-1/10}).$$

Therefore,

$$\begin{aligned}
\langle \nu_n^{(l_1)}, X^{(l_2)}/\sqrt{n} \rangle &= \frac{s(\nu_n)}{\sqrt{w^\top \mathcal{Q}'(\sigma) w}} w^\top \left\{ \sqrt{\lambda} \odot [M(\sigma) V^{-1} e_{l_1}] \odot [B e_{l_2}] \right\} + \mathcal{O}_<(n^{-1/10}) \\
&= \frac{s(\nu_n)}{\sqrt{w^\top \mathcal{Q}'(\sigma) w}} \sum_{s=1}^L w_s \sqrt{\lambda_s} [M(\sigma) V^{-1}]_{sl_1} B_{sl_2} \\
&= \frac{s(\nu_n)}{\sqrt{w^\top \mathcal{Q}'(\sigma) w}} \left\{ V^{-1} M(\sigma) \text{Diag}(w \odot \sqrt{\lambda}) B \right\}_{l_1 l_2} + \mathcal{O}_<(n^{-1/10}).
\end{aligned}$$

This proves the claimed matrix formula for  $\text{mat}(\nu_n)^\top X/\sqrt{n}$ .  $\square$

**Lemma 6.4.** *For any  $T \in \text{Sym}_L(\mathbb{R})$  and  $|\sigma_n - \sigma| = \mathcal{O}_<(n^{-1/10})$ , we have*

$$\begin{aligned}
&\left\| U^\top (H_1 - \sigma_n I_{nL})^{-1} (T \otimes I_n) (H_1 - \sigma_n I_{nL})^{-1} U \right. \\
&\quad \left. - \left( \sqrt{\Lambda} B \sqrt{\Lambda} \right) \odot (\mathcal{P}_\sigma [V^{-1} T V^{-1}]) \right\| = \mathcal{O}_<(n^{-1/20}),
\end{aligned}$$

where  $\mathcal{P}_\sigma$  is defined in (6.3).

*Proof.* If we take  $\Gamma = \kappa T$  in the generalized resolvent (5.1) with some fixed  $T \in \text{Sym}_L(\mathbb{R})$  and  $\kappa$  in a sufficiently small fixed neighborhood of zero, then

$$\begin{aligned}
&U^\top (H_1 - \sigma_n I_{nL})^{-1} (T \otimes I_n) (H_1 - \sigma_n I_{nL})^{-1} U \\
&= -\frac{d}{d\kappa} \left\{ U^\top (H_1 + \kappa [T \otimes I_n] - \sigma_n I_{nL})^{-1} U \right\} \Big|_{\kappa=0}.
\end{aligned} \tag{6.4}$$

As in Lemma 6.1, the quadratic form  $U^\top (H_1 + \kappa [T \otimes I_n] - z I_{nL})^{-1} U$  satisfies the deterministic estimate

$$\left\| U^\top (H_1 + \kappa [T \otimes I_n] - z I_{nL})^{-1} U + \sqrt{\Lambda} [B \odot M_\kappa(z)] \sqrt{\Lambda} \right\| = \mathcal{O}_<(n^{-1/10}), \quad M_\kappa(z) := M(z; \kappa T),$$

uniformly for  $z$  in a fixed neighborhood of  $\sigma$  separated from the corresponding perturbed bulk support and for  $\kappa$  in the same neighborhood of zero. We apply this estimate at  $z = \sigma_n$ , using  $|\sigma_n - \sigma| = \mathcal{O}_<(n^{-1/10})$ . Here  $M_\kappa(z)$  solves the following equation

$$M_\kappa(z)^{-1} = z B^{-1} - \kappa V^{-1} T V^{-1} + \text{Diag}(\lambda) - \text{Diag}\{\lambda \odot \text{diag}(M_\kappa(z))\}.$$

Differentiating with respect to  $\kappa$  and restricting to  $\kappa = 0$ , we derive that

$$M(\sigma)^{-1} \left[ \frac{dM_\kappa(\sigma)}{d\kappa} \Big|_{\kappa=0} \right] M(\sigma)^{-1} = V^{-1} T V^{-1} + \text{Diag} \left\{ \lambda \odot \text{diag} \left[ \frac{dM_\kappa(\sigma)}{d\kappa} \Big|_{\kappa=0} \right] \right\},$$

which can be then transformed into

$$\begin{aligned}
\frac{dM_\kappa(\sigma)}{d\kappa} \Big|_{\kappa=0} &= M(\sigma) V^{-1} T V^{-1} M(\sigma) \\
&\quad + M(\sigma) \text{Diag} \left\{ \lambda \odot \text{diag} \left[ \frac{dM_\kappa(\sigma)}{d\kappa} \Big|_{\kappa=0} \right] \right\} M(\sigma).
\end{aligned}$$

Applying  $\text{diag}(\cdot)$  onto it, we have that

$$(I_L - M(\sigma)^{\odot 2} \Lambda) \text{diag} \left[ \frac{dM_\kappa(\sigma)}{d\kappa} \Big|_{\kappa=0} \right] = \text{diag} [M(\sigma) V^{-1} T V^{-1} M(\sigma)].$$

Therefore,

$$\frac{dM_\kappa(\sigma)}{d\kappa} \Big|_{\kappa=0} = \mathcal{P}_\sigma [V^{-1} T V^{-1}]. \quad (6.5)$$

To justify differentiating the deterministic equivalent, we use a difference quotient. Let

$$\begin{aligned} \mathcal{F}_n(\kappa) &:= U^\top (H_1 + \kappa [T \otimes I_n] - \sigma_n I_{nL})^{-1} U, \\ \mathcal{F}(\kappa) &:= -\sqrt{\Lambda} [B \odot M_\kappa(\sigma_n)] \sqrt{\Lambda}. \end{aligned}$$

Under the event  $\mathcal{E}$ , after shrinking the fixed neighborhood of zero if necessary, the resolvent  $(H_1 + \kappa [T \otimes I_n] - \sigma_n I_{nL})^{-1}$  stays uniformly bounded for all  $\kappa$  in that neighborhood. Hence, for  $\kappa_n = n^{-1/20}$ ,

$$\left\| \frac{d\mathcal{F}_n}{d\kappa}(0) - \frac{\mathcal{F}_n(\kappa_n) - \mathcal{F}_n(0)}{\kappa_n} \right\| \leq C |\kappa_n| = C n^{-1/20}.$$

The deterministic equivalent gives  $\|\mathcal{F}_n(\kappa) - \mathcal{F}(\kappa)\| = \mathcal{O}_<(n^{-1/10})$  for  $\kappa = 0, \kappa_n$ . Hence

$$\left\| \frac{\mathcal{F}_n(\kappa_n) - \mathcal{F}_n(0)}{\kappa_n} - \frac{\mathcal{F}(\kappa_n) - \mathcal{F}(0)}{\kappa_n} \right\| = \mathcal{O}_<(n^{-1/20}).$$

Moreover, since  $\mathcal{F}$  is continuously differentiable in this neighborhood of zero,

$$\left\| \frac{\mathcal{F}(\kappa_n) - \mathcal{F}(0)}{\kappa_n} - \frac{d\mathcal{F}}{d\kappa}(0) \right\| \leq C |\kappa_n| = C n^{-1/20}.$$

Therefore,

$$\left\| \frac{d\mathcal{F}_n}{d\kappa}(0) - \frac{d\mathcal{F}}{d\kappa}(0) \right\| = \mathcal{O}_<(n^{-1/20}).$$

From (6.5) and the continuity in the spectral parameter, we find that

$$\frac{d\mathcal{F}}{d\kappa}(0) = -\left(\sqrt{\Lambda} B \sqrt{\Lambda}\right) \odot (\mathcal{P}_\sigma [V^{-1} T V^{-1}]) + \mathcal{O}_<(n^{-1/10}).$$

Combining this identity with (6.4) gives the claim.  $\square$

*Proof of Proposition 6.3(c).* By definition,

$$H_1 \nu_n + U U^\top \nu_n = \sigma_n \nu_n,$$

which yields that

$$\nu_n = -(H_1 - \sigma_n I_{nL})^{-1} U U^\top \nu_n.$$

Then

$$\begin{aligned} \langle \nu_n^{(l_1)}, \nu_n^{(l_2)} \rangle &= \nu_n^\top (e_{l_1} \otimes I_n) (e_{l_2}^\top \otimes I_n) \nu_n \\ &= \nu_n^\top U U^\top (H_1 - \sigma_n I_{nL})^{-1} (e_{l_1} \otimes I_n) (e_{l_2}^\top \otimes I_n) (H_1 - \sigma_n I_{nL})^{-1} U U^\top \nu_n \\ &= \nu_n^\top U U^\top (H_1 - \sigma_n I_{nL})^{-1} (T \otimes I_n) (H_1 - \sigma_n I_{nL})^{-1} U U^\top \nu_n \end{aligned} \quad (6.6)$$

where  $T = \frac{1}{2}e_{l_1}e_{l_2}^\top + \frac{1}{2}e_{l_2}e_{l_1}^\top$ ; only the symmetric part contributes to the quadratic form. Lemma 6.4 gives

$$\left\| U^\top (H_1 - \sigma_n I_{nL})^{-1} (T \otimes I_n) (H_1 - \sigma_n I_{nL})^{-1} U - \left( \sqrt{\Lambda} B \sqrt{\Lambda} \right) \odot (\mathcal{P}_\sigma [V^{-1} T V^{-1}]) \right\| = \mathcal{O}_<(n^{-1/20}).$$

Moreover, Proposition 6.3(a) gives

$$\left\| U^\top \nu_n - s(\nu_n) \frac{w}{\sqrt{w^\top \mathcal{Q}'(\sigma) w}} \right\| = \mathcal{O}_<(n^{-1/10}).$$

Substituting these two estimates into (6.6) and telescoping the errors gives the claimed self-overlap formula. Together with Proposition 6.3(b), this proves Proposition 3.5.  $\square$

## 7 Variational analysis of the matrix Dyson equation at $z = 1$

Recall from Section 4 that, when the auxiliary perturbation  $\Gamma$  is set to zero, the matrix Dyson equation takes the form

$$M^{-1} = zB^{-1} + \Lambda - \text{Diag} \{ \lambda \odot \text{diag}(M) \}, \quad M \in \text{Sym}_L(\mathbb{C}), \quad (7.1)$$

where  $\Lambda = \text{Diag}(\lambda)$ . The solution for  $z \in \mathbb{C}^+$  is the deterministic object that controls the bulk law, but for the phase transition we need to understand its valid continuation to the special real point  $z = 1$ .

**Proposition 7.1.** *When  $\text{SNR}(\lambda, B) \neq 1$ , there exists some  $\epsilon > 0$  such that the valid solution  $M(z)$  to (7.1) can be continuously extended to  $(1 - \epsilon, +\infty)$  with  $M(\sigma) \in \text{Sym}_L(\mathbb{R})$  for any  $\sigma > 1 - \epsilon$ . Specifically, if  $\text{SNR}(\lambda, B) < 1$ , we have  $M(1) = B$ ; if  $\text{SNR}(\lambda, B) > 1$ , we have  $0 < M(1) < B$ .*

Together with Proposition 4.5, this shows that the interval  $(1 - \epsilon, +\infty)$  lies outside the limiting bulk spectrum. The proof of Proposition 7.1 has two steps. First, we rewrite the real MDE as the first-order condition for a finite-dimensional variational problem. Second, we analyze the local minimizers of this variational objective and show that the trivial minimizer changes stability exactly when  $\text{SNR}(\lambda, B)$  crosses one.

### 7.1 Variational formulation

The variational objective is

$$\mathcal{R}(\chi, \sigma) = \log \left\{ \det \left[ \sigma B^{-1} + \text{Diag}(\lambda \odot (\chi + 1)) \right] \right\} + \frac{1}{2} \sum_{l=1}^L \lambda_l \chi_l^2, \quad (7.2)$$

defined on

$$\mathcal{D} = \{ (\chi, \sigma) \in \mathbb{R}^L \times \mathbb{R} : \sigma B^{-1} + \text{Diag}(\lambda \odot (\chi + 1)) > 0 \}.$$

This objective is motivated by the replica-symmetric prediction for the Bayesian inference problem (1.1); see, for example, [MS24]. More concretely, (7.2) is the finite-dimensional replica-symmetric free energy for the Gaussian-prior version of the model, where  $\text{vec}(X^{(1)}, \dots, X^{(L)}) \sim \mathcal{N}(0, B)$ .

For  $(\chi, \sigma) \in \mathcal{D}$ , define

$$M_\chi(\sigma) := \left[ \sigma B^{-1} + \text{Diag} \{ \lambda \odot (\chi + 1) \} \right]^{-1}. \quad (7.3)$$

The point of this change of variables is that the stationarity condition for  $\mathcal{R}$  is equivalent to the MDE. Indeed,  $\nabla_\chi \mathcal{R}(\chi, \sigma) = 0$  gives  $\chi = -\text{diag}(M_\chi(\sigma))$ , and substituting this identity into (7.3) gives (7.1).

**Lemma 7.2.** *If  $\sigma > 0$ , the functional  $\chi \mapsto \mathcal{R}(\chi, \sigma)$  is analytic on  $[-1, +\infty)^L$ . Its first and second derivatives are*

$$\frac{\partial \mathcal{R}}{\partial \chi} = \lambda \odot \left[ \chi + \text{diag} \left\{ \left[ \sigma B^{-1} + \text{Diag}(\lambda \odot (\chi + 1)) \right]^{-1} \right\} \right], \quad (7.4)$$

$$\frac{\partial^2 \mathcal{R}}{(\partial \chi)^2} = \text{Diag}(\lambda) - \text{Diag}(\lambda) \left\{ \left[ \sigma B^{-1} + \text{Diag}(\lambda \odot (\chi + 1)) \right]^{-1} \right\}^{\odot 2} \text{Diag}(\lambda). \quad (7.5)$$

*Proof.* For any differentiable family of invertible matrices  $C(x)$ ,

$$\frac{d}{dx} \log \{ \det [C(x)] \} = \text{tr} \left[ C(x)^{-1} \frac{dC(x)}{dx} \right].$$

Applying this identity with  $C(\chi) = \sigma B^{-1} + \text{Diag}(\lambda \odot (\chi + 1))$  gives

$$\frac{\partial \mathcal{R}}{\partial \chi_l} = \text{tr} \{ C(\chi)^{-1} \lambda_l e_l e_l^\top \} + \lambda_l \chi_l = \lambda_l e_l^\top C(\chi)^{-1} e_l + \lambda_l \chi_l.$$

Differentiating once more gives

$$\begin{aligned} \frac{\partial^2 \mathcal{R}}{\partial \chi_l \partial \chi_k} &= -\lambda_l \lambda_k e_l^\top C(\chi)^{-1} e_k e_k^\top C(\chi)^{-1} e_l + \lambda_l \mathbf{1}_{l=k} \\ &= -\lambda_l \lambda_k \{ e_l^\top C(\chi)^{-1} e_k \}^2 + \lambda_l \mathbf{1}_{l=k}, \end{aligned}$$

which is exactly (7.5). □

The next lemma explains why strict local minimizers of  $\mathcal{R}$  produce the valid real branch of the MDE.

**Lemma 7.3.** *Suppose that for every  $\sigma \geq 1$  there exists  $\chi^*(\sigma) \in [-1, 0)^L$  such that*

$$\frac{\partial \mathcal{R}}{\partial \chi}(\chi^*(\sigma), \sigma) = 0, \quad \frac{\partial^2 \mathcal{R}}{(\partial \chi)^2}(\chi^*(\sigma), \sigma) > 0. \quad (7.6)$$

*Define*

$$M^o(\sigma) := \left[ \sigma B^{-1} + \text{Diag} \{ \lambda \odot (\chi^*(\sigma) + 1) \} \right]^{-1}. \quad (7.7)$$

*Then the solution  $M(z)$  of (7.1) on  $\mathbb{C}^+$  admits a real analytic continuation to a neighborhood of every point in  $[1, +\infty)$ , and this continuation agrees with  $M^o(\sigma)$  on  $[1, +\infty)$ . Consequently,  $M(z)$  extends to  $(1 - \epsilon, +\infty)$  for some  $\epsilon > 0$ , and  $M(\sigma) \in \text{Sym}_L(\mathbb{R})$  on this interval.*

*Proof.* The stationarity condition and Lemma 7.2 imply that

$$[M^o(\sigma)]^{-1} = \sigma B^{-1} + \Lambda - \text{Diag} \{ \lambda \odot \text{diag} [M^o(\sigma)] \}.$$

We next identify this real solution with the valid continuation from  $\mathbb{C}^+$ . Fix  $\sigma \in [1, +\infty)$ , and let

$$T(m, z) := -m^{-1} + zB^{-1} + \Lambda - \text{Diag} \{ \lambda \odot \text{diag}(m) \}.$$

Then  $T(M^o(\sigma), \sigma) = 0$ . The derivative with respect to the first argument is the linear operator

$$\nabla_R^{(1)} T(m, z) = m^{-1} R m^{-1} - \text{Diag} \{ \lambda \odot \text{diag}(R) \}, \quad R \in \text{Sym}_L(\mathbb{C}).$$

We claim that  $\nabla^{(1)} T(M^o(\sigma), \sigma)$  is invertible. Given  $\Delta \in \text{Sym}_L(\mathbb{C})$ , solving

$$\Delta = [M^o(\sigma)]^{-1} R [M^o(\sigma)]^{-1} - \text{Diag} \{ \lambda \odot \text{diag}(R) \}$$

reduces, after multiplying by  $M^o(\sigma)$  on both sides and taking diagonals, to

$$[I - (M^o(\sigma) \odot M^o(\sigma)) \Lambda] \text{diag}(R) = \text{diag} [M^o(\sigma) \Delta M^o(\sigma)].$$

By (7.5) and the strict Hessian condition in (7.6),

$$\Lambda - \Lambda (M^o(\sigma) \odot M^o(\sigma)) \Lambda > 0.$$

Equivalently, by conjugating with  $\Lambda^{-1/2}$ , the matrix  $\Lambda^{1/2} (M^o(\sigma) \odot M^o(\sigma)) \Lambda^{1/2}$  has spectral radius strictly smaller than one. Since this matrix is similar to  $(M^o(\sigma) \odot M^o(\sigma)) \Lambda$ , we have

$$\rho((M^o(\sigma) \odot M^o(\sigma)) \Lambda) < 1.$$

Hence  $I - (M^o(\sigma) \odot M^o(\sigma)) \Lambda$  is invertible, so the diagonal of  $R$  is uniquely determined. The whole matrix is then recovered from

$$R = M^o(\sigma) \{ \Delta + \text{Diag} \{ \lambda \odot \text{diag}(R) \} \} M^o(\sigma).$$

This inverse is positivity preserving. Indeed, if  $\Delta > 0$ , then  $\text{diag} [M^o(\sigma) \Delta M^o(\sigma)]$  has strictly positive entries. Moreover, the spectral-radius bound above gives the convergent Neumann series

$$[I - (M^o(\sigma) \odot M^o(\sigma)) \Lambda]^{-1} = \sum_{k \geq 0} [(M^o(\sigma) \odot M^o(\sigma)) \Lambda]^k,$$

whose coefficients are nonnegative.

Lemma 4.10 therefore gives an analytic solution  $M^o(z)$  to the MDE in a complex neighborhood of  $\sigma$ . Moreover,

$$\frac{dM^o}{dz}(\sigma) = - \left\{ \nabla^{(1)} T(M^o(\sigma), \sigma) \right\}^{-1} B^{-1} < 0,$$

where the negativity follows from the positivity-preserving form of the inverse displayed above. Thus, for  $\eta > 0$  sufficiently small,  $\Im M^o(\sigma + i\eta) < 0$ . By uniqueness of the MDE solution in Proposition 4.2, this local branch agrees with  $M(z)$  on its intersection with  $\mathbb{C}^+$ .

Since  $\sigma \geq 1$  was arbitrary, the solution from  $\mathbb{C}^+$  extends analytically to an open set containing  $[1, +\infty)$  and agrees there with  $M^o$  on the real line. Taking a small interval below 1 inside this open set and using Schwarz reflection across the real axis gives  $\Im M(\sigma) = 0$  for all  $\sigma \in (1 - \epsilon, 1)$ . This proves the claimed real continuation.  $\square$

## 7.2 Local minimizers of the variational objective

It remains to prove the existence of the strict local minimizers required in Lemma 7.3. The result we need is the following.

**Lemma 7.4.** *Assume that  $\text{SNR}(\lambda, B) \neq 1$ .*

- (i) For every  $\sigma > 1$ , the map  $\chi \mapsto \mathcal{R}(\chi, \sigma)$  has a global minimizer  $\chi^*(\sigma) \in (-1, 0)^L$  on  $[-1, +\infty)^L$  satisfying (7.6).
- (ii) If  $\text{SNR}(\lambda, B) < 1$ , then  $\chi^*(1) = -\mathbf{1}_L$  satisfies (7.6).
- (iii) If  $\text{SNR}(\lambda, B) > 1$ , then  $\chi \mapsto \mathcal{R}(\chi, 1)$  has a global minimizer  $\chi^*(1) \in (-1, 0)^L$  on  $[-1, +\infty)^L$  satisfying (7.6).

We prove the three cases separately, and then verify the strict Hessian condition for the interior minimizers.

**Lemma 7.5.** For any  $\sigma > 1$ , the map  $\chi \mapsto \mathcal{R}(\chi, \sigma)$  has a global minimizer in  $(-1, 0)^L$  over the domain  $[-1, +\infty)^L$ .

*Proof.* It suffices to minimize over  $[-1, 0]^L$  and check that the minimizer cannot lie on the boundary. If  $\chi_l \geq 0$  for some  $l \in [L]$ , then

$$\begin{aligned} \frac{\partial \mathcal{R}}{\partial \chi_l}(\chi, \sigma) &= \lambda_l e_l^\top [\sigma B^{-1} + \text{Diag}(\lambda \odot (\chi + 1))]^{-1} e_l + \lambda_l \chi_l \\ &> 0. \end{aligned}$$

If  $\chi_l = -1$  for some  $l \in [L]$ , then, using  $B_{ll} = 1$  from Assumption A4,

$$\frac{\partial \mathcal{R}}{\partial \chi_l}(\chi, \sigma) \leq \lambda_l e_l^\top B e_l / \sigma - \lambda_l < 0.$$

Therefore every boundary point can be improved by moving into  $(-1, 0)^L$ , and the global minimizer over the compact set  $[-1, 0]^L$  lies in  $(-1, 0)^L$ .  $\square$

**Lemma 7.6.** If

$$\text{SNR}(\lambda, B) = \sigma_{\max} \left( \text{Diag}(\sqrt{\lambda}) (B \odot B) \text{Diag}(\sqrt{\lambda}) \right) < 1, \quad (7.8)$$

then  $\chi^*(1) = -\mathbf{1}_L$  is a strict local minimizer of  $\mathcal{R}(\cdot, 1)$  and satisfies (7.6).

*Proof.* By (7.4), the identity  $\partial \mathcal{R} / \partial \chi(-\mathbf{1}_L, 1) = 0$  holds for all parameters. At this point,

$$\frac{\partial^2 \mathcal{R}}{(\partial \chi)^2}(-\mathbf{1}_L, 1) = \Lambda - \Lambda (B \odot B) \Lambda.$$

The condition (7.8) is equivalent to this Hessian being positive definite.  $\square$

When  $\text{SNR}(\lambda, B) > 1$ , the trivial stationary point  $-\mathbf{1}_L$  becomes unstable, and an interior minimizer appears.

**Lemma 7.7.** If

$$\text{SNR}(\lambda, B) = \sigma_{\max} \left( \text{Diag}(\sqrt{\lambda}) (B \odot B) \text{Diag}(\sqrt{\lambda}) \right) > 1, \quad (7.9)$$

then  $\mathcal{R}(\cdot, 1)$  has a global minimizer  $\chi^* \in (-1, 0)^L$  over  $[-1, +\infty)^L$ .

*Proof.* If  $\chi_l \geq 0$  for some  $l \in [L]$ , then

$$\frac{\partial \mathcal{R}}{\partial \chi_l}(\chi, 1) = \lambda_l e_l^\top [B^{-1} + \text{Diag}(\lambda \odot (\chi + 1))]^{-1} e_l + \lambda_l \chi_l > 0.$$

Hence the infimum over  $[-1, +\infty)^L$  is attained on the compact set  $[-1, 0]^L$ . Moreover, the same derivative check at  $\chi_l = 0$  shows that any global minimizer satisfies  $\chi_l^* < 0$  for every  $l$ .

We next rule out the boundary  $\chi_l^* = -1$ . Since (7.9) holds, Perron-Frobenius applied to the irreducible nonnegative matrix  $\text{Diag}(\sqrt{\lambda})(B \odot B)\text{Diag}(\sqrt{\lambda})$  gives a nonnegative direction along which the Hessian at  $-\mathbf{1}_L$  is negative. Thus  $-\mathbf{1}_L$  is not a local minimizer.

Let  $\mathcal{A} = \{l \in [L] : \chi_l^* = -1\}$  be the inactive set. Suppose that  $\mathcal{A}$  is nonempty and not all of  $[L]$ . Choose  $l \in \mathcal{A}$  and  $k \in \mathcal{A}^c$ . With  $D = \text{Diag}(\lambda \odot (\chi^* + 1))$ , we have  $D \geq \mu e_k e_k^\top$  for some  $\mu > 0$ . Since a one-sided derivative at the boundary must be nonnegative,

$$\begin{aligned} 0 &\leq \frac{\partial \mathcal{R}}{\partial \chi_l}(\chi^*, 1) = \lambda_l \left\{ (B^{-1} + D)^{-1} \right\}_{ll} - \lambda_l \\ &\leq \lambda_l \left\{ (B^{-1} + \mu e_k e_k^\top)^{-1} \right\}_{ll} - \lambda_l \\ &= \lambda_l \left\{ B - \frac{B e_k e_k^\top B}{1/\mu + B_{kk}} \right\}_{ll} - \lambda_l \\ &= -\frac{\lambda_l B_{kl}^2}{1/\mu + 1} \leq 0, \end{aligned}$$

where we again used  $B_{kk} = B_{ll} = 1$ . Therefore  $B_{kl} = 0$  for every  $l \in \mathcal{A}$  and  $k \in \mathcal{A}^c$ , contradicting the irreducibility of  $B$  in Assumption A4. Since  $\mathcal{A} = [L]$  has already been ruled out, we must have  $\mathcal{A} = \emptyset$ .  $\square$

**Lemma 7.8.** *Let  $\sigma \geq 1$  and let  $\chi_* \in (-1, 0)^L$  be a local minimizer of  $\mathcal{R}(\cdot, \sigma)$ . If*

$$\frac{\partial \mathcal{R}}{\partial \chi}(\chi_*, \sigma) = 0,$$

then

$$\frac{\partial^2 \mathcal{R}}{(\partial \chi)^2}(\chi_*, \sigma) > 0.$$

*Proof.* Since  $\chi_*$  is an interior local minimizer, the Hessian is positive semidefinite. Suppose, for contradiction, that it is singular. Let

$$M_* = [\sigma B^{-1} + \text{Diag}\{\lambda \odot (\chi_* + 1)\}]^{-1}.$$

Stationarity and Lemma 7.2 give

$$\sigma B^{-1} = M_*^{-1} - \Lambda + \text{Diag}\{\lambda \odot \text{diag}(M_*)\}, \quad (7.10)$$

$$0 = \sigma_{\min} [\Lambda - \Lambda(M_* \odot M_*)\Lambda]. \quad (7.11)$$

Since  $\sigma \geq 1$  and  $\chi_* \in (-1, 0)^L$ , we have  $M_* < B$ .

From (7.11), the matrix  $\Lambda^{1/2}(M_* \odot M_*)\Lambda^{1/2}$  has largest eigenvalue one. Equivalently, the non-negative matrix  $\Lambda(M_* \odot M_*)$  has Perron-Frobenius eigenvalue one. Choose a nonzero vector  $v \in \mathbb{R}_+^L$  such that

$$\Lambda(M_* \odot M_*)v = v,$$

and set  $W = \text{Diag}(v)$ . For the operators  $\mathcal{S}[R] = \text{Diag}\{\lambda \odot \text{diag}(R)\}$  and  $\mathcal{C}_{M_*}[R] = M_*RM_*$ , this choice gives

$$\mathcal{S}\mathcal{C}_{M_*}[W] = W.$$

Taking the inner product of (7.10) with  $M_*WM_*$  yields

$$\begin{aligned} \sigma \langle B^{-1}, M_*WM_* \rangle &= \langle W, M_* \rangle + \langle M_*WM_*, \mathcal{S}[M_* - B] \rangle \\ &= \langle W, M_* \rangle + \langle \mathcal{S}\mathcal{C}_{M_*}[W], M_* - B \rangle \\ &= \langle W, 2M_* - B \rangle. \end{aligned}$$

On the other hand,

$$\begin{aligned} \langle B^{-1}, M_*WM_* \rangle &= \langle W, M_*B^{-1}M_* \rangle, \\ B + M_*B^{-1}M_* - 2M_* &= \sqrt{M_*} \left[ M_*^{-1/2}BM_*^{-1/2} + M_*^{1/2}B^{-1}M_*^{1/2} - 2I_L \right] \sqrt{M_*} > 0, \end{aligned}$$

where the last inequality follows from  $M_* < B$ . Since  $W \geq 0$  and  $W \neq 0$ , this implies

$$\langle W, 2M_* - B \rangle < \langle B^{-1}, M_*WM_* \rangle.$$

Therefore

$$\sigma = \frac{\langle W, 2M_* - B \rangle}{\langle B^{-1}, M_*WM_* \rangle} < 1,$$

contradicting  $\sigma \geq 1$ . □

*Proof of Lemma 7.4.* For  $\sigma > 1$ , Lemma 7.5 gives an interior global minimizer, and Lemma 7.8 gives the strict Hessian condition. If  $\sigma = 1$  and  $\text{SNR}(\lambda, B) < 1$ , Lemma 7.6 gives the required minimizer directly. If  $\sigma = 1$  and  $\text{SNR}(\lambda, B) > 1$ , Lemma 7.7 gives an interior global minimizer, and Lemma 7.8 again gives the strict Hessian condition. □

### 7.3 Proof of Proposition 7.1

*Proof.* By Lemma 7.4, the hypotheses of Lemma 7.3 hold whenever  $\text{SNR}(\lambda, B) \neq 1$ . Thus the valid solution of (7.1) extends to  $(1 - \epsilon, +\infty)$  and is real on this interval.

It remains only to identify the value at  $\sigma = 1$ . If  $\text{SNR}(\lambda, B) < 1$ , Lemma 7.6 gives  $\chi^*(1) = -\mathbf{1}_L$ , and therefore (7.7) gives  $M(1) = B$ . If  $\text{SNR}(\lambda, B) > 1$ , Lemma 7.7 gives  $\chi^*(1) \in (-1, 0)^L$ . Hence

$$M(1) = [B^{-1} + \text{Diag}\{\lambda \odot (\chi^*(1) + 1)\}]^{-1},$$

where the diagonal perturbation is strictly positive definite. Consequently  $0 < M(1) < B$ . □

As a byproduct, Proposition 7.1 also implies that the local minimizers selected above are unique on the valid branch.

## 8 Emergence of outlier eigenvalues

This section proves the phase-transition statements in Theorems 2.7 and 2.9, as well as the outlier-counting statement in Proposition 2.8. The inputs have been established in the preceding sections. Section 6 reduces outlier eigenvalues to the finite-dimensional equation  $\det \mathcal{Q}(\sigma) = 0$  and gives the corresponding eigenvector-overlap formulas. Section 7 analyzes the valid solution of the matrix

Dyson equation at  $z = 1$  and shows that it changes behavior exactly when  $\text{SNR}(\lambda, B)$ , defined in (1.2), crosses one. We now combine these inputs.

Throughout this section, let

$$\sigma_+ := \sup \text{supp}(\mu)$$

be the right edge of the limiting bulk spectrum. Whenever it is used below,  $M_+$  denotes the one-sided limit of the valid real solution  $M(\sigma)$  as  $\sigma \downarrow \sigma_+$ ; the existence of this limit follows from the monotonicity argument in the proof of Proposition 2.8.

We first prove Proposition 2.8. This argument counts the deterministic roots of the outlier equation from Section 6, and then uses Proposition 3.3 to transfer the count to the random eigenvalues. The subcritical simplification is included in the same proof. Above the threshold, the special point  $\sigma = 1$  becomes a root of the outlier equation. We then identify the corresponding null vector and simplify the overlap formulas before stating the final local proposition used in Theorem 2.9.

### 8.1 Counting outliers to the right

*Proof of Proposition 2.8.* For any  $\sigma > \sigma_+$ , the self-consistent equation (mat) is solvable at  $z = \sigma, \Gamma = 0$ . In other words, there exists  $M : (\sigma_+, \infty) \rightarrow \text{Sym}_L^+(\mathbb{R})$  such that

$$M(\sigma)^{-1} = \sigma B^{-1} + \text{Diag}(\lambda) - \text{Diag}\{\lambda \odot \text{diag}(M(\sigma))\}, \quad (8.1)$$

and  $M(\sigma)$  is strictly decreasing in  $\sigma$ . The monotonicity and boundedness of  $M(\sigma)$  imply that the one-sided limit

$$M(\sigma_+) := \lim_{\sigma \downarrow \sigma_+} M(\sigma)$$

exists; we write it as  $M_+$ . We therefore extend  $\mathcal{Q}(\sigma) = I_L - \sqrt{\Lambda} [B \odot M(\sigma)] \sqrt{\Lambda}$  continuously to  $\sigma = \sigma_+$  by using this boundary value. Letting  $\sigma \rightarrow +\infty$  in (8.1), we also have

$$\lim_{\sigma \rightarrow +\infty} M(\sigma) = 0.$$

By Proposition 3.3, outlier eigenvalues outside the bulk are determined by

$$\mathcal{Q}(\sigma) = I_L - \sqrt{\Lambda} [B \odot M(\sigma)] \sqrt{\Lambda}.$$

Let  $f_1, \dots, f_L : [\sigma_+, \infty) \rightarrow \mathbb{R}$  be the eigenvalues of this continuous extension of  $\mathcal{Q}(\sigma)$ , counted continuously with multiplicity. Up to multiplicity, the number of real roots of  $\det \mathcal{Q}(\sigma) = 0$  on  $(\sigma_+, \infty)$  is

$$\begin{aligned} |\{\sigma > \sigma_+ : \det \mathcal{Q}(\sigma) = 0\}| &= \sum_{j \in [L]} |\{\sigma > \sigma_+ : f_j(\sigma) = 0\}| \\ &= \sum_{j \in [L]} \mathbf{1}\{f_j(\sigma_+) < 0\} = L_0. \end{aligned}$$

Indeed,  $\mathcal{Q}(\sigma)$  is strictly increasing in  $\sigma$ , and  $\lim_{\sigma \rightarrow \infty} \mathcal{Q}(\sigma) = I_L$ . Thus each eigenvalue branch can cross zero at most once, and it crosses precisely when its boundary value at  $\sigma_+$  is negative. Since there are only finitely many such roots, we may choose  $\epsilon_0 > 0$  so that the roots in  $(\sigma_+, \infty)$  all lie to the right of  $\sigma_+ + 2\epsilon_0$ . Proposition 3.3 then converts this deterministic root count into the asserted high-probability count of outlier eigenvalues.

When  $\text{SNR}(\lambda, B) < 1$ , Proposition 7.1 gives  $\sigma_+ < 1$  and  $M(1) = B$ . We claim that

$$\sqrt{\Lambda} [B \odot M(\sigma)] \sqrt{\Lambda} < I_L, \quad \sigma > \sigma_+. \quad (8.2)$$

To prove this, first note that for every  $\sigma > \sigma_+$  the matrix

$$I_L - (M(\sigma) \odot M(\sigma)) \Lambda$$

is invertible. Indeed, if it were singular, then for some nonzero vector  $d$  the matrix

$$A = M(\sigma) \text{Diag}(\lambda \odot d) M(\sigma)$$

would satisfy  $\text{diag}(A) = d$  and hence

$$A - M(\sigma) \text{Diag} \{ \lambda \odot \text{diag}(A) \} M(\sigma) = 0,$$

contradicting the invertibility of the stability operator away from  $\text{supp}(\mu)$  in Lemma 4.9, after taking the limit from  $\sigma + i\eta$  as  $\eta \downarrow 0$ . Since

$$\lambda_{\max} \left( \sqrt{\Lambda} [B \odot B] \sqrt{\Lambda} \right) = \text{SNR}(\lambda, B) < 1$$

at  $\sigma = 1$ , continuity in  $\sigma$  gives

$$\lambda_{\max} \left( \sqrt{\Lambda} [M(\sigma) \odot M(\sigma)] \sqrt{\Lambda} \right) < 1, \quad \sigma > \sigma_+. \quad (8.3)$$

We now compare the mixed Schur product with the two square Schur products. Let

$$A_B := \sqrt{\Lambda} [B \odot B] \sqrt{\Lambda}, \quad A_M := \sqrt{\Lambda} [M(\sigma) \odot M(\sigma)] \sqrt{\Lambda}.$$

Both are entrywise nonnegative. For nonnegative matrices  $A_B, A_M$ , the Collatz–Wielandt formula and Cauchy’s inequality imply

$$\rho \left( \left| \sqrt{\Lambda} [B \odot M(\sigma)] \sqrt{\Lambda} \right| \right) \leq \sqrt{\rho(A_B) \rho(A_M)}.$$

Since the spectral radius of a matrix is bounded by the spectral radius of its entrywise absolute value, combining this bound with  $\rho(A_B) = \text{SNR}(\lambda, B) < 1$  and (8.3) proves (8.2). Letting  $\sigma \downarrow \sigma_+$  gives

$$\lambda_{\max} \left( \sqrt{\Lambda} [B \odot M_+] \sqrt{\Lambda} \right) \leq \sqrt{\text{SNR}(\lambda, B)} < 1.$$

Thus no eigenvalue of  $\sqrt{\Lambda} (B \odot M_+) \sqrt{\Lambda}$  is larger than one, and  $L_0 = 0$ .

It remains to record the additional conclusion in the informative regime. If  $\text{SNR}(\lambda, B) > 1$ , Proposition 7.1 gives  $\sigma_+ < 1$ , while Lemma 8.1 below shows that  $\mathcal{Q}(1)$  has a nontrivial kernel. Thus 1 is a root of  $\det \mathcal{Q}(\sigma) = 0$  in  $(\sigma_+, \infty)$ , and the preceding root count implies  $L_0 \geq 1$ . The same high-probability count gives exactly  $L_0$  outliers above  $\sigma_+ + \epsilon$ , while the bulk law and the no-outside-spectrum estimate from Section 5 give the matching localization of the remaining eigenvalues at the right edge. Hence  $\sigma_{L_0+1}(H) \xrightarrow{\mathbb{P}} \sigma_+$ .  $\square$

## 8.2 Top outlier eigenvalue at 1

**Lemma 8.1.** *When  $\text{SNR}(\lambda, B) > 1$ , we always have  $\mathcal{Q}(1) = I_L - \sqrt{\Lambda} [B \odot M(1)] \sqrt{\Lambda} \geq 0$  and  $\mathcal{Q}(1)w = 0$  for*

$$w = \sqrt{\lambda} \odot (\mathbf{1}_L - \text{diag} [M(1)]) \in \mathbb{R}^L.$$

*Moreover, thanks to the irreducibility of  $B$  in Assumption A4, we also have  $\dim[\ker \mathcal{Q}(1)] = 1$ . Finally,  $\mathcal{Q}(\sigma) > 0$  for every  $\sigma > 1$ .*

*Proof.* We take several steps to build this lemma.

*Step 1. Constructively finding a null vector.* As established in Proposition 7.1, the solution  $M(1)$  must satisfy that  $B - M(1) > 0$ . Therefore,  $w = \sqrt{\lambda} \odot \text{diag}(B - M(1))$  is non-zero. By definition,  $M(1)$  satisfies

$$M(1)^{-1} = B^{-1} + \text{Diag}(\lambda) - \text{Diag}\{\lambda \odot \text{diag}(M(1))\}. \quad (8.4)$$

Multiplying  $B$  from the left and  $M(1)$  from the right, we conclude that

$$M(1) - B + M(1) \begin{bmatrix} \lambda_1(1 - M(1)_{11}) & 0 & \cdots & 0 \\ 0 & \lambda_2(1 - M(1)_{22}) & \cdots & 0 \\ & & \cdots & \\ 0 & 0 & \cdots & \lambda_L(1 - M(1)_{LL}) \end{bmatrix} B = 0. \quad (8.5)$$

Recall the identity that  $\text{diag}[A_1 \text{Diag}(b)A_2] = (A_1 \odot A_2)b$  for any  $A_1, A_2 \in \mathbb{R}^L, b \in \mathbb{R}^L$ . Now applying  $\text{diag}(\cdot)$  to (8.5), we obtain

$$- \begin{bmatrix} 1 - M(1)_{11} \\ 1 - M(1)_{22} \\ \cdots \\ 1 - M(1)_{LL} \end{bmatrix} + (B \odot M(1)) \begin{bmatrix} \lambda_1(1 - M(1)_{11}) \\ \lambda_2(1 - M(1)_{22}) \\ \cdots \\ \lambda_L(1 - M(1)_{LL}) \end{bmatrix} = 0.$$

Then multiply  $\sqrt{\Lambda}$  from the left to deduce that  $\mathcal{Q}(1)w = 0$ .

*Step 2. Proving  $\mathcal{Q}(1)$  to be positive semi-definite.* The key idea is to transform both  $B$  and  $M(1)$  so that they become commutative. Let

$$\begin{aligned} \Psi_1 &:= \text{Diag} \left[ \sqrt{\lambda} \odot \sqrt{\mathbf{1}_L - \text{diag}(M(1))} \right] B \text{Diag} \left[ \sqrt{\lambda} \odot \sqrt{\mathbf{1}_L - \text{diag}(M(1))} \right], \\ \Psi_2 &:= \text{Diag} \left[ \sqrt{\lambda} \odot \sqrt{\mathbf{1}_L - \text{diag}(M(1))} \right] M(1) \text{Diag} \left[ \sqrt{\lambda} \odot \sqrt{\mathbf{1}_L - \text{diag}(M(1))} \right]. \end{aligned}$$

Then (8.4) yields that

$$\Psi_2^{-1} = \Psi_1^{-1} + I_L,$$

which further implies that  $\Psi_1 \Psi_2 = \Psi_1 - \Psi_2 = \Psi_2 \Psi_1$ . Henceforth,  $\Psi_1$  and  $\Psi_2$  are commutable, thus simultaneously diagonalizable: there exists orthogonal  $Q$  and scalars  $\psi_1, \dots, \psi_L, \xi_1, \dots, \xi_L > 0$  such that

$$\begin{aligned} \Psi_1 &= Q \text{Diag}(\psi_1, \dots, \psi_L) Q^\top, \\ \Psi_2 &= Q \text{Diag}(\xi_1, \dots, \xi_L) Q^\top. \end{aligned}$$

Then  $\Psi_2^{-1} = \Psi_1^{-1} + I_L$  gives

$$\xi_l^{-1} = \psi_l^{-1} + 1, \quad \text{or equivalently} \quad \xi_l = \frac{\psi_l}{1 + \psi_l}, \quad l = 1, \dots, L.$$

Subsequently, we claim that  $\Psi_1 \odot \Psi_2 \leq \text{Diag}(\text{diag}(\Psi_1 \Psi_2))$ . It can be shown in the following way,

$$\begin{aligned} \Psi_1 \odot \Psi_2 &= \sum_{k,l=1}^L \psi_k \xi_l (q_k q_k^\top) \odot (q_l q_l^\top) \\ &= \sum_{k,l=1}^L \psi_k \xi_l (q_k \odot q_l) (q_k \odot q_l)^\top. \end{aligned}$$

At the same time,

$$\begin{aligned}
\text{Diag}(\text{diag}(\Psi_1 \Psi_2)) &= \sum_{k=1}^L \psi_k \xi_k \text{Diag}(\text{diag}(q_k q_k^\top)) \\
&= \sum_{k=1}^L \psi_k \xi_k \text{Diag}(q_k) \left[ \sum_{l=1}^L q_l q_l^\top \right] \text{Diag}(q_k) \\
&= \sum_{k,l=1}^L \psi_k \xi_k (q_k \odot q_l) (q_k \odot q_l)^\top.
\end{aligned}$$

Consequently, by subtracting the two equations,

$$\begin{aligned}
F &:= \text{Diag}(\text{diag}(\Psi_1 \Psi_2)) - \Psi_1 \odot \Psi_2 \\
&= \sum_{1 \leq l < k \leq L} (\psi_k \xi_k + \psi_l \xi_l - \psi_k \xi_l - \psi_l \xi_k) (q_k \odot q_l) (q_k \odot q_l)^\top \\
&= \sum_{1 \leq l < k \leq L} (\psi_k - \psi_l) (\xi_k - \xi_l) (q_k \odot q_l) (q_k \odot q_l)^\top.
\end{aligned}$$

Since  $\xi = \psi/(1 + \psi)$  is an increasing function of  $\psi > 0$ , we always have  $(\psi_k - \psi_l) (\xi_k - \xi_l) \geq 0$ . Thus  $\Psi_1 \odot \Psi_2 \leq \text{Diag}(\text{diag}(\Psi_1 \Psi_2))$ . Lastly, we need to put it back into an inequality of  $B$  and  $M(1)$ . Let  $u = \lambda - \lambda \odot \text{diag}(M(1))$ , then (8.4) deduces that  $B - M(1) = M(1) \text{Diag}(u) B$  so that

$$\begin{aligned}
\text{Diag}(\text{diag}(\Psi_1 \Psi_2)) &= \text{Diag} \left\{ \text{diag} \left[ \sqrt{\text{Diag}(u)} B \text{Diag}(u) M(1) \sqrt{\text{Diag}(u)} \right] \right\} \\
&= \sqrt{\text{Diag}(u)} \text{Diag} \left\{ \text{diag} [B \text{Diag}(u) M(1)] \right\} \sqrt{\text{Diag}(u)} \\
&= \sqrt{\text{Diag}(u)} \text{Diag} \{ \mathbf{1}_L - \text{diag}(M(1)) \} \sqrt{\text{Diag}(u)}
\end{aligned}$$

On the other hand,

$$\Psi_1 \odot \Psi_2 = \text{Diag}(u) [B \odot M(1)] \text{Diag}(u).$$

Therefore,  $\Psi_1 \odot \Psi_2 \leq \text{Diag}(\text{diag}(\Psi_1 \Psi_2))$  implies that  $\sqrt{\Lambda} [B \odot M(1)] \sqrt{\Lambda} \leq I_L$ , i.e.  $\mathcal{Q}(1) \geq 0$ .

*Step 3. Establishing the null space dimension.* It remains to show that  $\dim[\ker \mathcal{Q}(1)] = 1$ . Continue using the notations in Step 2. Since  $B$  is irreducible and the diagonal conjugation defining  $\Psi_1$  has strictly positive diagonal entries,  $\Psi_1$  is irreducible as well. Recall that

$$F = \sum_{1 \leq l < k \leq L} (\psi_k - \psi_l) (\xi_k - \xi_l) (q_k \odot q_l) (q_k \odot q_l)^\top$$

is always PSD. Now take  $z \in \ker F \subseteq \mathbb{R}^L$ . It follows that

$$\sum_{1 \leq l < k \leq L} (\psi_k - \psi_l) (\xi_k - \xi_l) \left[ (q_k \odot q_l)^\top z \right]^2 = z^\top F z = 0.$$

Consequently,  $\psi_k \neq \psi_l$  immediately deduces that  $(q_k \odot q_l)^\top z = 0$ . Furthermore, letting  $D_z = \text{Diag}(z)$ , the previous fact implies that

$$\begin{aligned}
D_z \Psi_1 - \Psi_1 D_z &= \left( \sum_l q_l q_l^\top \right) D_z \left( \sum_k \psi_k q_k q_k^\top \right) - \left( \sum_l \psi_l q_l q_l^\top \right) D_z \left( \sum_k q_k q_k^\top \right) \\
&= \sum_{k,l} [(\psi_k - \psi_l) q_l^\top D_z q_k] q_l q_k^\top = 0,
\end{aligned}$$

where the last step is due to  $q_l^\top D_z q_k = (q_k \odot q_l)^\top z$ . Since  $D_z$  is diagonal, it holds that

$$z_i(\Psi_1)_{ij} = (D_z \Psi_1)_{ij} = (\Psi_1 D_z)_{ij} = z_j(\Psi_1)_{ij}.$$

Lastly, since  $\Psi_1$  is irreducible, we can find  $L - 1$  edges  $e_1, \dots, e_{L-1} \in [L]^2$  to connect every index such that we always have  $(\Psi_1)_{e_j} \neq 0$  for  $1 \leq j \leq L - 1$ . Since  $e_1, \dots, e_{L-1}$  connect every index, it is enough to conclude that  $z_1 = z_2 = \dots = z_L$ . Therefore, we learn that  $\ker F = \text{span}(\mathbf{1}_L)$ , which further implies that  $\dim[\ker \mathcal{Q}(1)] = 1$ .

Since  $M(\sigma)$  is strictly decreasing in  $\sigma$  on  $(\sigma_+, \infty)$ , the matrix  $\mathcal{Q}(\sigma)$  is strictly increasing. Therefore  $\mathcal{Q}(\sigma) > \mathcal{Q}(1) \geq 0$  for every  $\sigma > 1$ .  $\square$

### 8.3 Simplifying the overlap formulas

Section 6.3 gives matrix overlap formulas for a general simple outlier. At the special outlier  $\sigma = 1$ , Lemma 8.1 gives an explicit null vector  $w$ , and the remaining task is to simplify the two-resolvent term that appears in the self-overlap formula. Recall the notion  $\mathcal{P}_\sigma$  from (6.3). This linear operator naturally arises when we differentiate such an equation

$$M_\kappa(z)^{-1} = zB^{-1} - \kappa V^{-1}TV^{-1} + \text{Diag}(\lambda) - \text{Diag}\{\lambda \odot \text{diag}(M_\kappa(z))\}.$$

When  $\sigma = 1$ , we can establish the following identity. Using it, we can bypass  $\mathcal{P}_1$  when simplifying the expression for the asymptotic limits of  $\text{mat}(\nu_n)^\top \text{mat}(\nu_n)$ . It is proved purely exploiting linear algebra.

**Lemma 8.2.** *For any symmetric  $T \in \text{Sym}_L(\mathbb{R})$ , it holds that*

$$w^\top \left\{ \left( \sqrt{\Lambda} B \sqrt{\Lambda} \right) \odot (\mathcal{P}_1 [V^{-1}TV^{-1}]) \right\} w = \text{tr} [T(I - V^{-1}M(1)V^{-1})], \quad (8.6)$$

where  $w$  is the null vector from Lemma 8.1.

*Proof.* Proving this identity is pretty involved. We begin by introducing a few notations for shorthand. Recall that  $M := M(1)$  is given subject to

$$M^{-1} = B^{-1} + \text{Diag}(\lambda) - \text{Diag}\{\lambda \odot \text{diag}(M)\}. \quad (8.7)$$

Let  $\Delta := \mathcal{P}_1 [V^{-1}TV^{-1}] \in \text{Sym}_L(\mathbb{R})$ . Since  $\mathcal{P}_1$  is defined in order to differentiate  $M_\kappa(1)$  with respect to  $\kappa$ , the following equation actually implicitly defines  $\Delta$ ,

$$M^{-1}\Delta M^{-1} = V^{-1}TV^{-1} + \text{Diag}(\lambda \odot \text{diag}(\Delta)). \quad (8.8)$$

These two equations suffice for all subsequent derivation. Let

$$s := \lambda - \lambda \odot \text{diag}(M) \in \mathbb{R}^L, \quad d := \text{diag}(\Delta) \in \mathbb{R}^L, \quad U := V^{-1}TV^{-1} \in M_L(\mathbb{R}).$$

Then the two sides of (8.6) becomes

$$\begin{aligned} \text{LHS} &= s^\top (B \odot \Delta) s, \\ \text{RHS} &= \text{tr} [T(I - V^{-1}MV^{-1})]. \end{aligned}$$

Using (8.8), we can write

$$U = M^{-1}\Delta M^{-1} - \text{Diag}(\lambda \odot d).$$

Hence

$$MV^{-1}TV = MUB = \Delta M^{-1}B - M \text{Diag}(\lambda \odot d)B. \quad (8.9)$$

Taking diagonals and using

$$M^{-1}B = I + \text{Diag}(s)B,$$

we obtain

$$\text{diag}(\Delta M^{-1}B) = \text{diag}(\Delta) + \text{diag}(\Delta \text{Diag}(s)B).$$

Moreover, using  $\text{diag}(\Delta \text{Diag}(s)B) = (B \odot \Delta)s$ , we can go from (8.9) to find that

$$\text{diag}(MV^{-1}TV) = d + (B \odot \Delta)s - \text{diag}(M \text{Diag}(\lambda \odot d)B),$$

which can be further rearranged into

$$(B \odot \Delta)s - \text{diag}(MV^{-1}TV) = \text{diag}(M \text{Diag}(\lambda \odot d)B) - d. \quad (8.10)$$

In the following, we will verify that  $s$  is orthogonal to the right-handed side term of (8.10). To do so, let's derive the following:

$$\begin{aligned} & s^\top \text{diag}(M \text{Diag}(\lambda \odot d)B) \\ &= \text{tr}[\text{Diag}(s)M \text{Diag}(\lambda \odot d)B] \\ &= \text{tr}[\text{Diag}(\lambda \odot d)B] - \text{tr}[M \text{Diag}(\lambda \odot d)] \\ &= \lambda^\top d - [\lambda \odot \text{diag}(M)]^\top d \\ &= s^\top d, \end{aligned} \quad (8.11)$$

where the first equality is by the definition of those algebra notations, the second equality is from  $\text{Diag}(s) = M^{-1} - B^{-1}$  as seen from (8.7), the third equality is because of  $\text{diag}(B) = \mathbf{1}_L$  and the last equality uses the definition of  $s$ .

Henceforth, continuing from (8.10) and (8.11), we conclude that

$$\begin{aligned} \text{LHS} &= s^\top (B \odot \Delta) s \\ &= s^\top \text{diag}(MV^{-1}TV) \\ &= \text{tr}[\text{Diag}(s)MV^{-1}TV] \\ &= \text{tr}[(M^{-1} - B^{-1})MV^{-1}TV] \\ &= \text{tr}[T(I - V^{-1}MV^{-1})] = \text{RHS}, \end{aligned}$$

where we have used  $B = V^2$  in the middle.  $\square$

We can now combine the outlier statement from Section 6 with the two special-point identities above. This gives the eigenvalue and overlap asymptotics at the outlier  $\sigma = 1$ .

**Proposition 8.3.** *Let  $\sigma_n$  be the top eigenvalue of  $H$ , and let  $\nu_n \in \mathbb{R}^{nL}$  be a corresponding unit eigenvector. Split  $\nu_n$  into  $L$  segments written as  $\nu_n^{(1)}, \dots, \nu_n^{(L)} \in \mathbb{R}^n$ . Recall the sign flipping  $s(\nu_n)$  in (6.2) and denote*

$$\begin{aligned} w &:= \sqrt{\lambda} \odot (\mathbf{1}_L - \text{diag}[M(1)]) \in \mathbb{R}^L, \\ c^* &:= \sum_{l=1}^L \lambda_l M_{ll}(1) [1 - M_{ll}(1)] > 0, \\ \Sigma_1 &:= \frac{1}{\sqrt{c^*}} \{V^{-1}[B - M(1)]\} \in \mathbb{R}^{L \times L}, \\ \Sigma_2 &:= \frac{1}{c^*} \{I - V^{-1}M(1)V^{-1}\} \in \text{Sym}_L^+(\mathbb{R}). \end{aligned} \quad (8.12)$$

Moreover,  $c^* = w^\top \mathcal{Q}'(1)w$ . Then  $|\sigma_n - 1| = \mathcal{O}_<(n^{-1/10})$ , and

$$\left\| \frac{s(\nu_n)}{\sqrt{n}} \text{mat}(\nu_n)^\top X - \Sigma_1 \right\| = \mathcal{O}_<(n^{-1/10}), \quad (8.13)$$

$$\left\| \text{mat}(\nu_n)^\top \text{mat}(\nu_n) - \Sigma_2 \right\| = \mathcal{O}_<(n^{-1/20}). \quad (8.14)$$

Compared to the overlaps that can be obtained via Cauchy residue theorems for a general outlier eigenvalue, shown in Proposition 3.4 and 3.5, the expressions are much more simplified at the special value  $z = 1$ . We manage to guess the final simplified expressions, via state evolution of a Bayes optimal approximate message passing algorithm under a Gaussian prior distribution (see Appendix A.2), but the simplification process is rigorously proved via linear algebra identities in Lemma 8.2.

*Proof of Proposition 8.3.* The convergence of  $|\sigma_n - 1|$  follows from Proposition 3.3. Use Lemma 8.1 to obtain the simplified expression for  $w$ . Recall the statements of Proposition 6.3 to find that

$$\left\| \text{mat}(\nu_n)^\top \text{mat}(\nu_n) - \frac{1}{c^*} \tilde{\Sigma}_2 \right\| = \mathcal{O}_<(n^{-1/20}), \quad c^* = w^\top \mathcal{Q}'(1)w,$$

for some  $\tilde{\Sigma}_2 \in \text{Sym}_L^+(\mathbb{R})$  defined through  $\mathcal{P}_1$ . Utilizing the identity stated in Lemma 8.2 about  $\mathcal{P}_1$ , we can simplify  $\tilde{\Sigma}_2$  to

$$\tilde{\Sigma}_2 = I - V^{-1}M(1)V^{-1}.$$

Since  $\|\nu_n\| = 1$  is well-normalized,

$$\begin{aligned} c^* &= \text{tr} \left( \tilde{\Sigma}_2 \right) \\ &= \text{tr} [I - M(1)B^{-1}] \\ &= \text{tr} \{M(1) [\text{Diag}(\lambda) - \text{Diag} [\lambda \odot \text{diag}(M(1))]]\} \\ &= \sum_{l=1}^L \lambda_l M_{ll}(1)(1 - M_{ll}(1)). \end{aligned}$$

In this way, we have obtained all the simplification in (8.12). Then the quantitative convergence in (8.13) and (8.14) follow immediately from Proposition 6.3(b) and Proposition 6.3(c) respectively.  $\square$

## 8.4 Proofs of the main spectral theorems

*Proof of Theorem 2.7.* First suppose  $\text{SNR}(\lambda, B) < 1$ . Proposition 7.1 gives  $\sigma_+ < 1$ . The argument leading to (8.2) shows that the deterministic outlier equation has no root to the right of  $\sigma_+$ . Hence, for every fixed  $\epsilon > 0$ , with high probability there is no eigenvalue of  $H$  above  $\sigma_+ + \epsilon$ . Together with the bulk convergence from Theorem 2.6, this implies  $\sigma_1(H) \xrightarrow{\mathbb{P}} \sigma_+$ .

Now suppose  $\text{SNR}(\lambda, B) > 1$ . Proposition 7.1 again gives  $\sigma_+ < 1$ , and Lemma 8.1 shows that  $\det \mathcal{Q}(1) = 0$  with a one-dimensional kernel spanned by  $w$ . The crossing at 1 is simple because Proposition 8.3 gives  $w^\top \mathcal{Q}'(1)w = c^* > 0$ . Proposition 3.3 therefore gives a simple eigenvalue of  $H$  converging to 1. The same lemma also gives  $\mathcal{Q}(\sigma) > 0$  for every  $\sigma > 1$ , so the determinant equation has no root to the right of 1. Thus the outlier at 1 is the top eigenvalue, and  $\sigma_1(H) \xrightarrow{\mathbb{P}} 1$ . All other outliers are associated with roots of  $\det \mathcal{Q}(\sigma) = 0$  in  $[\sigma_+, 1)$ , while the remaining eigenvalues stay at the bulk edge by the no-outside-spectrum estimate. Therefore  $\sigma_2(H)$  converges in probability to a deterministic point in  $[\sigma_+, 1)$ .  $\square$

*Proof of Theorem 2.9.* The existence of the valid solution  $M(1)$  with  $0 < M(1) < B$  is Proposition 7.1. By the informative part of Theorem 2.7, the top eigenvalue is simple and converges to 1. Proposition 8.3 gives the unit-eigenvector limits

$$\frac{s(\nu_n)}{\sqrt{n}} \text{mat}(\nu_n)^\top X \xrightarrow{\mathbb{P}} \Sigma_1, \quad \text{mat}(\nu_n)^\top \text{mat}(\nu_n) \xrightarrow{\mathbb{P}} \Sigma_2.$$

After choosing the global sign so that  $s(\nu_n) = 1$  and setting  $\hat{X} = \sqrt{n} \text{mat}(\nu_n)$ , these are exactly

$$\frac{1}{n} \hat{X}^\top X \xrightarrow{\mathbb{P}} \Sigma_1, \quad \frac{1}{n} \hat{X}^\top \hat{X} \xrightarrow{\mathbb{P}} \Sigma_2.$$

Finally, since  $M(1) < B$ , the matrix  $\Sigma_1 = (c^*)^{-1/2} V^{-1} (B - M(1))$  is nonzero, so the top eigenvector has nontrivial overlap with the signal.  $\square$

## 9 Derivation of the spectral algorithm

In this section, we derive a spectral method for signal recovery in (1.1). To this end, we linearize an appropriate message passing algorithm around the “non-informative” fixed point. This general strategy has been successful for diverse high-dimensional models, including community detection, single-index and multi-index models, contextual block models, and spiked models with heterogeneous noise. In the present multi-view problem, the linearization produces the matrix  $H$  studied in the main text, whose correlated noise component is described by the matrix Dyson equation introduced in Section 4.

We start with a general family of AMP algorithms to estimate  $X$  from  $A$ . Similar algorithms have been explored in several recent works [NM24, RR23]. The formulation below follows recent work by two of the present authors [YLS25]. The general iterations take the form

$$m_i^{t+1} := \sum_{k=1}^n \sqrt{\frac{\lambda_l}{n}} A_{i,k}^{(l)} \mathcal{E}_t^{(l)}(m_k^t) - \lambda_l \mathbf{d}_t^{(l)} \mathcal{E}_{t-1}^{(l)}(m_i^{t-1}), \quad (9.1)$$

$$\mathbf{d}_t^{(l)} := \frac{1}{n} \sum_{k=1}^n \partial_l \mathcal{E}_t^{(l)}(m_k^t), \quad (9.2)$$

where  $\mathcal{E}_0, \mathcal{E}_1, \mathcal{E}_2, \dots : \mathbb{R}^L \rightarrow \mathbb{R}^L$  are a series of *non-linear denoisers*. Assuming that the latent features  $X_i^{(1:L)}$  are sampled i.i.d from a distribution  $p$ , one can select denoisers sequentially to maximize the correlation with the latent signal. This denoiser is related to a natural fixed-dimensional denoising problem. Specifically, for hidden  $\mathcal{X} \sim p(x)$ , if we observe  $m_l := \lambda_l q_l \mathcal{X}_l + \mathcal{N}(0, \lambda_l q_l)$  for every  $l \in [L]$ , the optimal denoiser  $\hat{\mathcal{X}}$  is the posterior expectation

$$\hat{\mathcal{X}} \equiv \mathcal{E}_{\text{Bayes}}(m; q) := \frac{\int x \exp \left\{ -\sum_{l=1}^L (m_l - \lambda_l q_l x_l)^2 / 2\lambda_l q_l \right\} dp(x)}{\int \exp \left\{ -\sum_{l=1}^L (m_l - \lambda_l q_l x_l)^2 / 2\lambda_l q_l \right\} dp(x)} \in \mathbb{R}^L, \quad \forall m \in \mathbb{R}^L.$$

The *Bayes optimal* AMP algorithm keeps track of a series of state evolution parameters  $q^0, q^1, q^2, \dots \in [0, +\infty)^L$  and adopts  $\mathcal{E}_t(\cdot) = \mathcal{E}_{\text{Bayes}}(\cdot; q^t)$  in (9.1) and (9.2). Heuristics from spin glass theory suggest that this algorithm should be optimal among computationally efficient algorithms for recovering the latent signal in (1.1).

We derive the relevant spectral operator by linearizing this iterative algorithm. Assuming  $\mathcal{E}_{\text{Bayes}}(0; q) \equiv \mathbb{E}[x] = 0$  and  $\nabla_m \mathcal{E}_{\text{Bayes}}(0; q) \equiv \mathbb{E}[xx^\top] = B$  for any  $q \in [0, +\infty)^L$ , such an expansion

$$\mathcal{E}_{\text{Bayes}}(m; q) \approx \mathcal{E}_{\text{Bayes}}(0; q) + \nabla_m \mathcal{E}_{\text{Bayes}}(0; q) m \equiv Bm$$

linearizes the iterations while preserving the correlation structure contained in the prior  $p(x)$ . Assuming that the algorithm converges to a fixed point, the limit can be written, after the change of variables detailed in Appendix A.1, as an eigenvalue equation for the matrix  $H$  defined in (2.1). The decomposition  $H = H_0 + H_1$  used throughout the spectral analysis is given in (2.3), with  $H_0$  and  $H_1$  defined in (2.4)–(2.5). Using a slightly different perspective, we can also obtain the same linearized AMP matrix by imposing a Gaussian prior distribution on the spikes; see Appendix A.2.

## 10 Discussion

We have analyzed the spectral behavior of the linearized AMP matrix for the multi-view spiked Wigner model. The main conclusion is that the emergence of an informative spectral direction is governed by the explicit quantity  $\text{SNR}(\lambda, B)$  in (1.2). Below the threshold  $\text{SNR}(\lambda, B) = 1$ , the largest eigenvalue remains at the right edge of the limiting bulk spectrum; above the threshold, a distinguished outlier appears at the point 1, and its eigenvector has nontrivial matrix-valued overlaps with the latent signals. This gives an explicit spectral weak-recovery threshold for the linearized AMP method.

The proof also identifies the deterministic mechanism behind this transition. The bulk spectrum is controlled by a matrix Dyson equation associated with the correlated Gaussian noise component, while the outliers are described by a finite-dimensional determinant equation involving its solution. At the special point  $z = 1$ , the matrix Dyson equation admits an explicit characterization that connects the sign of  $\text{SNR}(\lambda, B) - 1$  to the creation of a root of the outlier equation. This is the step that turns the general outlier theory into the sharp phase-transition formula.

On the technical side, the proof keeps the matrix Dyson equation in an explicit finite-dimensional form. This makes it possible to use the same deterministic objects in the bulk law, the spike-direction deterministic equivalents, and the outlier equation, which is what ultimately produces a single spectral characterization of the transition.

The variational analysis in Section 7 suggests a deeper structural connection between the matrix Dyson equation for the linearized AMP matrix and the TAP free energy associated with the underlying inference problem. The proof uses the variational characterization directly, but the TAP interpretation gives a useful perspective on why the same finite-dimensional objects appear both in the spectral analysis and in the fixed-point description of the inference problem.

Finally, we expect the spectral threshold  $\text{SNR}(\lambda, B) = 1$ , with  $\text{SNR}(\lambda, B)$  defined in (1.2), to be the algorithmic threshold for the multi-view spiked model (1.1). A rigorous proof of this conjecture is an interesting direction for future inquiry.

**Acknowledgments.** SS gratefully acknowledges support from NSF grant DMS CAREER 2239234, ONR grant N00014-23-1-2489, and AFOSR grant FA9950-23-1-0429. Y.M.L. gratefully acknowledges support from a Harvard College Professorship, the Harvard FAS Dean’s Fund for Promising Scholarship, and DARPA grant DIAL-FP-038. The authors thank Hang Du, Henry Hu, and Saba Lepsveridze for stimulating discussions and for sharing an early version of their manuscript.

## References

- [AEK19] Oskari H Ajanki, László Erdős, and Torben Krüger. Stability of the matrix dyson equation and random matrices with correlations. *Probability Theory and Related Fields*, 173:293–373, 2019.
- [AEK20] Johannes Alt, László Erdős, and Torben Krüger. The dyson equation with linear self-energy: spectral bands, edges and cusps. *Documenta Mathematica*, 25:1421–1539, 2020.
- [AEKN19] Johannes Alt, László Erdős, Torben H Krüger, and Yuriy Nemish. Location of the spectrum of kronecker random matrices. In *Annales de l’institut Henri Poincaré*, volume 55, 2019.
- [AEKS20] Johannes Alt, László Erdős, Torben H Krüger, and Dominik J Schröder. Correlated random matrices: Band rigidity and edge universality. *Annals of Probability*, 48(2), 2020.
- [AGZ10] Greg W Anderson, Alice Guionnet, and Ofer Zeitouni. *An introduction to random matrices*. Number 118. Cambridge university press, 2010.
- [BBAP05] Jinho Baik, Gérard Ben Arous, and Sandrine Péché. Phase transition of the largest eigenvalue for nonnull complex sample covariance matrices. *Annals of Probability*, pages 1643–1697, 2005.
- [BCSvH24] Afonso S Bandeira, Giorgio Cipolloni, Dominik Schröder, and Ramon van Handel. Matrix concentration inequalities and free probability ii. two-sided bounds and applications. *arXiv preprint arXiv:2406.11453*, 2024.
- [BGN11] Florent Benaych-Georges and Raj Rao Nadakuditi. The eigenvalues and eigenvectors of finite, low rank perturbations of large random matrices. *Advances in Mathematics*, 227(1):494–521, 2011.
- [Bol14] Erwin Bolthausen. An iterative construction of solutions of the tap equations for the sherrington–kirkpatrick model. *Communications in Mathematical Physics*, 325(1):333–366, 2014.
- [CLM22] Shuxiao Chen, Sifan Liu, and Zongming Ma. Global and individualized community detection in inhomogeneous multilayer networks. *The Annals of Statistics*, 50(5):2664–2693, 2022.
- [DAM17] Yash Deshpande, Emmanuel Abbe, and Andrea Montanari. Asymptotic mutual information for the balanced binary stochastic block model. *Information and Inference: A Journal of the IMA*, 6(2):125–170, 2017.
- [DHL26] Hang Du, Henry Hu, and Saba Lepsveridze. Optimal spectral algorithms for correlated two-view models in high dimensions. *personal communication*, 2026.
- [EKY13] László Erdős, Antti Knowles, and Horng-Tzer Yau. Averaging fluctuations in resolvents of random band matrices. In *Annales Henri Poincaré*, volume 14, pages 1837–1926. Springer, 2013.

- [EKYY13] László Erdos, Antti Knowles, Horng-Tzer Yau, and Jun Yin. The local semicircle law for a general class of random matrices. *Electron. J. Probab*, 18(59):1–58, 2013.
- [Erd19] Laszlo Erdos. The matrix dyson equation and its applications for random matrices. *arXiv preprint arXiv:1903.10060*, 2019.
- [EY17] László Erdős and Horng-Tzer Yau. *A dynamical approach to random matrix theory*, volume 28. American Mathematical Soc., 2017.
- [Flu84] Bernhard N Flury. Common principal components in k groups. *Journal of the American Statistical Association*, 79(388):892–898, 1984.
- [FVRS22] Oliver Y Feng, Ramji Venkataramanan, Cynthia Rush, and Richard J Samworth. A unifying tutorial on approximate message passing. *Foundations and Trends® in Machine Learning*, 15(4):335–536, 2022.
- [GHL26] Shuyang Gong, Dong Huang, and Zhangsong Li. Fundamental limits of community detection in contextual multi-layer stochastic block models. *arXiv preprint arXiv:2602.08173*, 2026.
- [HFS07] J William Helton, Reza Rashidi Far, and Roland Speicher. Operator-valued semicircular elements: solving a quadratic matrix equation with positivity constraints. *International Mathematics Research Notices*, 2007(9):rnm086–rnm086, 2007.
- [HLN07] Walid Hachem, Philippe Loubaton, and Jamal Najim. Deterministic equivalents for certain functionals of large random matrices. *The Annals of Applied Probability*, 17(3):875–930, 2007.
- [Joh01] Iain M Johnstone. On the distribution of the largest eigenvalue in principal components analysis. *The Annals of statistics*, 29(2):295–327, 2001.
- [KMM<sup>+</sup>13] Florent Krzakala, Cristopher Moore, Elchanan Mossel, Joe Neeman, Allan Sly, Lenka Zdeborová, and Pan Zhang. Spectral redemption in clustering sparse networks. *Proceedings of the National Academy of Sciences*, 110(52):20935–20940, 2013.
- [KY13] Antti Knowles and Jun Yin. The isotropic semicircle law and deformation of wigner matrices. *Communications on Pure and Applied Mathematics*, 66(11):1663–1749, 2013.
- [KZ25] Christian Keup and Lenka Zdeborová. Optimal thresholds and algorithms for a model of multi-modal learning in high dimensions. *Journal of Statistical Mechanics: Theory and Experiment*, 2025(9):093302, 2025.
- [LAL19] Wangyu Luo, Wael Alghamdi, and Yue M Lu. Optimal spectral initialization for signal recovery with applications to phase retrieval. *IEEE Transactions on Signal Processing*, 67(9):2347–2356, 2019.
- [Leh99] Franz Lehner. Computing norms of free operators with matrix coefficients. *American Journal of Mathematics*, 121(3):453–486, 1999.
- [Li25] Zhangsong Li. The algorithmic phase transition in symmetric correlated spiked wigner model. *arXiv preprint arXiv:2511.06040*, 2025.

- [LL20] Yue M Lu and Gen Li. Phase transitions of spectral initialization for high-dimensional non-convex estimation. *Information and Inference: A Journal of the IMA*, 9(3):507–541, 2020.
- [LM19] Marc Lelarge and Léo Miolane. Fundamental limits of symmetric low-rank matrix estimation. *Probability Theory and Related Fields*, 173:859–929, 2019.
- [MKK24] Pierre Mergny, Justin Ko, and Florent Krzakala. Spectral phase transition and optimal pca in block-structured spiked models. In *Proceedings of the 41st International Conference on Machine Learning*, pages 35470–35491, 2024.
- [MM17] Catherine Matias and Vincent Miele. Statistical clustering of temporal networks through a dynamic stochastic block model. *Journal of the Royal Statistical Society Series B: Statistical Methodology*, 79(4):1119–1141, 2017.
- [MM18] Marco Mondelli and Andrea Montanari. Fundamental limits of weak recovery with applications to phase retrieval. In *Conference On Learning Theory*, pages 1445–1450. PMLR, 2018.
- [MS24] Andrea Montanari and Subhabrata Sen. A friendly tutorial on mean-field spin glass techniques for non-physicists. *Foundations and Trends® in Machine Learning*, 17(1):1–173, 2024.
- [MV21] Andrea Montanari and Ramji Venkataramanan. Estimation of low-rank matrices via approximate message passing. *The Annals of Statistics*, 49(1), 2021.
- [MZ25] Pierre Mergny and Lenka Zdeborová. Spectral thresholds in correlated spiked models and fundamental limits of partial least squares. *arXiv preprint arXiv:2510.17561*, 2025.
- [NM24] Sagnik Nandy and Zongming Ma. Multimodal data integration and cross-modal querying via orchestrated approximate message passing. *arXiv preprint arXiv:2407.19030*, 2024.
- [PWBM18] Amelia Perry, Alexander S Wein, Afonso S Bandeira, and Ankur Moitra. Optimality and sub-optimality of pca i: Spiked random matrix models. *The Annals of Statistics*, 46(5):2416–2451, 2018.
- [Ree20] Galen Reeves. Information-theoretic limits for the matrix tensor product. *IEEE Journal on Selected Areas in Information Theory*, 1(3):777–798, 2020.
- [RR23] Riccardo Rossetti and Galen Reeves. Approximate message passing for the matrix tensor product model. *arXiv preprint arXiv:2306.15580*, 2023.
- [Ver18] Roman Vershynin. *High-dimensional probability: An introduction with applications in data science*, volume 47. Cambridge university press, 2018.
- [Wai19] Martin J Wainwright. *High-dimensional statistics: A non-asymptotic viewpoint*, volume 48. Cambridge university press, 2019.
- [YLS25] Xiaodong Yang, Buyu Lin, and Subhabrata Sen. Fundamental limits of community detection from multi-view data: multi-layer, dynamic and partially labeled block models. *The Annals of Statistics*, 53(6):2728–2756, 2025.

- [ZJVM24] Yihan Zhang, Hong Chang Ji, Ramji Venkataramanan, and Marco Mondelli. Spectral estimators for structured generalized linear models via approximate message passing. In *The Thirty Seventh Annual Conference on Learning Theory*, pages 5224–5230. PMLR, 2024.
- [ZM24] Yihan Zhang and Marco Mondelli. Matrix denoising with doubly heteroscedastic noise: Fundamental limits and optimal spectral methods. *Advances in Neural Information Processing Systems*, 37:93060–93117, 2024.
- [ZMV22] Yihan Zhang, Marco Mondelli, and Ramji Venkataramanan. Precise asymptotics for spectral methods in mixed generalized linear models. *arXiv preprint arXiv:2211.11368*, 2022.

## A Linearizing Bayes optimal AMP

### A.1 Expansion around the origin

Continued from the derivation in the start of Section 2, we provide a detailed derivation for the object in (2.1). Recall that a Bayes optimal AMP algorithm proceeds by

$$m_{i,l}^{t+1} := \sum_{k=1}^n \sqrt{\frac{\lambda_l}{n}} A_{i,k}^{(l)} \mathcal{E}_t^{(l)}(m_k^t) - \lambda_l \mathbf{d}_t^{(l)} \mathcal{E}_{t-1}^{(l)}(m_i^{t-1}),$$

$$\mathbf{d}_t^{(l)} := \frac{1}{n} \sum_{k=1}^n \partial_l \mathcal{E}_t^{(l)}(m_k^t),$$

where the denoisers are explicitly given as

$$\mathcal{E}_t(m) \equiv \mathcal{E}_{\text{Bayes}}(m; q^t) := \frac{\int x \exp \left\{ -\sum_{l=1}^L (m_l - \lambda_l q_l^t x_l)^2 / 2\lambda_l q_l^t \right\} dp(x)}{\int \exp \left\{ -\sum_{l=1}^L (m_l - \lambda_l q_l^t x_l)^2 / 2\lambda_l q_l^t \right\} dp(x)} \in \mathbb{R}^L. \quad (\text{A.1})$$

Here  $q^0, q^1, \dots$  are a series of state evolution parameters that are sequentially defined by

$$q^{t+1} = \mathbb{E} \left[ \mathcal{X} \odot \mathcal{E}_{\text{Bayes}} \left( \lambda \odot q^t \odot \mathcal{X} + \sqrt{\lambda \odot q^t} \odot \mathcal{W}; q^t \right) \right]$$

It is easy to verify that  $q_* = 0$  is always a trivial fixed point of this equation, in which case the algorithmic iterates are also fixed at  $m_* = 0$ .

To proceed, the high-level idea is to do Taylor expansion for  $\mathcal{E}_{\text{Bayes}}$  around  $m = 0$ . Via taking derivative in  $m_{l_2}$ , we find

$$\begin{aligned} \frac{\partial \mathcal{E}_{\text{Bayes}}^{(l_1)}}{\partial m_{l_2}}(m; q) &= \frac{\int x_{l_1} x_{l_2} \exp \left\{ -\sum_{l=1}^L (m_l - \lambda_l q_l x_l)^2 / 2\lambda_l q_l \right\} dp(x)}{\int \exp \left\{ -\sum_{l=1}^L (m_l - \lambda_l q_l x_l)^2 / 2\lambda_l q_l \right\} dp(x)} \\ &\quad - \frac{\int x_{l_1} \exp \left\{ -\sum_{l=1}^L (m_l - \lambda_l q_l x_l)^2 / 2\lambda_l q_l \right\} dp(x)}{\int \exp \left\{ -\sum_{l=1}^L (m_l - \lambda_l q_l x_l)^2 / 2\lambda_l q_l \right\} dp(x)} \\ &\quad \times \frac{\int x_{l_2} \exp \left\{ -\sum_{l=1}^L (m_l - \lambda_l q_l x_l)^2 / 2\lambda_l q_l \right\} dp(x)}{\int \exp \left\{ -\sum_{l=1}^L (m_l - \lambda_l q_l x_l)^2 / 2\lambda_l q_l \right\} dp(x)}. \end{aligned}$$

Henceforth, when taking  $m_* = 0$  and  $q_* = 0$ , the partial derivative boils down to the correlations under the original prior  $p(x)$ ,

$$\frac{\partial \mathcal{E}_{\text{Bayes}}^{(l_1)}}{\partial m_{l_2}}(0; 0) = \mathbb{E}_p [X_{l_1} X_{l_2}] = B_{l_1 l_2}.$$

A Taylor expansion of this denoising function at  $m \approx 0$  yields that

$$\mathcal{E}_{\text{Bayes}}^{(l)}(m; 0) = \mathcal{E}_{\text{Bayes}}^{(l)}(0; 0) + \sum_{l_1 \in [L]} \frac{\partial \mathcal{E}_{\text{Bayes}}^{(l_1)}}{\partial m_{l_2}}(0; 0) m_{l_1} + o(|m|).$$

Now suppose we choose the denoising function to be the linear component of this Taylor expansion,  $\bar{\mathcal{E}}^{(l)}(m) = \sum_{l_1} \mathbb{E}_p [X^{(l)} X^{(l_1)}] m_{l_1}$  for any  $l \in [L]$ . Then the Onsager term (9.2) would be greatly simplified to  $\mathbf{d}_t^{(l)} \equiv 1$ . Assume the updating equation (9.1) has reached a new equilibrium with the linearized denoisers, i.e.  $m^t = m^*$  for any  $t$ , then  $m^*$  must solve the following linear equations

$$m_{:,l}^* = \left( \sqrt{\frac{\lambda^{(l)}}{n}} A^{(l)} - \lambda^{(l)} I_n \right) \left( m_{:,l}^* + \sum_{l_1 \neq l} B_{ll_1} m_{:,l_1}^* \right), \quad \forall l \in [L]. \quad (\text{A.2})$$

To simplify this set of equations furthermore, we rearrange  $m^* \in \mathbb{R}^{n \times L}$  into a vector of dimension  $nL$  by

$$\mathbf{m}^* = \begin{bmatrix} m_{:,1}^* \\ m_{:,2}^* \\ \dots \\ m_{:,L}^* \end{bmatrix} \in \mathbb{R}^{nL}.$$

Then (A.2) can be written into a matrix form

$$\begin{aligned} \mathbf{m}^* &= \left\{ \left[ \text{diag} \left( \sqrt{\Lambda/n} \right) \otimes I_n \right] \mathbf{A} - \text{diag}(\Lambda) \otimes I_n \right\} \{ B \otimes I_n \} \mathbf{m}^*, \\ \mathbf{A} &= \text{diag} \left\{ A^{(1)}, \dots, A^{(L)} \right\} \in \mathbb{R}^{nL \times nL}, \\ \Lambda &= \left( \lambda^{(1)}, \dots, \lambda^{(L)} \right) \in \mathbb{R}^L, \end{aligned}$$

where  $\otimes$  denotes Kronecker product between matrices with

$$B \otimes I_n = \begin{bmatrix} I_n & \mathbb{E}_p [X^{(1)} X^{(2)}] I_n & \dots & \mathbb{E}_p [X^{(1)} X^{(L)}] I_n \\ \mathbb{E}_p [X^{(1)} X^{(2)}] I_n & I_n & \dots & \mathbb{E}_p [X^{(2)} X^{(L)}] I_n \\ \dots & \dots & \dots & \dots \\ \mathbb{E}_p [X^{(1)} X^{(L)}] I_n & \mathbb{E}_p [X^{(2)} X^{(L)}] I_n & \dots & I_n \end{bmatrix} \in \mathbb{R}^{nL \times nL}.$$

**Remark A.1.** If  $L = 1$ , then (A.2) directly boils down to

$$m^* = \left( \sqrt{\frac{\lambda}{n}} A - \lambda I_n \right) m^* \quad \implies \quad \frac{1}{\sqrt{n}} A m^* = \frac{\lambda + 1}{\sqrt{\lambda}} m^*.$$

So we are actually solving for the eigenvector of  $A/\sqrt{n}$  when the corresponding eigenvalue is  $(\lambda + 1)/\sqrt{\lambda}$ . This is exactly the largest eigenvalue predicted by BBP phase transition when  $\lambda > 1$ .

The last step is to plug in  $B = V^2$ . It turns out that  $(V \otimes I_n) m^*$  should be an eigenvector of  $H$  given in (2.1) with eigenvalue exactly 1.

## A.2 Gaussian prior

While Section A.1 presents one way of linearizing AMP via expanding the non-linear denoisers around the origin, here is an alternative way by directly placing a Gaussian prior  $\mathcal{N}(0, B)$  as  $p(x)$ . In this case, those Bayes optimal denoisers (A.1) automatically become linear in  $m$ . Benefiting from this alternative, we can make educated guesses on the simplified asymptotic overlaps shown in Theorem 2.9.

Let  $m_t^{(1)}, \dots, m_t^{(L)} \in \mathbb{R}^n$  denote the running variables in our AMP algorithm. In our previous note, we have characterized its updating rule as

$$\begin{aligned} m_t^{t+1} &= \sqrt{\frac{\lambda_l}{n}} A^{(l)} \mathcal{E}_t^{(l)} \left( m_t^{(1)}, \dots, m_t^{(L)} \right) - \lambda_l \mathbf{d}_t^{(l)} \mathcal{E}_{t-1}^{(l)} \left( m_t^{(1)}, \dots, m_t^{(L)} \right) \in \mathbb{R}^n, \\ \mathbf{d}_t^{(l)} &= \frac{1}{n} \sum_{i=1}^n \partial_i \mathcal{E}_t^{(l)} \left( m_{t,i}^{(1)}, \dots, m_{t,i}^{(L)} \right) \in \mathbb{R}. \end{aligned}$$

By imposing a multivariate Gaussian prior  $\mathcal{N}(0, B)$  on each  $X_i^{(1)}, \dots, X_i^{(L)}$ , a closed form for the Bayes optimal denoisers can be obtained. Suppose the state evolution iterates at time  $t$  is  $q_t \in [0, 1]^L$ , it follows from (A.1) that

$$\mathcal{E}_t(a_1, \dots, a_L) := \left( \text{Diag}(\lambda \odot q_t) + B^{-1} \right)^{-1} a, \quad \forall a_1, \dots, a_L \in \mathbb{R},$$

which also deduces that  $\mathbf{d}_t^{(l)} = \left[ \left( \text{Diag}(\lambda \odot q_t) + B^{-1} \right)^{-1} \right]_{ll}$  for any  $l$  and  $t$ . Then the series of state evolution parameters evolve according to such a rule

$$\begin{aligned} q_{t+1}^{(l)} &= \mathbb{E} \left[ X^{(l)} \mathcal{E}_t^{(l)} (\lambda \odot q_t \odot X + \mathcal{N}(0, \text{diag}(\lambda \odot q_t))) \right] \\ &= \left[ \left( \text{Diag}(\lambda \odot q_t) + B^{-1} \right)^{-1} \text{Diag}(\lambda \odot q_t) B \right]_{ll} \\ &= 1 - \left[ \left( \text{Diag}(\lambda \odot q_t) + B^{-1} \right)^{-1} \right]_{ll}. \end{aligned}$$

**Conjecture A.2.** *We conjecture that this choice of AMP algorithm will converge to equilibrium, as  $t \rightarrow \infty$ . By equilibrium, we mean the following two statements:*

1. *The state evolution parameters converge  $q_t \rightarrow q_* \in \mathbb{R}^L$ , where  $q_*$  is the solution to the following fixed-point equation*

$$q_* = 1 - \text{diag} \left[ \left( \text{Diag}(\lambda \odot q_*) + B^{-1} \right)^{-1} \right].$$

*In comparison with our self-consistent equations (mat), it holds that  $q_*^{(l)} = 1 - M_{ll}(1)$ .*

2. *Let  $m_t \in \mathbb{R}^{nL}$  be the concatenation of  $m_t^{(1)}, \dots, m_t^{(L)}$ . Then it also converges to equilibrium, as  $m_t \rightarrow m_* \in \mathbb{R}^{nL}$ , where  $m_*$  satisfies that*

$$m_*^{(l)} = \sqrt{\frac{\lambda_l}{n}} A^{(l)} \mathcal{E}_*^{(l)}(m_*) - \lambda_l \left( 1 - q_*^{(l)} \right) \mathcal{E}_*^{(l)}(m_*), \quad (\text{A.3})$$

*where we use  $\mathcal{E}_*$  to denote the denoiser with the limiting state evolution parameters  $q_*$ . Moreover, we have the following distributional result*

$$m_*^{(l)} \stackrel{d.}{\approx} \lambda_l q_*^{(l)} X^{(l)} + \sqrt{\lambda_l q_*^{(l)}} \mathcal{N}(0, I_n), \quad l \in [L]. \quad (\text{A.4})$$

*Moreover, we also have  $X^{(l)\top} \mathcal{E}_*^{(l)}(m_*)/n \stackrel{d.}{\approx} q_*^{(l)}$ .*

By some additional algebraic transformation, we can go from (A.3) to have

$$\mathcal{E}_*(m_*) = (B \otimes I_n) \begin{bmatrix} \sqrt{\frac{\lambda_1}{n}} A^{(1)} - \lambda_1 I_n & & 0 \\ & \dots & \\ 0 & & \sqrt{\frac{\lambda_L}{n}} A^{(L)} - \lambda_L I_n \end{bmatrix} \mathcal{E}_*(m_*).$$

where we denote

$$\mathcal{E}_*(m_*) := \left[ (\text{Diag}(\lambda \odot q_*) + B^{-1})^{-1} \otimes I_n \right] m_* \in \mathbb{R}^{nL}.$$

We know that  $X^{(l)\top} \mathcal{E}_*^{(l)}(m_*)/n \approx q_*^{(l)}$ . By comparing to the definition of  $H$ , we find that

$$\bar{\nu}^* = n^{-1/2} (V \otimes I_n)^{-1} \mathcal{E}_*(m_*) \in \mathbb{R}^{nL}$$

is an eigenvector of  $H$  with eigenvalue 1. And  $\nu^* = \frac{\bar{\nu}^*}{\|\bar{\nu}^*\|}$  further normalizes its norm to 1.

At this stage, (A.4) becomes a powerful tool to compute some overlaps. Firstly,

$$\begin{aligned} u_l^\top \bar{\nu}^* &= \frac{\sqrt{\lambda_l}}{n} \left[ (V e_l) \otimes X^{(l)} \right]^\top (V \otimes I_n)^{-1} \mathcal{E}_*(m_*) \\ &= \frac{\sqrt{\lambda_l}}{n} \left[ e_l \otimes X^{(l)} \right]^\top \mathcal{E}_*(m_*) \\ &= \frac{\sqrt{\lambda_l}}{n} X^{(l)\top} \mathcal{E}_*^{(l)}(m_*) \\ &\approx \sqrt{\lambda_l} q_*^{(l)}. \end{aligned}$$

Similarly, it also follows that

$$\begin{aligned} \bar{\nu}^{*\top} \bar{\nu}^* &= \frac{1}{n} \mathcal{E}_*(m_*)^\top (B \otimes I_n)^{-1} \mathcal{E}_*(m_*) \\ &\approx \text{tr} \left\{ \frac{1}{n} (B^{-1} \otimes I_n) \mathcal{E}_*(m_*) \mathcal{E}_*(m_*)^\top \right\} \\ &= \text{tr} \left\{ B^{-1} [\text{diag}(\lambda \odot q_*) + B^{-1}]^{-1} [\text{Diag}(\lambda \odot q_*) + \text{Diag}(\lambda \odot q_*) B \text{Diag}(\lambda \odot q_*)] \right. \\ &\quad \left. [\text{diag}(\lambda \odot q_*) + B^{-1}]^{-1} \right\} \\ &= \text{tr} \left\{ \text{Diag}(\lambda \odot q_*) [\text{Diag}(\lambda \odot q_*) + B^{-1}]^{-1} \right\} \\ &= \sum_{l=1}^L \lambda_l q_*^{(l)} (1 - q_*^{(l)}). \end{aligned}$$

Therefore, we should conclude that as  $n \rightarrow \infty$

$$u_l^\top \nu^* \rightarrow \frac{\sqrt{\lambda_l} q_*^{(l)}}{\sqrt{\sum_{l=1}^L \lambda_l q_*^{(l)} (1 - q_*^{(l)})}}.$$

This is how we manage to guess  $\Sigma_1$  in Proposition 8.3.

Moreover, we can also compute

$$\begin{aligned}
& \bar{\nu}^{*\top} (e_{l_1} e_{l_2}^\top \otimes I_n) \bar{\nu}^* \\
&= \frac{1}{n} \mathcal{E}_*(m_*)^\top (V^{-1} e_{l_1} e_{l_2}^\top V^{-1} \otimes I_n) \mathcal{E}_*(m_*) \\
&\approx \text{tr} \left\{ \frac{1}{n} (V^{-1} e_{l_1} e_{l_2}^\top V^{-1} \otimes I_n) \mathcal{E}_*(m_*) \mathcal{E}_*(m_*)^\top \right\} \\
&= \text{tr} \left\{ V^{-1} e_{l_1} e_{l_2}^\top V^{-1} [\text{diag}(\lambda \odot q_*) + B^{-1}]^{-1} \right. \\
&\quad \left. [\text{Diag}(\lambda \odot q_*) + \text{Diag}(\lambda \odot q_*) B \text{Diag}(\lambda \odot q_*)] [\text{diag}(\lambda \odot q_*) + B^{-1}]^{-1} \right\} \\
&= \text{tr} \left\{ V^{-1} e_{l_1} e_{l_2}^\top V \text{Diag}(\lambda \odot q_*) [\text{diag}(\lambda \odot q_*) + B^{-1}]^{-1} \right\} \\
&= e_{l_1}^\top (I - V^{-1} M V^{-1}) e_{l_2}.
\end{aligned}$$

This is how we manage to guess  $\Sigma_2$  in Proposition 8.3. Note that our proof to it is completely rigorous via Propositions 3.5, and the linear algebra identity in Lemma 8.2.

## B Standard facts for the self-consistent equation

*Proof of Proposition 4.2.* Our first step is to transform the equation into the exact form of matrix Dyson equations in [AEK19]. With transformation  $M_0 = -V^{-1} M V^{-1}$ , the equation (mat) can be restated as

$$-M_0^{-1} = zI_L - \Gamma + V \Lambda V + V \text{Diag} \{ \lambda \odot \text{diag}(V M_0 V) \} V, \quad (\text{B.1})$$

which is exactly the same as equation (2.2) in [AEK19]. Then the results in [HFS07] suffice to establish the feasibility and uniqueness of the solution  $M_0(z; \Gamma)$  to the equation (B.1) under the additional constraint that  $\Im M_0(z; \Gamma) > 0$ . Then  $M(z; \Gamma) := -V M_0(z; \Gamma) V$  naturally becomes a solution to (mat) with  $\Im M(z; \Gamma) < 0$ .

What's more, [AEK19, Proposition 2.1] also implies that  $M_0(z; \Gamma)$  admits a Stieltjes transform representation. In more detail, there exists a compactly-supported  $\text{Sym}_L^+(\mathbb{R})$ -valued measure  $\rho_\Gamma$  on  $\mathbb{R}$  such that  $\rho_\Gamma(\mathbb{R}) = I_L$  and

$$M_0(z; \Gamma) = \int_{\mathbb{R}} \frac{\rho_\Gamma(d\tau)}{\tau - z} \in \text{Sym}_L(\mathbb{C}), \quad \forall z \in \mathbb{C}^+.$$

This representation then induces the following

$$M(z; \Gamma) = - \int_{\mathbb{R}} \frac{V \rho_\Gamma(d\tau) V}{\tau - z} \in \text{Sym}_L(\mathbb{C}),$$

Therefore, we can finish the proof by taking  $\nu_\Gamma = V \rho_\Gamma V$ .  $\square$

The proof of Proposition 4.7, including the invertibility estimate for the stability operator, is given in Section 4.

## C Proofs for the information-theoretical thresholds

Our information-theoretical impossibility results can be deduced easily based on [YLS25].

To this end, consider the following functional for any  $q \in [0, +\infty)^L$ ,

$$\mathcal{H}(q) := \sum_{l=1}^L \frac{\lambda_l(q_l^2 - 2q_l)}{4} - \mathbb{E} \log \left[ \int_{\mathbb{R}^L} \exp \left( -\frac{1}{2} \sum_{l=1}^L (\sqrt{\lambda_l q_l} \mathcal{X}_l + \mathcal{W}_l - \sqrt{\lambda_l q_l} x_l)^2 \right) dp(x) \right], \quad (\text{C.1})$$

where the expectation is taken over  $\mathcal{X} \sim p(x)$  and  $\mathcal{W} \sim \mathcal{N}(0, I_L)$ . This functional depends on both the prior  $p(x)$  and  $(\lambda, B)$ , and is motivated from the replica-symmetric prediction on the free energy of the observation model (1.1). Under the following generic condition on  $p(x)$ , the information-theoretic threshold coincides with the spectral threshold  $\text{SNR}(\lambda, B) \leq 1$ .

( $\star$ ) As long as  $\text{SNR}(\lambda, B) < 1$ , the functional  $\mathcal{H}(q)$  is uniquely minimized at  $q = 0$ .

While  $\text{SNR}(\lambda, B) < 1$  in fact ensures  $q = 0$  to be a local minimum of  $\mathcal{H}(q)$ , the prior distribution  $p(x)$  has to satisfy additional conditions to guarantee that  $q = 0$  is the global minimizer of the free energy landscape.

**Proposition C.1.** *Under Assumption 2.10, suppose further that condition ( $\star$ ) holds. Then for any estimator  $\hat{X}(A) \in \mathbb{R}^{n \times L}$  computed from the observation model (1.1), its overlap with the planted signal converges to 0 i.e.,*

$$\frac{1}{n} \hat{X}(A)^\top X \xrightarrow{\mathbb{P}} 0_{L \times L},$$

when  $\text{SNR}(\lambda, B) < 1$ .

*Proof of Proposition C.1.* Theorem A.2 of [YLS25] derives the asymptotic limit of the minimal mean squared error for  $X^{(l)} X^{(l)\top}$  for any  $l \in [L]$ ,

$$\inf_{\hat{X}(A)} \frac{1}{n^2} \mathbb{E} \left\| \hat{X}^{(l)} \hat{X}^{(l)\top} - X^{(l)} X^{(l)\top} \right\|_F^2 \xrightarrow{\mathbb{P}} 1 - (q_l^*)^2, \quad (\text{C.2})$$

where  $q^*$  is the global minimizer of the functional  $\mathcal{H}(q)$  in (C.1). Although all the results of [YLS25] are stated for priors supported on  $\{\pm 1\}^L$ , the free energy method adopted in proving their Theorem A.2 does not require  $x \in \{\pm 1\}^L$  at all. Under condition ( $\star$ ), we learn that  $q^* \equiv 0$  as long as  $\text{SNR}(\lambda, B) < 1$ .

Next, suppose that we manage to find an estimator  $\hat{X}$  such that

$$\hat{X}^{(l)\top} X^{(l)} / n \xrightarrow{\mathbb{P}} \alpha > 0.$$

Then writing  $\beta := \lim_{n \rightarrow \infty} \frac{1}{n^2} \mathbb{E} \left\| \hat{X}^{(l)} \hat{X}^{(l)\top} \right\|_F^2 > 0$ , we have

$$\begin{aligned} & \frac{1}{n^2} \mathbb{E} \left\| t \hat{X}^{(l)} t \hat{X}^{(l)\top} - X^{(l)} X^{(l)\top} \right\|_F^2 \\ &= \frac{1}{n^2} \mathbb{E} \left\| X^{(l)} X^{(l)\top} \right\|_F^2 + \frac{t^4}{n^2} \mathbb{E} \left\| \hat{X}^{(l)} \hat{X}^{(l)\top} \right\|_F^2 - 2t^2 \left( \hat{X}^{(l)\top} X^{(l)} / n \right)^2 \\ & \xrightarrow{\mathbb{P}} 1 - 2t^2 \alpha^2 + t^4 \beta < 1 \end{aligned}$$

if  $0 < t^2 < 2\alpha^2/\beta$ . This is contradictory to (C.2). So we can conclude this proposition.  $\square$

*Proof of Proposition 2.11.* We need to deal with the two conditions separately.

1. When condition  $(\#)$  holds, we can proceed to show that condition  $(\star)$  indeed holds as well. Firstly, by direct differentiation, we can verify that

$$\begin{aligned}\nabla\mathcal{H}(q) &= \frac{\lambda_l}{2} [q_l - T(\lambda \odot q)], \\ \nabla^2\mathcal{H}(0) &= \Lambda - \Lambda(B \odot B)\Lambda.\end{aligned}$$

The detailed computation can be found in Proposition A.7 of [YLS25]. Therefore, when  $\text{SNR}(\lambda, B) < 1$ , we immediately have that  $\nabla\mathcal{H}(0) = 0$  and  $\nabla^2\mathcal{H}(0) \geq 0$ , so that  $q = 0$  becomes a local minimum of  $\mathcal{H}(q)$ . Subsequently, with the help of condition  $(\#)$ , we can use a contradiction argument. Suppose that  $\mathcal{H}(q)$  has some global minimizer  $q^* \neq 0$  elsewhere but still with  $q^* \in [0, +\infty)^L$ . There must exist an index  $l \in [L]$  such that  $q_l^* > 0$  and  $\nabla_l\mathcal{H}(q^*) = 0$ . As implied by condition  $(\#)$ , the following uni-variate function

$$t \in [0, 1] \rightarrow f(t) = \nabla_l\mathcal{H}(tq^*)$$

should be strictly concave yet  $f(0) = f(1) = 0$ . So we must have some small  $\epsilon > 0$  such that  $f(\epsilon) < 0$ , i.e.  $\nabla_l\mathcal{H}(\epsilon q^*) < 0$ . This is against the previous condition that  $\nabla^2\mathcal{H}(0) \geq 0$ . In conclusion,  $\mathcal{H}(q)$  cannot have any global minimizer but 0.

2. When condition  $(b)$  holds, we can use Theorem A.12 of [YLS25] to derive that

$$\inf_{\hat{X}(A)} \frac{1}{n^2} \mathbb{E} \left\| \hat{X}^{(l)} \hat{X}^{(l)\top} - X^{(l)} X^{(l)\top} \right\|_F^2 \xrightarrow{\mathbb{P}} 1,$$

for any  $l \in [L]$ . It is proved via the second moment method. Then the rest of the proof is the same as Proposition C.1. □

*Proof of Corollary 2.12.* In case  $(a)$ , it is crucial to realize that the functional  $\mathcal{H}(q)$  admits a closed-form expression, namely

$$\mathcal{H}(q) = \sum_{l=1}^L \frac{\lambda_l(q_l^2 - 2q_l)}{4} - \frac{1}{2} \log \left\{ \det \left[ (B^{-1} + \text{Diag}(\lambda \odot q))^{-1} \right] \right\} + C,$$

where  $C$  is a constant that does not depend on  $q$ . Via a change-of-variable  $q = \chi + 1$ , it is equivalent to our objective (7.2) with  $z = 1$ . Then condition  $(\star)$  follows immediately from Lemma 7.6.

In case  $(b)$ , Proposition A.14 and Lemma A.15 of [YLS25] together yield our claim. □

## D Gaussian concentration for the noise resolvent

This appendix records the standard Gaussian concentration input used in Section 5. Although the entries of  $H_1$  are correlated after conjugation by  $V \otimes I_n$ , the underlying variables are independent Gaussian entries of the matrices  $W^{(l)}$ , and the usual Lipschitz concentration argument applies.

**Lemma D.1.** *For any  $z \in \mathbb{C}^+$ ,  $\Gamma \in \text{Sym}_L(\mathbb{R})$ , and any  $A \in \mathbb{C}^{nL \times nL}$  with  $\|A\| = 1$ , the normalized trace  $\frac{1}{n} \text{tr}[AG(z; \Gamma)]$  concentrates around its mean. Namely, for any  $\delta > 0$ ,*

$$\mathbb{P} \left( \left| \frac{1}{n} \text{tr}[AG(z; \Gamma)] - \mathbb{E} \left\{ \frac{1}{n} \text{tr}[AG(z; \Gamma)] \right\} \right| \geq \delta \right) \leq 2 \exp \left( -C (\Im z)^4 n^2 \delta^2 \right).$$

In the display above,  $C := C(B, \lambda) = 1/\left(\|V\|^4 L \max_l \lambda_l\right)$ . Moreover, for any deterministic  $A \in \mathbb{C}^{nL \times nL}$ ,

$$\mathrm{tr}[A(G(z; \Gamma) - \mathbb{E}G(z; \Gamma))] = \mathcal{O}_{<} \left( \frac{\|A\|_F}{\sqrt{n}(\Im z)^2} \right). \quad (\text{D.1})$$

*Proof.* The core step is to view  $\frac{1}{n} \mathrm{tr}[AG(z; \Gamma)]$  as a function of the independent Gaussian scalars  $\{W_{ij}^{(l)} : l \in [L], 1 \leq i \leq j \leq n\}$ . Specifically, let

$$\Phi(W) = \frac{1}{n} \mathrm{tr} \left[ A (H_1(W) + \Gamma \otimes I_n - zI_{nL})^{-1} \right].$$

We estimate the Lipschitz constant of  $\Phi$  with respect to the Frobenius norm on the collection  $W$ . Since  $\|A\| = 1$ , for another realization  $\bar{W}$ ,

$$\begin{aligned} & |\Phi(W) - \Phi(\bar{W})| \\ &= \frac{\sqrt{L}}{n} \left| \mathrm{tr} \left[ A (H_1(W) + \Gamma \otimes I_n - zI_{nL})^{-1} (H_1(W) - H_1(\bar{W})) (H_1(W) + \Gamma \otimes I_n - zI_{nL})^{-1} \right] \right| \\ &\leq \frac{\sqrt{L}}{\sqrt{n}} \left\| (H_1(W) + \Gamma \otimes I_n - zI_{nL})^{-1} (H_1(W) - H_1(\bar{W})) (H_1(W) + \Gamma \otimes I_n - zI_{nL})^{-1} \right\|_F \\ &\leq \frac{\sqrt{L}}{\sqrt{n}(\Im z)^2} \|H_1(W) - H_1(\bar{W})\|_F \\ &\leq \frac{1}{n} \frac{\|V\|^2 \sqrt{L \max_l \lambda_l}}{(\Im z)^2} \left( \sum_{l=1}^L \|W^{(l)} - \bar{W}^{(l)}\|_F \right). \end{aligned}$$

We used  $\|(H_1 + \Gamma \otimes I_n - zI_{nL})^{-1}\| \leq 1/\Im z$  and the concrete form of  $H_1$  in (2.5). Thus the Lipschitz constant of  $\Phi$  is of order  $1/n$ . The result follows from standard concentration for Lipschitz functions of independent Gaussian variables, for instance [Wai19, Theorem 2.26] or [Ver18, Theorem 5.2.3].

The proof of (D.1) is the same, but without the normalization by  $n$  and with the Frobenius norm of the test matrix retained. For

$$\Psi_A(W) = \mathrm{tr} \left[ A (H_1(W) + \Gamma \otimes I_n - zI_{nL})^{-1} \right],$$

the preceding resolvent identity and Cauchy-Schwarz give

$$|\Psi_A(W) - \Psi_A(\bar{W})| \leq \frac{C(B, \lambda) \|A\|_F}{\sqrt{n}(\Im z)^2} \left( \sum_{l=1}^L \|W^{(l)} - \bar{W}^{(l)}\|_F \right).$$

Gaussian concentration for this Lipschitz functional gives (D.1).  $\square$